1.0 EUR

HUNGARIAN GROUP OF *fib*

CONCRETE STRUCTURES

ANNUAL TECHNICAL JOURNAL

2017

Vol. 18

CONCRETE STRUCTURES
Journal of the Hungarian Group of ***fib***

Founded by: Hungarian Group of ***fib***
Publisher: Hungarian Group of ***fib***
(***fib*** = International Federation for Structural Concrete)

Editorial office:
Budapest University of Technology and Economics (BME)
Department of Construction Materials and Engineering Geology
Műegyetem rkp. 3., H-1111 Budapest
Phone: +36-1-463 4068
Fax: +36-1-463 3450
WEB http://www.fib.bme.hu
WEB editor: Olivér Czoboly

Layout and print:
Csaba Halmai
Navigar Ltd.

Price: 10 EUR
Printed in 1000 copies

HU ISSN 2062-7904
online ISSN: 1586-0361

Cover photo:
Cold store made of special reinforced concrete produced by FERROBETON Co, CRH Group

FERROBETON

CONTENT

CRACK CONTROL: AN ADVANCED CALCULATION MODEL – PART II: THE MODEL

Dedicated to Prof. Gallus Rehm on the occasion of his 90th birthday

Andor Windisch

Crack control is a fundamental part of dimensioning: in many cases it governs the amount of reinforcement in R.C. members. In Part I - instead of inscrutable databanks - the data, records and notations of four classical papers with excellently documented tests were studied and evaluated. In Part II –after a critical review of the influencing factors- the well-known formula of the design value of crack width gets an advanced interpretation. All influencing factors –e.g. bond, concrete contribution, effective concrete tension area, shrinkage- are taken into consideration at their proper position.

Keywords: cracking, Goto-cracks, primary cracks, secondary cracks, bond, concrete cover, concrete elongation, effective distance

1. THEORETICAL CONSIDERATIONS AND COMMENTS

1.1 Development of crack pattern

At dimensioning a R.C. member the dimensions of the load bearing element, the dead and live loads, the class of concrete, the type of reinforcing steel and thus the cracking force/moment are known. Varying the rate/amount of reinforcement the steel stress at cracking and the ultimate force/moment can be calculated. Depending on the chosen rate of reinforcement steel stresses at cracking from 450 N/mm² to 45 N/mm² and ratios of ultimate force/moment to cracking force/moment 1 to 10 arise.

In the cross section with the lowest concrete tensile strength (which might be any value between $f_{ct\,0.05}$ and $f_{ct\,0.95}$) the first primary crack develops. The crack unloads the concrete in its both sides. Depending on the steel stress in the crack and the chosen rebar diameter load transfer lengths are developed on both sides of the crack. The load transfer length depends on the steel stress in the crack, on the diameter of the rebar and on the bond characteristics rebar/concrete. The load transfer length increases as the steel stress in the crack increases. The next primary crack can develop at any next weak section outside of the actual load transfer sections. The distance between the neighboring primary cracks can be at least the actual load transfer length. If the crack distance is two times the actual load transfer length, then a further primary crack might occur during an increase of the loading. Achieving the $f_{ct\,0.95}$ value at the most stressed fiber of the member the primary crack pattern is considered as stabilized.

Depending on the steel stress and slip in the crack a pattern of the well-known Goto-cracks around the rebar can develop immediately after the occurrence of the primary crack, or later. The extent of the Goto-cracks decreases away from the crack, whereas the tensile stresses in the concrete around the rebar increase due to the bond forces transmitted. This occurs rather symmetric to the rebar's axis. Where the most tensioned circular area reaches the outer surface of the R.C. member a secondary crack occur. It is easy to recognize that in this section the stress in the rebar is less than the stress in the crack (i.e. uncracked concrete regions around do exist). It is a further reason why data banks containing all cracks found on the surface of a R.C. member cannot yield any feasible rule or formula. It can be recognized that the crack width control means the control of the width of the primary cracks. The test results of Rüsch and Rehm (1963) revealed that the development of secondary cracks on both sides of the first or the widest primary crack is not necessary.

The detailing rules serve for the activation of the concrete tensile contribution.

Applying small number of big diameter rebars instead of many small diameter rebars for the same rate of reinforcement the transfer length increases: hence less primary cracks can develop and the slip increases. As an example: changing the diameter from Ø10 to Ø20 and Ø32 the transfer length increases with ~60% and ~160%, whereas the slip (depending on the steel stress) with ~ (110-60)% and ~ (230-150)%, resp. Note: the corresponding values were calculated taking into account the local bond-slip relationship as given in Eq. (6.1-1) of MC2010 (2013).

1.2 Bond, concrete contribution and tension stiffening

Structural concrete has four "constituents": concrete, reinforcement, cracks and bond.

The interaction between rebar and the surrounding concrete is characterized by the bond stresses. Bond reduces the strain in the rebars between two adjacent cracks. This phenomenon is named tension stiffening. In case of deformation and cyclic load etc. the mean value along the R.C. member is governing. At crack control a lower fractile value is decisive.

For stiffness related characteristics (deflection and dynamic behaviour) of R.C. members the mean values of crack distance and crack width are of interest whereas for crack width control the 95% upper fractile value.

1.3 Local bond stress-slip relationship vs. Goto-cracks

The local bond-slip relationship as given e.g. in MC2010 (2013) assigns an imaginary layer between rebar surface and concrete around. In reality the concrete cannot withstand such high slips of the rebar ribs against the concrete without creating inhomogeneity: these are the well-known Goto-cracks. Between the inclined bent-compression struts inclined Goto-cracks develop. Their length and width obey the rules of equilibrium and compatibility. Their lengths decrease away from the primary crack. They form a circular domain around the rebar. When occurring, the Goto-crack does not change the sign of the slip in the direction of the primary crack: the steel stress increases in the Goto-crack. In general, the Goto-cracks reduce the concrete contribution between two adjacent primary cracks.

The Goto-cracks might extend into the primary crack therefore even if we assume that with the help of the local bond stress-slip relationship the real crack width on the surface of the rebar is calculated, the accuracy of the theory can never be proven with measurements of the actual crack width profiles: the deformation of the concrete cone on the front of the first Goto-crack disturbs the profile (see Borosnyói et al. (2010)). Therefore, from the measured profiles along a crack no reliable correlations between crack width on the rebar surface and on the concrete surface can be deduced (Borosnyói et al. (2010), Husain et al. (1968)).

When the Goto-crack 'arrives' at the nearest concrete surface, a secondary crack will be observed. This secondary crack needs not intersect the whole cross section: the crack width on the rebar surface (i.e. the steel stress) and the length of this secondary crack obey the equilibrium and compatibility conditions. This means that the limited length of the secondary crack influences the crack distance in a limited region only: this is the reason why the crack distance (especially the mean one) might differ in a wall or in a slab along the rebar's axis and between two rebars.

Secondary cracks have the same impacts on the concrete contribution like the Goto-cracks.

If – on equilibrium and compatibility reasons – the secondary crack intersects the whole cross section, then in the following the crack shows the characteristics of a primary crack.

1.4 Comments on the bond stress-slip relationship given in MC2010

The parameters defining the mean bond stress-slip relationship of deformed bars, given in Table 6.1-1 of MC2010 (2013) can be commented as follows:

- The relationship attests a much stiffer bond characteristic than in the reality. The parameters are deduced from the results of RILEM pull-out tests. The 5Ø long bonded length is in the upper part of a cube with 10Ø side lengths. The cube is supported by the plate of a tensile machine. The slip of the rebar against of the concrete is measured on the unloaded end of the bonded length. As it can easily be recognized (and was shown by Windisch (1985) on the loaded end of the bonded length the slip values are greater than at the unloaded end hence the real stiffness is much less than generally considered and accepted. The support conditions of the cube hinder the development of the Goto-cracks around the rebar hence make the bond even stiffer. Moreover, the compressive forces supporting the cube specimen "prestress" the bond region around the rebar.
- The parameters s_1 and s_2 are not constant for all bar diameters, but (as shown by Windisch et al. (1984)) similar to the s_3 parameter, they depend on the clear distance between the ribs.

It must be concluded that the bond stress-slip relationship given in MC2010 cannot be taken into account for calculation of crack widths.

As shown in Part I of this paper (Windisch, 2016) based on the measured steel stresses by Scott et al. (1987) the bond stress shows a rather constant course along the transfer length, its value is around f_{ct}.

1.5 The effective tension area of concrete ($A_{c,ef}$)

Balázs et al. (2013) wrote: "The effective tension area of concrete ($A_{c,ef}$) has been earlier developed as a computational tool in order to demonstrate the part of the concrete surrounding the reinforcement that is considerably influenced by the force transfer. It is normally a concrete area in tension with the same centroid as that of the reinforcement. By detailed analyses we can realize that it is not so easy and not so evident how to define the sizes and forms of this effective tension area of concrete. By considering didactical reasons as well as advantageous use of it for crack control in thick elements, we kept using effective tension area of concrete in our model."

According to the explanation in *fib* Bulletin (in press) the equation for the maximum crack spacing is derived from the equilibrium of a R.C. member with the cross section $A_{c,ef}$, with the length of the transfer length (the distance of the crack considered and of the next section of no-slip), reinforced with a rebar of diameter Ø and the cross section of A_s.

Allowing for that a model might contain simplifications, nevertheless this explanation is multiple questionable: the definitions of transfer length, of the effective tension area of concrete and of the ratio of mean concrete tensile strength to the bond stress are not correct. The transfer length is the length where the tensile forces necessary to let occur a cracking of the effective concrete area are transferred by bond, hence the remote end of the transfer length is not the section of no-slip. As the transfer by bond forces does not occur like in a "tube" with a cross section of $A_{c,ef}$, but disperse into the

Fig. 1 – Effective tension area of concrete Ac,ef for (a) beam; (b) slab; (c) wall in tension (shaded areas), see Figure 7.6-4 in MC 2010 (2012)

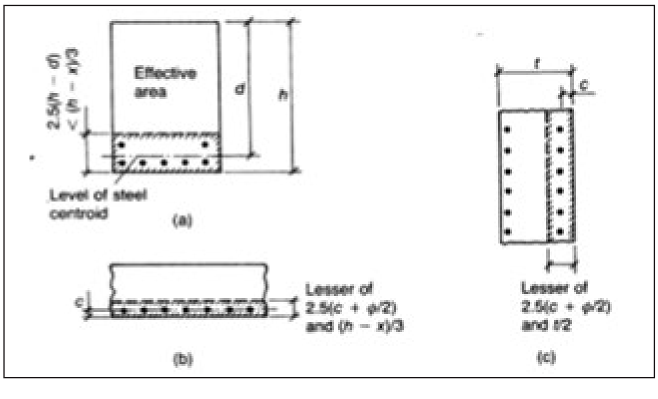

Table 1 – *Comparison of test values of Broms (1965) with results of models given in MC2010 (2013)*

	Concrete cover, t	25		43		54		76		94		107	
	Steel stress	MC	m*	MC	m*	MC	m*	MC	m*	MC	m*	MC	m*
T-RC6	314	0,37	0,40			0,44	0,59			0,53	0,85	0,56	0,93
	471	0,62	0,69			0,74	0,98			0,89	1,39	0,95	1,52
	604	0,81	0,84			0,96	1,14			1,17	1,56	1,24	1,69
T-RC5	314	0,22	0,30	0,26	0,43			0,34	0,66				
	471	0,36	0,43	0,43	0,61			0,56	0,95				
	628	0,51	0,54	0,60	0,74			0,79	1,12				

Legend: m* - measured max. crack width

regions outside, therefore the bond stress referred to in the formula must be a modified one which depends on the ratio of effective tension area to the total tensile zone hence cannot be simply related to the concrete tensile strength.

A look at the definition of the effective concrete areas shown in *Fig. 1* (Fig. 7-6.4 in MC2010) reveals that $A_{c,ef}$ refers to the cross section of a secondary crack only, hence – according to the former explanations on the function of secondary cracks in this paper – it is irrelevant for the calculation of the design crack width. Its definition became necessary as in the databanks primary and secondary cracks of members after their failure were considered as evenly matched.

1.6 The pitfalls of databanks and average value-oriented models

In this section the problems connected with the uncritical use of databanks are tackled.

For the development of mean values the subsequent occurrence of all cracks (i.e. secondary cracks too) are of interest. Some comments:

- The stress in the rebars at development of the primary cracks depends on the rate of reinforcement and can be between 50 N/mm² and up to f_{sy}.
- Before introduction of the partial safety factor-concept the working stress in the rebars at controlling the crack width was f_{sy} /1.7, i.e. in case of B400 steel grade 235 N/mm² and of B500 294 N/mm², respectively.
- In SLS the characteristic value of crack width shall be controlled under quasi-permanent loading conditions. Depending on the ratio of dead load to live load, the actual steel stress can vary from <100 N/mm² up to >300 N/mm². It can easily be recognized that under these conditions an average value oriented databank cannot function.
- The databanks contain mostly data of stabilized crack patterns. Stabilized crack patterns are consisted of primary and secondary cracks. As shown before, the actual steel stress in secondary cracks is as a rule smaller than in the primary cracks hence the data are not consistent they generate two disjunctive sets of data. Moreover, the width of primary and secondary cracks occur in completely different ways: in case of primary cracks the slip between rebar and concrete on both sides of the crack sum up whereas in case of secondary cracks their width compensates the difference between the concrete's elongations and its limited ultimate tensile strain.
- Mean values are quite insensitive to variations of the main influencing factors. The results of Rüsch/Rehm (1963) verify this: both, the mean crack distance and mean crack width do not change very much when increasing the concrete grade, while the 95% fractile values show a pronounced impact.
- In case of primary cracks stabilized cracking stage can be assumed when the concrete tensile stress in the cross section calculated with the Bernoulli-Navier-hypothesis is beyond the $f_{ct0.95}$ value. Thereafter (or in case of high steel stresses even before) with increasing steel stress secondary cracks might develop continuously, incessantly decreasing the mean values of crack distance and width, resp. Nevertheless, this has no impact on the upper fractile values of both, the crack distance and crack width.
- Certainly, at control of the deflection, vibrations, etc. the scatter of mean values is decisive; the databanks could yield valuable contribution.

1.7 Influence of $Ø/\rho_{s,ef}$

In 2004 Beeby (2004) agitated a debate publishing an article heavily defending the thesis that crack spacing is independent of parameter $Ø/\rho_{s,ef}$ and depends only on the distance of the crack from the nearest reinforcing bar. This was a very controversial statement and a huge discussion against arouse, since the defendants of the doctrine meant that the dependence of crack spacing on $Ø/\rho_{s,ef}$ is a "direct consequence of theory", whereas dependence of crack spacing on cover and bar distance are "more empirical". Despite a database with more than 300 tests from various researchers, it was not possible to obtain conclusive evidence that could settle this question. (The reason was the fundamental erroneous main feature of databanks: they scramble primary and secondary cracks thus the different characteristics of these two sets of cracks fade.) Remember to the note of Ferry Borges (1966): neither $Ø/\rho_{s,ef}$ nor concrete cover alone can characterize the function of crack width as basic variable.

The evaluation of the results of literature reveals that for the control of max. crack width the effective tension area of concrete ($A_{c,ef}$) is not relevant.

1.8 RECENT TRENDS

Referring to 'difficulties' at evaluation of databases due to the alleged inhomogeneity of the tests and their results and the subjective factors at direct observation of the crack widths some authors renounce totally the measurement of crack widths. Instead the strains along the compression face as well along the tension face corresponding to the location of the corresponding longitudinal reinforcement in the side of the beam using a digital extensometer with a 20 cm base will be measured. The mean crack spacing is determined by dividing the length of the constant moment zone (L) at the end of test when the crack pattern can be considered to be stabilized with the number of cracks along the length L. The mean crack width is considered to be equal with the mean strain in the tension chord multiplied with the mean crack spacing. The maximum crack width is approximated by multiplying the maximum measured strain in tension chord with the measurement length of extensometer. Especially this latter has no physical and theoretical background, hence any conclusion is erroneous. As shown by Beeby (1978), the mean crack width and the average crack spacing multiplied by the measured average surface strain show absolutely no relationship. Moreover, the crack pattern in ULS can be completely different from that in SLS, when the steel stress under quasi-permanent loading could be as 100 N/mm² low. Therefore, neither qualitative nor quantitative conclusions concerning the crack control can be deduced from the results of tests as reported in (Pérez et al., 2013).

1.9 Influence of stirrup spacing

In their recent paper Pérez et al. (2013) make the following correct conclusions:

- It is not correct to assimilate crack spacing and stirrup spacing. Cracks sometimes develop between stirrups and sometimes they do not develop at stirrup locations. Transfer length clearly still plays a role in crack formation.
- Although stirrup spacing has a significant effect on the mean crack spacing, the test results show that their influence on the maximum crack spacing is negligible.
- What matters for crack control is maximum crack spacing and not mean crack spacing, excluding stirrup spacing from the cracking models of current and future standards seems justified.

The same conclusions are valid for the role and impact of any "transverse" reinforcement: in slabs and walls.

2. NEW, THEORY BASED FORMULA FOR THE DESIGN CRACK WIDTH

This paper presents a cracking model which shows that the $A_{c,ef}$ is not a necessary component. Moreover, applying this method at control of the crack width in SLS no fundamental difference between R.C. members under pure tension or bending exists.

2.1 Design crack width formula

The formula is quite similar to that in MC 2010 (2012), nevertheless with some (quite fundamental) modifications:

$$w_{k,i} = 2 \cdot l_{s,max} \cdot (\varepsilon_{sm} - \varepsilon_{cm,t,i}) + 2 \cdot l_c \cdot \varepsilon_{cs} \qquad (1)$$

whereas

- w_k is the design crack width of a "primary" crack: Primary cracks are those cracks which develop at the "weakest" cross sections, i.e. with the tensile force or bending moment inducing say $f_{ct,0.95}$ acc. to the Bernoulli-Navier hypothesis. These "primary" cracks can be well recognized along the webs of higher bent members or at the mid-width of wide members in tension with poorly distributed reinforcement. At the development of any "secondary" cracks between two "primary" cracks along an R.C. member in flexure the compressive stresses have no influence, these "secondary" cracks serve the compatibility between the high strain in the rebar and the limited tensile elongation of concrete.
- $l_{s,max}$ is the transfer length on both sides of the crack with the width of w_k, up to the section with no slip between rebar and concrete around. $l_{s,max}$ is independent from the mean crack distance. Our task is to find $l_{s,\,max}$ which "survived" up to the SLS load level. With the increase of the loading the crack width increases, too, and the max. bond stress at the crack increases as well. It is common sense that the crack unloads the tensile concrete there. Away from the crack the tensile stresses increase in the concrete around the rebars due to the bond forces. Two types of cracks/tensile failures may occur: If a Goto-crack reaches the surface of the member, a "secondary" crack develops. If the tensile force reaches the failure load of a concrete cone around the bar then this cone bursts out into the crack. After this cone failure no bond forces from the rebar are transmitted here to the concrete ("zone of deactivated bond due to internal cracks"). This cone lets decrease the crack width around the rebar. This phenomenon is the reason for the "jump" in the crack widths measured by Borosnyói et al. (2010), and Tammo et al. (2006). Even if the reduction of the crack width could be interpreted as a decrease of the risk of corrosion there, nevertheless along the inclined surfaces of the failed cone corrosion inducing media could penetrate to the rebars surface. As higher the steel stress at SLS in the cracks, as more "secondary" cracks might develop. In case of standards/codes where the design is based on global safety factors, i.e. the crack width must be controlled at a given level of the steel stress simple detailing rules can be given in order to control the crack widths. ACI 318 follows this strategy. In case of a design using partial safety factors at SLS the steel stress in the cracks might vary between approx. 100 and 320 N/mm².
- $\varepsilon_{cm,t,i}$ is the mean concrete strain in a fibre in distance *t* from the steel surface. This term refers to the concrete contribution. It considers the development of the crack width along the cover, and in concrete fibres more remote from the rebar.
- l_c is the length on the side of the relevant primary crack where the concrete shrinkage ε_{cs} can influence the width of the primary crack. Note that here the secondary cracks have a substantial impact as each concrete mass between primary and/or secondary cracks shrinks for itself, producing a rather complicated state of strain/stress. The "free" shrinkage is impeded by the embedded reinforcement and by the uncracked concrete outside the secondary cracks. Here further research is needed..

The bond has twofold influence on the crack pattern:

- Along the transfer lengths on both sides of the "primary" cracks no further "primary" cracks can develop (the crack unloads the concrete in tension on its both sides).
- Increasing the load the steel stress in the crack, the crack width, the slips there and the bond stresses, too, increase.

Consequently, higher and higher tensile stresses develop in the concrete around the rebars which can cause “secondary” cracks. These “secondary” cracks need not expand to the whole tension zone of the concrete. The steel stress in these cracks “jumps”, too, unless equilibrium and compatibility are fulfilled. Note, that in these “load transfer” regions the Bernoulli-Navier hypothesis does not apply.

At the deduction of the formula for the design crack width the following assumptions are made:

- The crack with the design crack width, w_d, is that primary crack where the distance to the no-slip section on its both sides are ~0.9 times of the load transmission length at cracking of the R.C. member.
- The bond stress is uniformly distributed along the bond lengths.

The design crack width at the rebar-concrete interface is

$$w_d = 2 \cdot l_{s,max} \cdot (\varepsilon_{sm} - \varepsilon_{cm\,(t=0)}) \tag{2}$$

(Note: for reasons of simplification the influence of the shrinkage will not be tackled here.)

The bond transmission length, l_{s0}, at developing of the primary crack is

$$l_{s0} = \frac{A_{s1} \cdot \sigma_{s,cr}}{\emptyset \cdot \pi \cdot \tau_{cr}} \tag{3}$$

The steel stress in the primary crack is

- in case of uniaxial tension

$$\sigma_{s,cr} = f_{ct,i} \cdot \left(\frac{1}{\rho} + (\alpha - 1)\right)$$

- in case of pure bending

$$\sigma_{s,cr} = f_{ct,i} \cdot \left(\frac{1}{\rho} + (\alpha - 1)\right)$$

$$l_{s,max} = 0.9 \cdot l_{s0} \tag{4}$$

Fig. 2 – Comparison of measured max. crack widths, Rüsch/Rehm (1963) with those calculated from the reduced steel elongation only

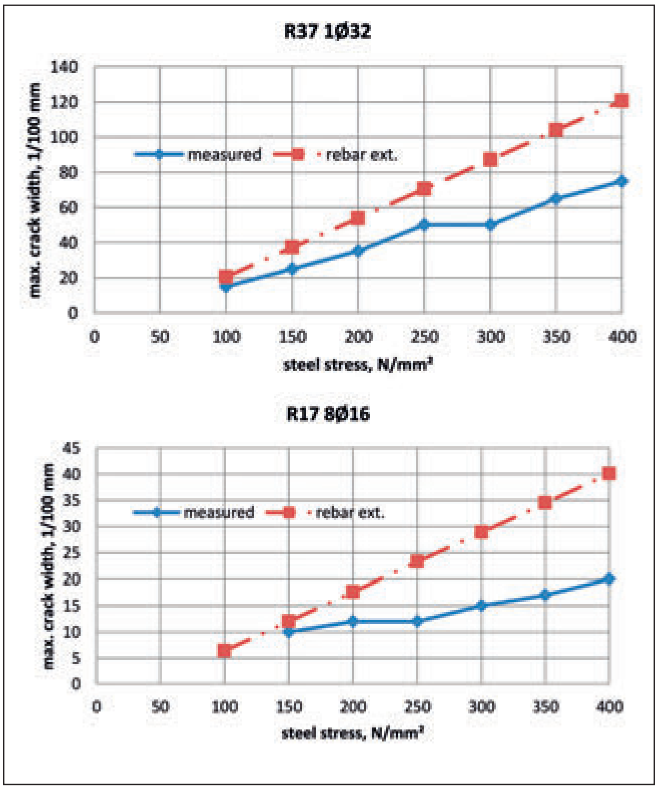

$$\varepsilon_{sm} = \frac{1}{E_s}\left(\sigma_{s,SLS} - \frac{0.5 \cdot l_{s,max} \cdot \tau_{SLS} \cdot \emptyset \cdot \pi}{A_{s1}}\right) \tag{5}$$

Substituting Eqs. (3) and (4) into Eq. (5) yields

$$\epsilon_{sm\,(t=0)} = \frac{1}{E_s}\left(\sigma_{s,SLS} - 0.45 \cdot \sigma_{scr} \cdot \frac{\tau_{SLS}}{\tau_{cr}}\right) \tag{5a}$$

The ratio τ_{SLS} / τ_{cr} must be estimated. This ratio increases with increasing load level/rebar stress/slip. The increase is as greater as greater the difference between the steel stress at cracking and in SLS. In order to keep the formula simple the ratio will be implemented into the constant rounded it up to 0.5.

A problem is to set the proper and actual values of f_{ct} and τ_{cr}:

If the bond stress τ_{cr} is related to the tensile strength then l_{s0} becomes independent of the concrete class. Note: the bond stress has no strength character, as with increasing slip (crack width) the actual bond stress increases as well. Nevertheless, the evaluation of the stress distribution measured by Scott et al. (1987) yielded the value of the uniformly distributed assumed bond stresses near to the value of the splitting tensile strength.

Substituting Eqs. (3), (4) and (5a) into Eq. (2) the design crack width is

$$w_d = 1.8 \cdot \frac{A_{s1} \cdot \sigma_{s\,cr}}{\emptyset \cdot \pi \cdot \tau_{cr}} \cdot \left(\frac{1}{E_s} \cdot (\sigma_{s\,SLS} - 0.5 \cdot \sigma_{s\,cr}) - \epsilon_{cm,t,i}\right) \tag{6}$$

Fig. 2 compares the measured max. crack widths with the crack widths calculated without the concrete elongation, i.e. resulting from the steel elongation reduced by the bond forces only (without $\varepsilon_{cm,t,i}$ see Eq. (6)). At the calculation the bond stress was taken as 1/10 of the 200 mm cube strength, the steel stress at cracking as given in the report Rüsch/Rehm (1963). The difference between the “theory” (i.e. from the mean steel elongation only) and “measured” reveals the effect of concrete elongation. *Fig. 3* shows these concrete elongations for beams reinforced with deformed rebars in Rüsch/Rehm (1963). Conclusion must be that the concrete elongation must be taken into account.

2.2 The variation of crack width along the cover

The measured maximum crack widths of the T-RC6 specimen with one 25 mm (#8) rebar and those with four 12.7 mm (#4) rebars of Broms et al. (1965) make possible to determine the variation of the crack width along the concrete cover. *Fig. 4* shows the variation of the max. measured crack widths for

Fig. 3 – Concrete elongation Rüsch/Rehm (1963) (calc. steel elongation - measured max crack width)

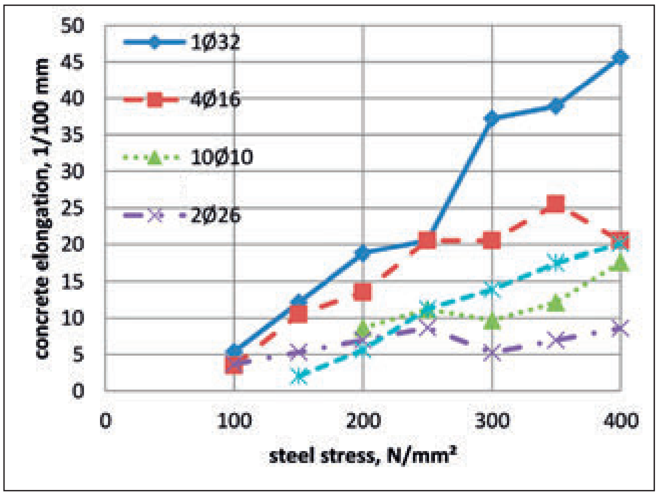

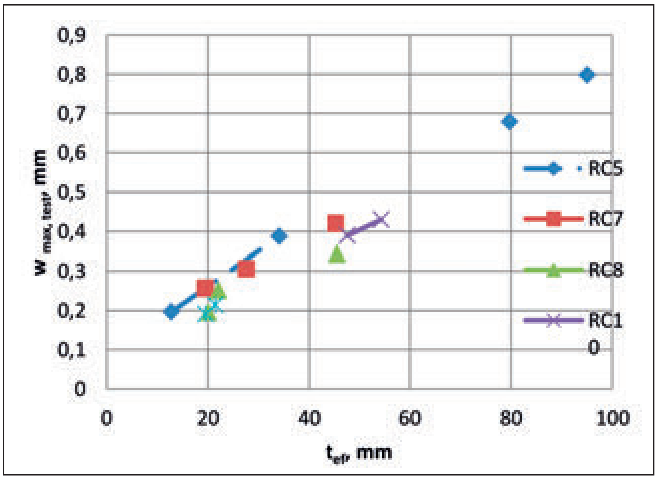

Fig. 4 – The max. measured crack widths of the specimens with Ø12.7 mm rebars at steel stress of 314 N/mm² in Broms et al. (1965)

the specimens reinforced with Ø12.7 (#4) rebars as function of the effective distance from the rebar surface. In *Fig. 5* the measured crack widths for the three stress levels are shown. Here too, fairly linear characteristics can be realized.

The basic idea is that the crack width on the concrete surface in different distances from the rebar surface can be calculated as

$$w_{k,i} = 2 \cdot l_{s,max} \cdot (\varepsilon_{sm} - \varepsilon_{cm,t,i})$$

where

$l_{s,max}$ and ε_{sm} are the same as in Eq. (1) whereas $\varepsilon_{cm,t,i}$ is the mean concrete tensile strain which is different in each fiber in different distances from the rebar surface. The different concrete strains result from the different rates of transfer of the bond forces. The maximum possible crack width is the mean steel elongation multiplied with the two max. transmission lengths. The bond between rebar and concrete 'pulls' the concrete around, which results in a central symmetrical variation of the crack width.

Fig. 6 shows the application of this assumption to the results of specimen T-RC6 of Broms et al. (1965):

The constant terms are the crack widths on the rebar surface. (Note: it might occur that this crack width cannot be directly measured on the rebar surface due to the concrete deformations around the rebar related to the Goto-cracks.) The crack width increases linearly with the distance between the rebar and the considered location along the concrete cover or on the concrete surface. The gradient (the multiplier of t_{ef}) gives the rate of the concrete contribution. This linearity is the logical consequence of the linear character of load

Fig. 5 – The max. measured crack widths of the specimens with Ø12.7 mm rebars at steel stress of 314, 471 and 628 N/mm², resp. in Broms et al. (1965)

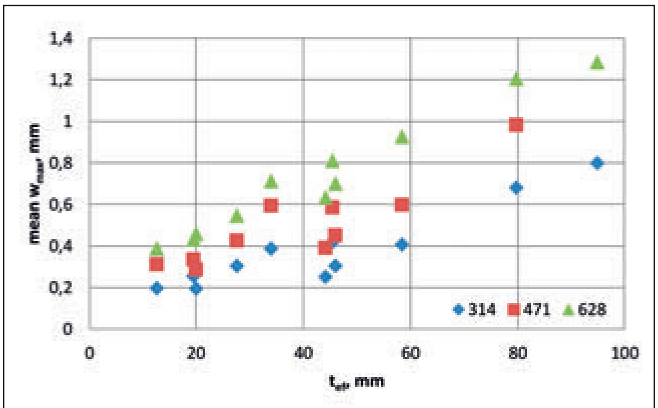

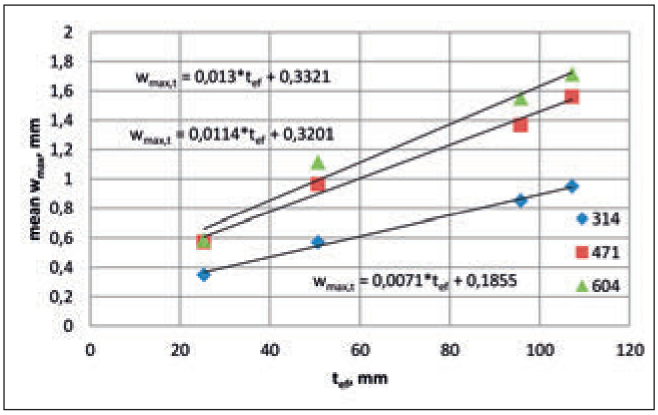

Fig. 6 – The variation of the mean wmax value as function of the effective distances tef and the steel stress in case of specimen T-RC6 in Broms et al. (1965)

transmission. Certainly this linearity stops at the maximum of t_{ef} where the concrete contribution tends to zero. Practically a t_{ef} = ~ 100 mm can be assumed.

Here further research is needed.

Applying the same assumption to the other specimens with the four #4 rebars *Fig. 7* shows the course of the biggest measured max. crack widths for the specimens T-RC5, 7 and 8, and (we look for the upper 5% fractile value of the crack widths). The interrelated courses follow a fairly linear relationship.

Note: the four Ø12.7 mm (#4) rebars of the specimens were anchored at their ends in a common concrete block. The different number of cracks and crack widths along the specimens resulted in different effective stiffnesses of the rebars (that is the real tension stiffening!). This means that after the first cracking the four rebars were loaded with imposed deformations and their share in the tensile load became unequal! Therefore at the evaluation the mean values of max. crack widths were taken into account. Here, too, a quite pronounced linearity up to a limit value of ~100 mm can be realized.

Comparing the multipliers and the nominal crack widths at the rebar surface for the #4 and #8 rebars it can be realized that both, the crack widths on the rebar surface and the inclinations depend on the rebar diameter and the steel stress in the primary crack (SLS). Both are related to the bond: it changes with the rebar diameter and the steel stress level and certainly with concrete class, too. Here too, further focused research is needed!

The crack widths measured by Borosnyói et al. (2010), shown in *Fig. 8* reveal a similar, linear dependency. The crack widths close to the rebar surface did not obey this relationship: this is the region of the Goto-cracks.

Fig. 7 – The course of the measured wmax-values at specimens reinforced with Ø12.7 mm rebars the relevant max. values at different steel stress levels as function of the effective distance in Broms et al. (1965)

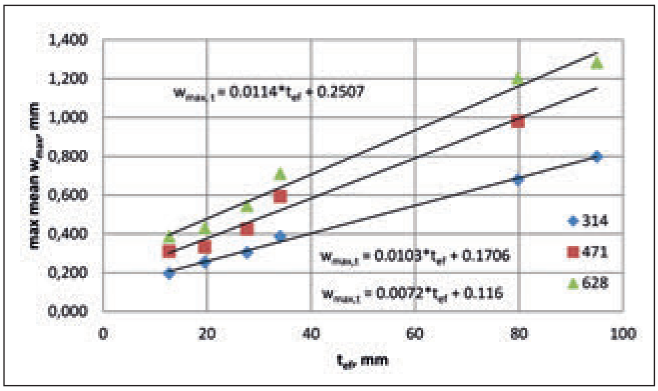

Fig. 8 – Linear course of crack widths out of the region of Goto-cracks, Borosnyói et al. (2010)

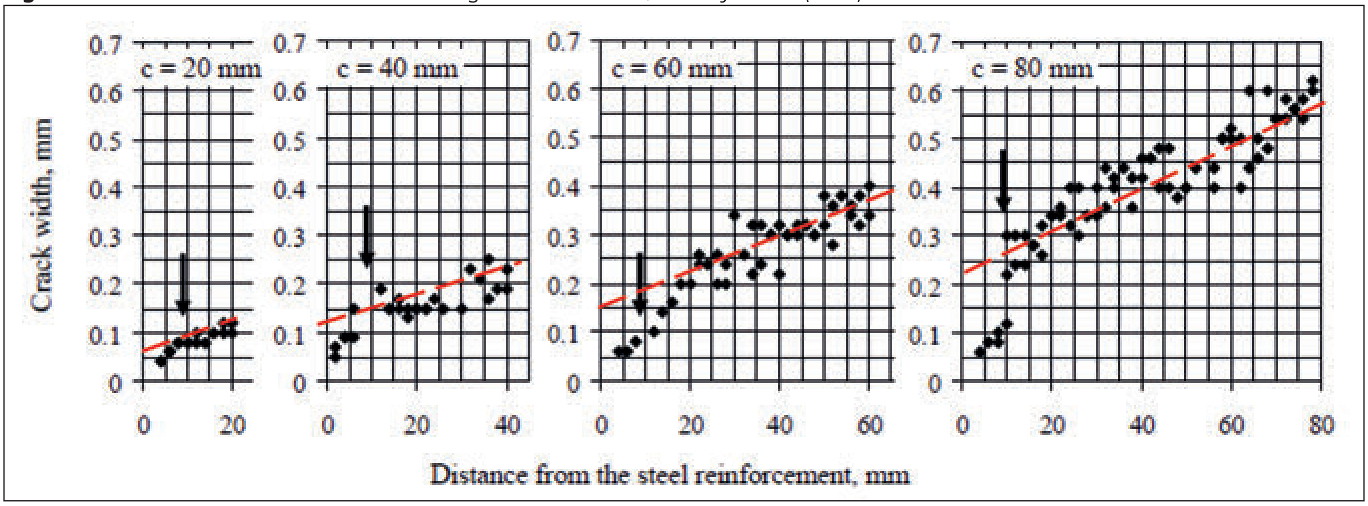

2.3 Crack width in the most tensioned fiber at members in flexure

Due to the curvature at members in flexure the width of the primary cracks in the utmost tensioned fiber is bigger than at the level of the main tensile reinforcement. If the concrete cover is the same on the side and on the bottom/top then the well-known multiplier:

$$\frac{h-x}{d-x}$$

can be applied. Otherwise, in addition the influence of the different covers must be taken into account, too.

2.4 Validation

First the test results of Broms et al. (1965) are recalculated with the models given in MC2010 (2013):

Comparing the calculated design crack widths (MC2010) with the measured (m*) values it can be seen that the definition of $A_{c,ef}$ according to Fig. 7.6-4 of MC 2010 must be corrected: for the concrete covers > 20 mm MC2010 yields too low values which are too much on the "economical" side, i.e. it does not warn the designing engineer.

A comparison of the Figs. 6 and 7 and the results of recalculations reveal the validity of the assumptions of the model described in this paper:

- the bond stress at development of the relevant primary crack depends on the actual crack width thus on the rebar diameter and the steel stress at cracking: this bond stress is definitively less than the mean tensile strength of concrete,
- the concrete deformations (strains) must be taken into account,
- the concrete deformation (strain) increases with the increasing steel stress in the primary crack and decreases linearly away from the rebar surface,
- the crack width increases linearly along the concrete cover/distance
- a limit value of effective distance exists beyond of which no concrete deformation can be considered hence the crack width there can be controlled through the steel amount and diameter only,
- the limit value depends on the bond characteristics, hence on the bar diameter,
- the secondary cracks need not be considered directly at the calculation of the design crack width.

2.5 Detailing

The purpose of the detailing is not the control of the mean crack width. The main criterions of detailing are:

- Minimize both, the mass of rebars and the time of installation.
- Create clear, practicable reinforcement patterns.
- Apply more thin rebars instead of a few thick ones: the shorter transfer length of thin rebars makes the development of closer primary cracks possible.
- The distance of two adjacent rebars shall not be more than 150-200 mm (if the design crack width at the position with the smallest t value is small enough then greater distances can be chosen as well).

2.6 Detailing rules for webs of deep beams, thick walls and slabs on grade

(Rules for thin webs under strong shear forces will be treated in another paper.)

After clarification of the course of crack development the 'roles' of the longitudinal web reinforcement are: reduction of the width of primary cracks and let develop the concrete deformation in its neighborhood.

The web reinforcement does not influence the distances of the relevant primary crack, it can reduce the crack width only. At the allocation of the web reinforcement the following influences shall be considered:

- the primary crack ends below the compression zone,
- approaching the neutral axis the tensile stresses diminish,
- the distance of the rebars along the concrete surface (along the depth over the main tensile reinforcement) should not be more than 150 mm (if the design crack width at the position with the smallest t value is small enough then greater distances can be chosen as well),
- As the durability of the RC member is not jeopardized by wider cracks, for aesthetic reasons 0.4 mm wide cracks can be tolerated. This could result in a relative 'weak' web reinforcement,
- The rebar pattern along the web must be simple and easy to be installed. Complicated pattern might result in faulty workmanship.

3. CONCLUSIONS

Based on the re-evaluation of results of four test series from the classical literature and a critical review of some relevant theoretical questions:

- An advanced calculation model is presented where in addition to the steel elongation the concrete contribution, the development of the crack width along the concrete/cover and the influence of concrete shrinkage are correctly considered.
- The bond stresses and the concrete contribution depend on the rebar diameter, the stress level in the primary crack and the concrete class.
- The concrete elongation is maximum at the rebar surface and decreases linearly away from it up to a limit distance.
- The crack width in a point of the relevant primary crack depends on the distance of the point to the next rebar. This distance controls the rate of concrete deformation hence the crack width at this point (see e.g. crack widths along a primary crack in a slab).
- A physically sound formula for calculation of the design crack width is proposed.
- An efficient distance (t_{ef}) is defined: if the distance t to the surface of next two rebars each is not greater than the limit distance (100 mm) then –due to the double concrete elongations- $t_{ef} = t/2$ shall be taken into account.
- For practical reasons a limit efficient distance of the concrete contribution must be defined
- The influence of flexure on the crack width is shown.
- Detailing rules for slabs and webs of deep beams are given.

Well planned and properly documented tests are necessary in order to further verify the proposed calculation method.

4. NOTATIONS

A_{s1}	cross section area of one rebar, mm²
E_s	Young's Modulus of Elasticity, N/mm²
W_{200}	20 cm cube strength
$W_{ci,I}$	section modulus of the uncracked ideal cross section for the concrete fibre in tension
$W_{si,II}$	section modulus for the rebar in the cracked cross-section
d	effective depth
$f_{ct,i}$	the actual concrete tensile strength
$f_{ct\,0.05}$	the 5% lower fractile value of concrete tensile strength
$f_{ct\,0.95}$	the 95% uppeer fractile value of concrete tensile strength
f_{sy}	yield strength of reinforcement
h	total depth of concrete cross section
l_c	length where the concrete shrinkage can influence the width of the primary crack
l_{s0}	bond transmission length
$l_{s,max}$	transfer length over which slip between steel and concrete occurs
s_1, s_2, s_3	characteristic slip values in the local bond stress-slip relationship
t	distance of the relevant concrete fibre from the nearest rebar surface
t_{ef}	effective distance of the concrete fibre at the half distance of two nearest rebars
w_d	design crack width
w_k	design crack width of a "primary" crack
x	depth of the concrete compression zone in SLS
Ø	rebar diameter, mm
α	E_s / E_c
$\varepsilon_{cm,\,t,\,I}$	mean concrete strain in distance t from the nearest rebar surface
ε_{sm}	the average steel strain over the length $l_{s,max}$
ε_{smi}	mean steel strain
ρ	ratio of steel and concrete cross sections ($A_s/A_{c,tot}$)
$\rho_{s,ef}$	ratio of steel and effective concrete cross sections ($A_s/A_{c,ef}$)
$\sigma_{s,SLS}$	steel stress under the loading in SLS, N/mm²
$\sigma_{s,cr}$	steel stress at the relevant primary crack when the crack occurred, N/mm²
τ_{cr}	actual bond stress at development of the primary crack
τ_{SLS}	bond stress at steel stress/slip conditions under SLS loading level, N/mm²
τ_{SLS}	bond stress at steel stress/slip conditions when the relevant primary crack occurred

5. REFERENCES

Balázs, L. Gy. et al., (2013), "Design for SLS according to fib Model Code 2010", *Structural Concrete*, 2/2013, June 2013, pp. 99-123.

Beeby. A. W., (1978), "Corrosion of reinforcing steel in concrete and its relation to cracking", *The Structural Engineer*, March 1978, pp. 77-81.

Beeby, A. W., (2004), "The influence of the parameter $Ø/\rho_{eff}$ on crack widths", *The Structural Concrete* 2004, Vol 5 No. 2. pp. 71-83.

Borosnyói, A., Snóbli, I. (2010), "Crack width variation within the concrete cover of reinforced concrete members", Építő*anyag*, 2010/3, Vol, 63. pp. 70-74.

Broms, B. B., Lutz, L. A. (1965), "Effects of Arrangement of Reinforcement on Crack Width and Spacing of Reinforced Concrete Members", *ACI Structural Journal* Nov. 1965, No. 62-77 pp. 1395-1410. + Part II Report.

Debernardi, P. G., Taliano, M. (2016), "An improvement of the Eurocode 2 and fib Model Code 2010 methods for the calculation of crack width in r.c. structures", *Structural Concrete*, September 2016, Vol 17, Issue 3, pp. 365-376.

Ferry Borges, J., (1966), "Cracking and Deformability of Reinforced Concrete Beams", *IABSE Publication*, Zürich, Vol. 26, pp. 75-95.

fib Model Code 2010 (MC2010), (2013), fib Model Code for Concrete Structures 2010, Wiley Ernst and Sohn

fib SLS according to MC2010. *fib* Bulletin (in preparation)

Husain, S. I., Ferguson, Ph. M., (1968), "Flexural crack width at the bars in reinforced concrete beams", *Research Report* 102-1F, Project 3-5-66-102. Center for Highway Research, The University of Texas at Austin, June 1968, 35 p.

Pérez Caldentey, A., Corres Peiretti, H., Peset Iribarren, J., Giraldo Soto, A. (2013), "Cracking of TC members revisited: influence of cover, $Ø/\rho_{s,ef}$ and stirrup spacing – an experimental and theoretical study", Structural Concrete, 14 (2013) No. 1, pp. 69-78.

Rüsch, H., Rehm G., (1963), „Versuche mit Betonformstählen", *Deutscher Ausschuss für Stahlbeton*. Heft 140, 182 p.

Scott, R. H., Gill, P. A. T., (1987), "Short term distributions of stand and bond stress along tension reinforcement", *The Structural Engineer*, 1987, 65B, No. 2, pp. 39-48.

Tammo, K., Thelandersson, S., (2006), "Crack opening near reinforcement bars in concrete structures", *Structural Concrete*, 2006, 7, No. 4, pp. 137-143.

Windisch, A., (1985), "A modified Pull-Out-Test and new evaluation methods for a more real local bond-slip relationship", *Matériaux et Constructions*, No. 105, 1985.

Windisch, A., Balázs, L.Gy., (1984), "A beton és az acélbetét együttdolgozásának jellemzése a fajlagos kapcsolati erö – relativ elmozdulás összefüggéssel", (The characterization of the interaction of concrete and rebar by the specific bond force – slip relationship. In Hungarian). *Mélyépítéstudományi Szemle*, Vol. XXXIV, 1984, pp. 265-271

Windisch, A., (2016), "Crack control: an advanced calculation model – Part I: review of classic tests", *Concrete Structures*, Vol. 17, pp. 41-48.

Andor Windisch PhD, Prof. h.c. retired as Technical Director of DYWIDAG-Systems International in Munich, Germany. He made his MSc and PhD at Technical University of Budapest, Hungary, where he served 18 years and is now Honorary Professor. Since 1970 he is member of different commissions of FIP, CEB and fib. He is author of more than 120 technical papers. e-mail: Andor.Windisch@web.de.

DURABILITY OF NATURAL FIBRES WITHIN CEMENT-BASED MATERIALS – REVIEW


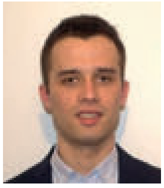


Ildikó Merta – Bojan Poletanovic – Katalin Kopecskó

Natural fibre reinforced cementitious composites have been recently considered as a viable replacement of highly resource- and energy-intensive traditional (steel- and synthetic) fibre reinforced composites. However, the major obstacle in their larger scale application remains the lack of long term durability of the natural fibres in the high alkaline environment of the Portland cement matrix. This review gives an insight in the ongoing research dealing with the two most effective ways of mitigating fibre degradation in the cementitious matrix, i) reducing the matrix alkalinity by partial replacement of Portland cement with supplementary cementitious materials (i.e. fly ash, metakaolin, silica fume, etc.), and ii) treating (protecting) the fibres with various chemical agents (alkaline-, silane-, sodium carbonate treatment, etc.) prior to adding them to the cement matrix.

Keywords: natural fibres, durability, cement-based materials, fibre reinforcement, degradation

1. INTRODUCTION

Concrete, as the most prominent representative of cement-based materials, is the most widely used man-made material in the world. Its yearly demand is estimated at 4 tons per person on the planet. Cement-based composites are quasi-brittle materials that are strong in compression but weak in tension. Their low tensile strength and strain capacity results in poor crack resistance and energy absorption capacity (toughness) of the material. These deficiencies can be effectively improved by incorporating randomly distributed short fibre reinforcement in the matrix and in such a way the transition from the brittle behaviour of the composite to quasi-ductile or even ductile behaviour with increased toughness and energy absorption capacity can be achieved. It has been reported that fibre reinforcement in cementitious materials substantially improve the material's tensile strain capacity, impact- and abrasion resistance, and reduce the cracking due to plastic- and drying shrinkage (Bentur and Mindess, 2007; Johnston, 2010; Mobasher, 2011). Generally fibres do not increase the tensile or flexural strength of concrete and are not capable to replace the structural reinforcement.

The most common fibre reinforcement in cementitious composites are made of steel, synthetic or glass (Balaguru and Shah, 1992; Bentur and Mindess, 2007). However, these traditional fibres are highly dependent on virgin material resources and are extremely resource and energy intensive to manufacture. Their production contributes to high pollution and carbon dioxide emissions. Recently, natural plant fibres, such as sisal, coir, flax, hemp, jute, cotton, coir, hibiscus cannabinus (kenaf), bamboo, banana, kraft pulp etc. have been considered as possible sustainable substituent fibres (Ardanuy et al., 2015; Swamy, 1990; Savastano et al., 2000; Tolêdo Filho et al., 2003; Silva et al., 2010a and 2010b; Torgal and Jalali, 2011; Sierra Beltran, 2011; Merta et al., 2011; Merta and Tschegg, 2013). Natural fibres are generally easily available and cheap, since they are produced from locally available renewable resources. They are biodegradable, recyclable, and non-abrasive and there is no concern with health and safety during their handling (Ranalli, 1999; Müssig, 2010). The substitution of traditional fibre reinforcement with natural fibres ensures the development of economically and ecologically sustainable cement-based composite materials that are considerably less dependent on non-renewable energy resources. This is an effective way to increase the sustainability of cement-based materials. Natural fibres in cementitious composites could: a) substantially improve the material's mechanical and physical properties (Silva et al., 2010a; Silva et al., 2010b; Merta et al., 2011; Merta et al., 2013; Hamzaoui et al., 2014; Agopyan et al., 2005; Rocha Almeida et al., 2002; Rodríguez et al., 2011), b) markedly reduce its production costs (Gunasekaran et al., 2011; Gunasekaran et al., 2015) and c) improve its environmental impact (Merta et al., 2017).

However, the great variability in mechanical and physical properties of natural fibres, their high moisture absorption capacity and the durability problem in the alkaline environment of cement matrix are the major concerns for their successful application. Degradation phenomenon is well known not only in natural fibres but also in glass, synthetic or steel fibres (Kopecskó 2004; Czoboly and Balázs, 2016a; Czoboly and Balázs, 2016b).

2. CHEMICAL COMPOSITION OF NATURAL FIBRES

Natural fibres are obtained from different parts of plants. Flax, hemp or kenaf fibres are so called bast fibres gained from the stem of the plant. Sisal, banana, agave fibres are taken from the leaves of the plants, whereas cotton fibres are derived from the seed of plant.

At the microscopic level, natural fibres are mainly composed of two outer cell walls (i.e. primary and secondary cell

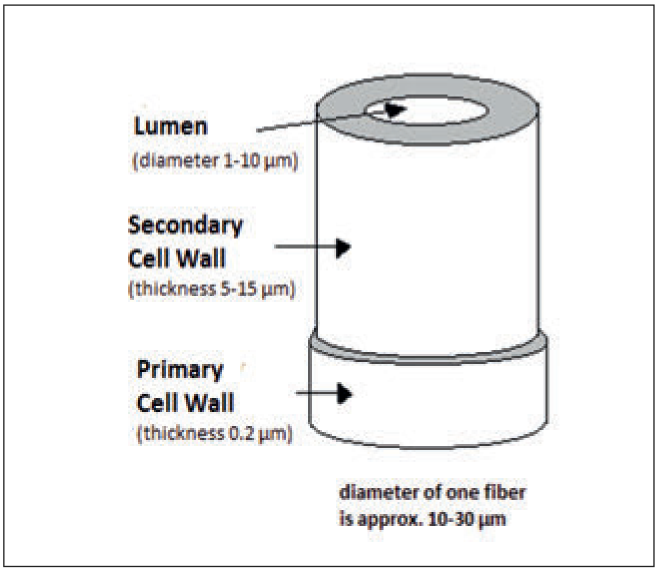

Fig. 1: *The structure of natural fibres (e.g. flax)*

wall), and one inner part, the lumen. The primary wall's role is to protect the secondary wall which is responsible for the tensile strength of the fibres. Inside of the secondary wall is the lumen, responsible for water uptake (*Fig. 1.*). Physical and chemical characteristics of natural fibres are hard to standardize as their properties change with harvest, climate zones, type of soil and fertilizer, etc.

The main chemical components of all natural fibres are cellulose, hemicellulose and lignin. From these natural polymers hemicellulose and lignin are amorphous, whereas cellulose is much more crystalline. Generally, the dominant chemical component of all natural fibres is cellulose (40-70 wt%), which is a linear polymer made of glucose subunits linked by β-1,4 bonds, and the basic repeating unit is cellobiose. Several different crystalline structures of cellulose are known, corresponding to the location of hydrogen bonds between and within strands. Cellulose has a significant contribution to strength and stiffness of fibres. The higher the cellulose content, the higher the tensile strength and Young's modulus (Bergström and Gram, 1984; Yan et al., 2016). The second major constituent of natural fibres is hemicellulose (10-30 wt%) which positively influences the Young's modulus. The main chain of hemicellulose is characterized by a β-1,4-linked-d-xylopyranosyl, which carries a variable number of neutral or uronic monosaccharide substituents (Joseleau et al., 1992). The third part is lignin (1-10 wt%), a substance which negatively influences the Young's modulus and tensile strength of fibres. Lignin is a kind of three-dimensional network heteropolymer (Hatfield and Vermerris, 2001; Sugimoto et al., 2002; Nadji et al., 2009). In addition to these three main components, natural fibres usually also contain some minor quantities of pectin, wax and water soluble substances. *Table 1* shows the composition of different natural (vegetable) fibres.

3. MECHANISM OF FIBRE DEGRADATION IN CEMENTITIOUS COMPOSITES

The most important factor affecting the large-scale use of natural fibres is associated with their weak durability within the alkaline environment of Portland cement matrix (pH > 12), caused mainly by the presence of calcium hydroxide, $Ca(OH)_2$ (portlandite). The interaction between the constituents of natural fibres and portlandite can occur resulting in the degradation of fibres (Savastano et al., 2009).

The two main mechanisms that cause degradation of natural fibres within cement-based matrices are: i) alkaline attack and ii) fibre mineralisation. In the first mechanism, the degradation of fibres in the cement matrix occurs as a consequence of dissolving of the lignin and the hemicellulose in the middle lamellae of the fibres through the alkaline pore water (due to adsorption of calcium and hydroxyl ions). In the second mechanism, fibre mineralization is caused by migration of hydration products (calcium hydroxide) onto fibre wall (surface) and into the fibre cell (lumen) (Toledo Filho et al., 2000; Toledo Filho et al., 2009). It has been widely reported that cementitious composites may undergo a serious reduction in strength and toughness as a result of weakening of the natural fibres by a combination of both mechanisms, alkali attack and mineralization (Bergström et al., 1984; Toledo Filho et al., 2000; Juárez et al., 2007; Kriker et al., 2008; Sedan et al., 2008; Troëdec et al., 2009; Merta et al., 2012; Melo Filho et al., 2013; Hamzaoui et al., 2014; Wei and Meyer, 2015).

Table. 1: *Physical properties and chemical composition of different cellulosic fibres (Dicker et al., 2014; Gurunathan et al., 2015)*

Natural fibres	Density (kg/m^3)	Young's modulus (GPa)	Tensile strength (MPa)	Cellulose (wt%)	Hemi-cellulose (wt%)	Lignin (wt%)	Pectin (wt%)	Wax (wt%)
Hemp	1470-1520	55-70	550-920	70.2-74.4	17.9-22.4	3.7-5.7	0.9	0.8
Flax	1420-1520	75-90	750-940	71-78	18.6-20.6	2.2	2.3	1.7
Jute	1440-1520	35-60	400-860	61-71.5	13.6-20.4	12-13	0.2	0.5
Kenaf	1435-1500	60-66	195-666	45-57	21.5	8-13	3-5	not specified
Ramie	1450-1550	38-44	500-680	68.6-76.2	13.1-16.7	0.6-0.7	1.9	0.3
Sisal	1400-1450	10-25	550-790	67-78	10-14	8-11	10	2
Coir	1150-1220	4-6	135-240	36-43	0.15-0.25	41-45	3-4	not specified

The durability of sisal and coir fibre reinforced concrete was studied first by Gram (1983). The fibre degradation was evaluated by exposing them to alkaline solutions, and then the variations in tensile strength were evaluated. The author reported a deleterious effect of Ca^{2+} cations on fibre degradation. He also stated that fibres were able to preserve their flexibility and strength in carbonated concrete where the pH value was 9 or less.

Toledo Filho et al. (2000) studied the durability of sisal and coconut fibres exposed to alkaline solutions of calcium and sodium hydroxide. The study found that fibres kept in a $Ca(OH)_2$ solution of pH 12 completely lost their flexibility and strength after 300 days. Fibres kept in sodium hydroxide solution retained around 70% of their initial strength after 420 days. The stronger attack by $Ca(OH)_2$ is believed to be the result of crystallization of lime in the fibre pores.

In the following chapters the most convenient methods for protecting natural fibres against degradation within cementitious composites will be reviewed.

4. MATRIX MODIFICATION

The primary cause of degradation of natural fibres in cement-based composites is the high alkalinity of the Portland cement matrix (pH>12). Regarding this, an effective way of mitigating the degradation is decreasing the matrix alkalinity by reducing the calcium hydroxide $Ca(OH)_2$ content. The addition of the following industrial by-products can decrease the alkalinity of the matrix enhancing the overall durability of the composite: fly ashes and slags (coal combustion-based fly ashes, biomass- or rice husk ashes, metallurgical slags, ground granulated blast furnace slag, etc.), metakaolin, thermally activated (calcined) clays, etc.

It has been reported that by replacing Portland cement with 30 w/w% metakaolin and 20 w/w% calcined waste crushed clay brick results in a matrix free of $Ca(OH)_2$ at 28 days of age (Silva et al., 2010b). After 6 months of aging in hot-water immersion, the $Ca(OH)_2$ free composites with sisal fibres showed 3.8 times higher bending strength and 42.4 times higher toughness than composites with Portland cement. The reduced alkalinity of the matrix slows down the fibres degradation process but it can have a beneficial influence on the fibre/matrix interface as well. A recent work (Alves Fidelis et al., 2016) reported that after 6 months of accelerated aging (40°C and 99% relative humidity) the maximal pull-out force of jute fibres from matrices with 50 w/w% replacement of cement with metakaolin decreased much less than in matrices with Portland cement.

Replacing cement with different quantities of metakaolin and bentonite has been reported to significantly improve the durability of sisal fibres in cement-based materials by increasing their flexural strength (Wei and Meyer, 2017). When replacing 50 w/w% of cement with metakaolin in sisal fibre reinforced matrices, after 10 wetting-drying cycles only a minor decrease in toughness has been observed (Melo Filho et al., 2013). Even a smaller replacement with metakaolin (30 w/w%) significant improvement in durability is achieved (Wei and Meyer, 2015). To consume the $Ca(OH)_2$ generated during the hydration of the Portland cement, metakaolin and calcined clay brick powder has been also used (Silva et al., 2006). Specimens containing industrial by-products showed three times higher flexural strength and up to 50 times higher toughness compared to specimens containing only Portland cement as binder after three days of freeze-thaw cycles in a forced air flow chamber.

Mohr et al. demonstrated that when replacing more than 30 w/w% of cement with silica fume no degradation of kraft pulp beams after 25 wet/dry cycles was achieved (Mohr et al., 2007). Similarly Wei et al. (2016) reported that the addition of supplementary cementitious materials (metakaolin, rice husk ash, fly ash, silica fume, etc.) can significantly slow down the degradation of natural fibres. Using a matrix with a lower content of cement protects coir fibres and improves their durability (Agopyan, 2005). With utilization of rice husk ashes (RHA) as a partial replacement of cement it is possible to achieve marked modification of the hydration of cement, which in turn reduces degradation of sisal fibres (Wei and Meyer, 2016). RHA is known as a high amorphous silica material with good pozzolanic behaviour.

5. FIBRE TREATMENT

Another effective way to mitigate the degradation of natural fibres within cementitious matrices is the treatment (protection) of the fibres prior to their addition to the matrix. The surface treatment of fibres does not only influence the surface (and lumen) of the fibres, but also the matrix/fibre interface region by changing the bond characteristics of the fibre. This in turn can significantly influence the overall behaviour of the composite.

The most common procedure of fibre treatment is to immerse the fibres in different chemical agents before adding them to the matrix. One of the most prevalent methods is alkaline treatment where the fibres are immersed in sodium hydroxide (NaOH) solution for a given period of time. The treatment changes the orientation of the highly packed crystalline cellulose order and forms an amorphous region by swelling the fibre cell wall. Alkali treatment also partially removes the hydrophilic hydroxyl groups of natural fibres which improves their moisture removal property. It is already proved that when using alkaline treatment the surface of fibres became rougher, which in turn has a positive influence on the durability of the entire composite (Weyenberg et al., 2003; Taallah and Guettala, 2016). The alkaline treatment primarily improves the fibre tensile strength was reported to increase by 32% for sisal fibres (Ferreira et al., 2015). Sodium carbonate ($NaCO_3$) was reported to be also a viable protective agent for natural fibres (Wei and Meyer, 2013). Another promising fibre surface protection that increases the durability of the composite is silane treatment (Weyenberg et al., 2003; Rong et al., 2001).

In addition to chemical treatments there are also mechanical treatments, such as the hornification process. Before adding fibres to the matrix, they are exposed to different wetting-drying cycles which lead to higher dimensional stability of the fibres and reduce the $Ca(OH)_2$ content on the surface of fibres. It is known that hornification can improve the performance of fibres by reducing their volumetric changes in the cement matrix (Ferreira et al., 2015). After 4 wet/dry cycles, cementitious composites containing previously hornified kraft pulp fibres showed approximately 13% higher flexural strength and 20% higher compressive strength compared to composites with untreated fibres (Claramunt, 2011). Cementitious matrices with hornified sisal fibres exhibit a better adhesional and frictional bond between the fibres and the matrix compared to matrices with untreated fibres (Ferreira et al., 2016). Similarly, by applying plasma pressure technology on the fibre surface better adhesion between fibres and matrix is obtained (Barra et al., 2012). Already after 10 minutes of plasma treatment of sisal fibres, significantly higher tensile strength was measured. Plasma treatment of coir fibres proved significant increase in surface roughness of fibres which led to better performance of the composite (Farias et al., 2017).

The treatment of the surface fibres with a natural latex polymer film combined with a pozzolanic layer (silica fume) in Portland cement composites showed an improved flexural strength and durability of the composite with deceleration of fibre degradation after aging (Silva et al., 2017). In contact with the cement matrix, latex causes a decrease in the ion transport in the aqueous medium that fills the pores of the cement paste. This may be related to the adsorption of CH in the polymeric film (Afridi et al., 1989). The latex layer around the fibre absorbs pozzolanic material, causing a reaction that produces a protective layer against alkaline attack resulting in greater mass conservation of fibres accompanied with a better preservation of the fibre structure.

The advantages of polymer modification of fibres are reported by Bijen (1990). Styrene-acrylic or acrylic types of polymers were used in the long-term experiments. Mechanical properties of the composite, such as tensile strength, strain capacity and impact strength were substantially improved for polymer modified fibres composite under natural weathering conditions.

Beneficial effect of surface treatment of poplar leaf fibres in cement-based materials were reported by means of improved compatibility between the fibres and cement-based materials with the following methods: pure acrylic polymer emulsion spraying, sodium silicate solution spraying and water dipping (Jiang et al., 2015). Accelerated ageing of hemp fibres and possible protection against deterioration due to the alkali environment of cement paste was studied by coating the fibres with linseed oil, linseed oil with catalyst, paraffin and beeswax (Merta et al., 2012). The results showed that linseed oil with a catalyst offered the best protection against alkaline environment; almost no loss of the fibre tensile strength after accelerated aging of simulated (elapsed) time of 5 years has been reported. Fibres treated with paraffin and beeswax in turn showed a moderate tension strength loss of up to 12% and 23%, respectively.

6. CONCLUSIONS

Recently, in certain industrial applications, natural fibre reinforced cementitious composites have been considered as a viable replacement for the highly resource- and energy-intensive traditional (steel and synthetic) fibre reinforced composites. However, the major concern in their larger scale application is still the lack of the long term durability of the natural fibres in the high alkaline environment of the Portland cement matrix.

This review gives a short overview of the ongoing research dealing with the two most effective ways to mitigate the fibre degradation in the cementitious matrix, namely i) the reduction of the matrix alkalinity by partial replacement of Portland cement with pozzolanic supplementary cementitious materials (i.e. fly ash, metakaolin, silica fume, etc.), and ii) treatment (protection) of the fibres with various chemical agents (alkaline-, silane-, sodium carbonate treatment, etc.) prior to their addition to the cement matrix.

The partial replacement of cement with supplementary cementitious materials efficiently decreases the alkalinity of the matrix and thus partially prevents the dissolving of the lignin and the hemicellulose in the middle lamellae of the fibres; however, it cannot protect the fibres from mineralisation. Supplementary cementitious materials are predominantly by-products from some industrial processes and are waste materials, thus their use as cementitious materials has a notable beneficial environmental effect.

The protection of natural fibres prior to their addition to the cement matrix with some chemical (or mechanical) treatment is indeed a cost intensive and challenging task considering the manufacturing process and quality control; however, it is so far the most effective method for preventing fibre mineralization.

7. ACKNOWLEDGEMENTS

This research is supported by the Stiftung Aktion Österreich-Ungarn in the frame of a bilateral research cooperation project Nr. 95öu6 and in the framework of a visiting student fellowship of the second author at the Budapest University of Technology.

Additionally, the first author would like to acknowledge the financial support of the Austrian Science Found (FWF) in the frame of her Hertha Firnberg post-doc fellowship for the research project *Biaxial Fracture Mechanical Properties of Natural Fibre Concrete*, grant Nr. T 503-N13.

8. REFERENCES

Afridi, M.U.K., Ohama Y., Zafar Iqbal M., Demura K. (1989), "Behaviour of $Ca(OH)_2$ in polymer modified mortars", *Int. J. Cem. Compos. Light. Concr.*, 11, pp. 235–244

Agopyan ,V., Savastano, Jr H., John, V.M., Cincotto, M.A. (2005), "Developments on vegetable fibre-cement based materials in Sao Paulo, Brazil: an overview", *Cem. Concr. Compos*, Volume 27, pp. 527-536

Alves Fidelis, M.E., Toledo Filho, R.D., Silva, F.A., Mechtcherine V., Butler M., Hempel S. (2016), "The effect of accelerated aging on the interface of jute textile reinforced concrete", *Cement and Concrete Composites*, Volume 74. pp. 7-15

Ardanuy, M., Claramunt, J., Toledo Filho, R.D. (2015), "Cellulosic fiber reinforced cement-based composites: A review of recent research", *Construction and Building Materials*, Vol 79, pp. 115-128.

Balaguru, P.N., Shah, S.P. (1992), "Fibre reinforced cement composites", *Civil Engineering Series*, McGraw-Hill. ISBN:0070564000

Barra B., Paulo, B., Alves Junior C., Savastano Junior H., Ghavami K. (2012), "Effects of Methane Cold Plasma in Sisal Fibers", *Key Engineering Materials*, Volume 517, pp. 458-468.

Bentur, A., Mindess, S. (2007), "Fibre reinforced cementitious composites", *Modern Concrete Technology Series*, CRC Press, Taylor & Francis Group, ISBN 978-0415250481.

Bergström, S.G., Gram, H.E. (1984), "Durability of alkali-sensitive fibres in concrete", *International Journal of Cement Composites and Lightweight Concrete*, Volume 6, (2), pp. 75-80

Bijen, J. (1990), "Improved mechanical properties of glass fibre reinforced cement by polymer modification", *Cem. Concr. Compos.*, 12 , pp. 95–101

Claramunt, J., Ardanuy, M., Garcia-Hortal, J.A., Filho, R.D.T. (2011), "The hornification of vegetable fibers to improve the durability of cement mortar composites". *Cement and Concrete Composites*. Volume 33.(5). pp. 586-595

Czoboly, O., Balázs, G.L. (2016a), "Possible deterioration mechanisms of fibres due to mixing", *Proceedings of the 9th RILEM International Symposium on Fiber Reinforced Concrete*. Eds.: N. Banthia, M. di Prisco, S. Soleimani-Dashtaki, Vancouver, Canada, RILEM Publications, pp. 593-606.

Czoboly, O., Balázs, G.L. (2016b), "Influence of mixing time to the properties of steel fibres and steel fibres reinforced concrete", *Concrete Structures: Annual Technical Journal, Journal of the Hungarian Group of fib*, 17:(1) pp. 23-28.

Dicker, M.P.M., Duckworth, P.F., Baker, A.B., Francois, G., Hazzard, M.K., Weaver, P.M. (2014), "Green composites: A review of material attributes and complementary applications. Composites Part A", *Applied Science and Manufacturing*. Volume 56, pp. 280-289.

Farias, J.G.G., Cavalcante, R. C., Canabarro, B.R., Viana, H.M., Scholz, S., Simao, R.A. (2017), *Carbohydrate Polymers*, Volume 165. pp. 429-436.

Ferreira, S.R., Silva, F.A., Lima, P.R.L., Toledo Filho, R.D. (2015), "Effect of fiber treatments on the sisal fiber properties and fiber-matrix bond in cement based systems", *Construction and Building Materials*, Volume 101, pp. 730-740.

Ferreira, S.R., Silva, F.A., Lima, P.R.L., Toledo Filho, R.D. (2016), "Effect of natural fiber hornification on the fiber matrix interface in cement based composite systems", *Key Engineering Materials*, Volume 668, pp. 118-125

Gram, H.E. (1983), "Durability of natural fibres in concrete", *Swedish Cement and Concrete Research Institute*, Research Fo. 1:83, Stockholm, 255 p.

Gunasekaran, K., Annadurai, R., Kumar P.S. (2015), "A study on some durability properties of coconut shell aggregate concrete", *Mater. Struct.*, 48, pp. 1253–1264

Gunasekaran, K., Kumar, P.S., Lakshmipathy, M. (2011), "Mechanical and bond properties of coconut shell concrete", *Constr. Build. Mater.,* 25 (2011), pp. 92–98

Gurunathan, T., Mohanty, S., Nayak, S.K. (2015), "Composites Part A", *Applied Science and Manufacturing*. Volume 77, pp. 1-25.

Hamzaoui, R., Guessasma, S., Mecheri, B., Eshtiaghi, A.M., Bennabi, A. (2014), "Microstructure and mechanical performance of modified mortar using hemp fibres and carbon nanotubes", *Materials & Design*, Volume 56, pp. 60-68

Hatfield, R., Vermerris, W. (2001), "Lignin formation in plants. The dilemma of linkage specificity", *Plant Physiol.*, 126, pp. 1351–1357.

Jiang, D., Cui, S., Xu, F., Tuo, T. (2015), "Impact of leaf fibre modification methods on compatibility between leaf fibres and cement-based materials", *Construction and Building Materials*, Volume 94, pp. 502–512,

Johnston, C.D., (2010), "Fiber-Reinforced Cements and Concretes", ISBN 90-5699-694-0, Taylor and Francis

Joseleau, J.P., Comtat, J., Ruel, K. (1992), "Chemical structure of xylans and their interaction in the plant cell walls". *Elsevier*, Amsterdam, pp. 1–15.

Juárez, C., Durán, A., Valdez, P., Fajardo, G. (2007), "Performance of "Agave lecheguilla" natural fiber in portland cement composites exposed to severe environment conditions", *Building and Environment*, Volume 42,(3), pp. 1151-1157.

Kopecskó, K. (2004), "Durability of Glass Fibres", BEFIB 2004: *Proceedings of the 6th RILEM Symposium on Fibre Reinforced Concrete (PRO 39)*. Eds.: di Prisco M., Felicetti R., Plizzari G.A. Varenna, Italy, pp. 583-592.

Kriker, A., Bali, A., Debicki, G., Bouziane, M., Chabannet, M. (2008), "Durability of date palm fibres and their use as reinforcement in hot dry climates", *Cement & Concrete Composites*, Volume 30, pp. 639-648.

Merta, I., Kopecskó, K., Tschegg, E.K. (2012), "Durability of hemp fibers in the alkaline environment of cement matrix", In: *8th RILEM International Symposium on fibre reinforced concrete: Challenges and Opportunities*. Guimaraes, Portugália, 19-21.09 2012, pp. 1-8.

Merta, I., Mladenovič, A., Turk, J., Šajna A., Mauko Pranjić A. (2017), "Life Cycle Assessment of Natural Fibre Reinforced Cementitious Composites", *Key Engineering Materials*, in press.

Merta, I., Tschegg, E.K. (2013), "Fracture energy of natural fibre reinforced concrete", *Original Research Article Construction and Building Materials*, Volume 40, 991-997

Merta, I., Tschegg, E., Tschegg, S., Kolbitsch, A. (2011), "Fracture Mechanics of Concrete Reinforced With Hemp, Straw and Elephant Grass Fibres, Composite Materials: Key to the Future", *18th International Conference on Composite Materials*, Jeju Island, Korea

Melo Filho, J.A., Silva, F.A., Toledo Filho, R.D. (2013), "Degradation kinetics and aging mechanisms on sisal fiber cement composite systems", *Cement and Concrete Composites*, Volume 40, pp 30-39, ISSN 0958-9465

Mobasher, B. (2011), "Mechanics of Fiber and Textile Reinforced Cement Composites", ISBN 978-1-4398-0660-9, CRC Press, Taylor & Fran,cis Group

Mohr, B.J. , Biernacki, J.J., Kurtis K.E. (2007), "Supplementary cementitious materials for mitigating degradation of kraft pulp fiber-cement composites", *Cem. Concr. Res*, Volume 37,(11), pp. 1531-1543

Müssig, J. (2010), "Industrial applications of natural fibres: structure, properties and technical applications (Wiley series in renewable resource)", *West Sussex (United Kingdom):* John Wiley & Sons. ISBN 978-0470695081

Nadji, H., Diouf, P.N., Benaboura, A., Bedard, Y., Riedl, B., Stevanovic, T. (2009), "Comparative study of lignins isolated from Alfa grass (Stipa tenacissima L.)", *Bioresour. Technol.*, 100, pp. 3585–3592.

Ranalli, P. (1999), "Agronomical and physiological advances in hemp crops. Advances in hemp research", *New York: The Haworth Press*, 61–84.

Rocha Almeida, R., Henrique Soares Del Menezzi, C., Eterno Teixeira, D. (2002), "Utilization of the coconut shell of babaçu (Orbignya sp.) to produce cement-bonded particleboard", *Bioresour. Technol*., 85, pp. 159–163

Rodríguez, N.J., Yáñez-Limón, M., Gutiérrez-Miceli, F.A., Gomez-Guzman, O., Matadamas-Ortiz, T.P., Lagunez-Rivera, L., Feijoo, J.A. (2011), "Assessment of coconut fibre insulation characteristics and its use to modulate temperatures in concrete slabs with the aid of a finite element methodology", *Energy Build*., 43, pp. 1264–1272

Rong, M.Z., Zhang, M.Q., Liu, Y., Yang, G.C., Zeng, H.M. (2001), "The effect of fiber treatment on the mechanical properties of unidirectional sisal-reinforced epoxy composites", *Composites Science and Technology*. Volume 61. (10). pp. 1437-1477.

Savastano, H., Santos, S.F., Radonjic, M., Soboyejo, W.O. (2009), "Fracture and fatigue of natural fiber-reinforced cementitious composites", *Cem. Concr. Compos.,* Volume 31, pp. 232–243

Savastano, J.H., Warden, P.G., Coutts, R.S.P. (2000), "Brazilian waste fibres as reinforcement for cement-based composites", *Cem. Concr. Compos*. Volume 22, 379–384.

Sedan, D., Pagnoux, C., Smith, A., Chotard, T. (2008), "Mechanical properties of hemp fibre reinforced cement: Influence of the fibre/matrix interaction", *J. Eur. Ceram. Soc*. Volume 28,(1) 183–192

Sierra Beltran, M.G. (2011), "Ductile cement-based composites with wood fibres – material design and experimental approach", *PhD Thesis*. ISBN 978-90-9026518-6. TU Delft, Netherlands.

Silva, E.J., Marques, M.L., Velasco, F.G., Fornari Junior C., Luzardo, F.M., Tashima, M.M. (2017), "A new treatment for coconut fibers to improve the properties of cement-based composites – Combined effect of natural latex/pozzolanic materials", *Sustainable Materials and Technologies*, Available online 17 April 2017,

Silva, F., Melo Filho, J.A., Toledo Filho, R.D., Fairbairn E.M.R. (2006), "Mechanical behavior and durability of compression molded sisal fiber cement mortar laminates (SFCML)", *1st International RILEM Conference on Textile Reinforced Concrete (ICTRC), Rilem Publications S.A.R.L*. pp. 171-180.

Silva, F.A., Mobasher B., Tolêdo Filho R.D. (2010a), "Fatigue behavior of sisal fiber reinforced cement composites", *Mat Sci Eng*: A; Volume 527(21–22): 5507–13.

Silva, F.A., Tolêdo Filho, R.D., Melo Filho, J.A., Rego, Fairbairn E.M. (2010b), "Physical and mechanical properties of durable sisal fiber–cement composites", *Constr Build Mater*; Volume 24(5): 777–785.

Sugimoto, T., Akiyama, T., Matsumoto, Y., Meshitsuka, G. (2002), "The erythro/threo ratio of beta-O-4 structures as an important structural characteristic of lignin – part 2. Changes in erythro/threo (E/T) ratio of beta-O-4 structures during delignification reactions", *Holzforschung*, 56, pp. 416–421.

Swamy, R.N. (1990), "Vegetable fibre reinforced cement composites – a false dream or a potential reality?" In: Sobral, H.S. (Ed.), Proceedings, *2nd International Symposium on Vegetable Plants and their Fibres as Building Materials. RILEM Proceedings 7. Chapman and Hall*, London, pp. 3–8.

Taallah, B, Guettala, A. (2016), "The mechanical and physical properties of compressed earth block stabilized with lime and filled with untreated and alkali-treated date palm fibers", *Construction and Building Materials*,Volume 104, pp. 52-62.

Tolêdo Filho, R.D.; Ghavami, K.; England, G.L.; Scrivener K. (2003), "Development of vegetable fibre-mortar composites of improved durability", *Cement & Concrete Composites*, Volume 25, 185–196.

Toledo Filho, R., Scrivener, K., England, G., Ghavami, K. (2000), "Durability of alkali-sensitive sisal and coconuts fibres in cement mortar composites", *Cem Concr Compos*, 22, pp. 127–143.

Tolêdo Filho, R.D., Silva, F.A., Fairbairn, E.M.R., Filho J.A.M. (2009), "Durability of compression molded sisal fiber reinforced mortar laminates*",* *Constr. Build. Mater*., 23, pp. 2409–2420

Torgal, F.P., Jalali, S. (2011), "Fibrous and Composite Materials for Civil Engineering Applications Natural fiber reinforced concrete", University of Minho, Portugal, edited by R. Fangueiro, *Woodhead Publishing Limited* ISBN: 978-1-84569-558-3

Troëdec, M., Peyratout, C.S., Smith, A., Chotard, T. (2009), "Influence of various chemical treatments on the interactions between hemp fibres and a lime matrix", *J. Eur. Ceram. Soc*. Volume 29 (10), pp 1861–1868.

Wei, J., Ma, S., Thomas, D.S.G. (2016), "Correlation between hydration of cement and durability of natural fiber-reinforced cement composites", *Corros. Sci.* ,Volume 106, pp. 1-15.

Wei, J., Meyer, C. (2013), "Improving degradation resistance of sisal fiber in concrete through fiber surface treatment", *Applied Surface Science*, Volume 289. pp. 511-523

Wei, J., Meyer, C. (2015), "Degradation mechanisms of natural fiber in the matrix of cement composites", *Cement and Concrete Research*, Volume 73, pp 1-16, ISSN 0008-8846

Wei, J., Meyer, C. (2016), "Utilization of rice husk in green natural fiber-reinforced cement composites: Mitigating degradation of sisal fiber". *Cement and Concrete Research*. Volume 81. pp. 94-11

Wei J., Meyer C. (2017), "Degradation of natural fiber in ternary blended cement composites containing metakaolin and montmorillonite", *Corrosion Science*, Volume 120, pp. 42-60

Weyenberg, I.V., Ivens, J., Coster, A., Kino, B., Beatens, E., Verpoest, I. (2003), "Influence of processing and chemical treatment of flax fibers on their composites", *Composites Science and Technology*. Volume 63. (9). pp. 1241-1246.

Yan, L., Kasal, B., Huang L. (2016), "A review of recent research on the use of cellulosic fibres, their fibre fabric reinforced cementitious, geo-polymer and polymer composites in civil engineering", *Composites Part B: Engineering*, Volume 92, pp. 94-132.

Ildikó Merta received her Ph.D. degree from the Technische Universität Wien, Austria (2006). She is currently holder of the Hertha Firnberg post-doc fellowship of the Austrian Science Fund for excellent female scientists. Her research interests focus on advanced fibre reinforced cementitious composites, natural fibre composites, fracture behaviour of quasi-brittle materials and optimization of concrete structures. For her research achievements she received the *Award for Excellent Female Scientist* (2013) from BAWAG PSK and for her research project of Natural Fibre Concrete the *Sustainability Award* (2016) from the Austrian Federal Ministry of Science, Research and Economy and Federal Ministry of Agriculture, Forestry, Environment and Water Management. ildiko.merta@tuwien.ac.at

Bojan Poletanović finished his bachelor (2014) and master studies (2015) in Civil Engineering at the Faculty of Technical Sciences, University of Novi Sad, Serbia at the structures course. Since 2016 he is a PhD student at the Faculty of Civil Engineering, Technische Universität Wien, Austria. Research area: geopolymers, cement-based materials reinforced with natural fibres. bojan.poletanovic@gmail.com

Katalin Kopecskó associate professor at the Budapest University of Technology and Economics in Hungary. Graduated in Chemical Engineering (1990) and has postgraduate studies in Concrete Technology (2004). She has PhD degree since 2006. Her PhD thesis was prepared on chloride ion binding capacity of steam-cured cement clinkers and cements. She teaches Chemistry for Civil Engineers both in BSc and MSc. Her research fields are: deterioration processes of construction materials, durability of concrete and other materials, cement hydration, diagnostics of historical buildings and ornamental stones, mineralogical properties of stones or soils, X-ray diffraction (XRD) and thermal analyses (TG/DTG/DTA). She is a member of the Hungarian Group of *fib* and of the Technical Committee MSZT/MB 102 (Cement and Lime) in the Hungarian Standards Institution. kopecsko.katalin@epito.bme.hu

SHEAR DESIGN FORMULAS FOR FRP AND SYNTHETIC FIBRE REINFORCED CONCRETE BEAMS

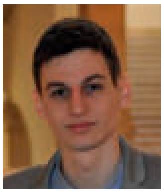

Péter Schaul – György L. Balázs

Synthetic reinforcements in concrete structures, such as macro synthetic fibres and fibre reinforced polymer bars are becoming more wide used nowadays, because of their most important advantage to be resistant against electrolytic corrosion. The fibre reinforced polymer (FRP) bars can increase the flexural capacity both as main reinforcement and shear capacity as stirrups. Macro synthetic fibres can increase the ductility of the elements and the shear capacity of the concrete structures as well. For design with FRP and synthetic fibre reinforcement concrete structures some guidelines exist (e.g. fib, ACI, CNR) but there is no standard available for them. In the literature many articles can be found which modify the formulas for steel bars and for steel fibres to be able to use for synthetic as well. One of the most dangerous failures in concrete structures is the shear failure owing to its rigid character. In this case inclined cracks are appearing on the side of the concrete beam, and the upper and the lower part of the structure start to be separated. Because of the above mentioned reasons it is really important to have a proper and accurate shear design.

In this article the available shear design formulas will be presented for FRP and for synthetic fibre reinforced concrete beams.

Keywords: FRP, synthetic fibre reinforced concrete, shear, non- metallic, design

1. INTRODUCTION

The shear and the punching shear failure is one of the most dangerous failure modes in all structural elements especially in reinforced concrete slabs and beams. The phenomena of the shear is complex, contains many different component (Balázs, 2010). During the shear failure of the reinforced concrete beams an inclined crack is appearing on the side of the concrete beam, and the beam start to separate along the crack. The mechanism can happened very quickly and sometimes there is no visible sign before the total failure. Because this failure mode is very rigid all the reinforced concrete standards (ACI, JSCE, Eurocode) have a different section for the shear design. These standards usually calculate the shear capacity of the concrete and the steel stirrups separately.

These standards specify the stirrups as they are made from steel and the formulas are only valid for steel as well. However, the synthetic reinforcements, such as fibre reinforced polymer (FRP) rebars and synthetic fibre reinforcement in concrete become a well-used alternative non- metallic reinforcement for concrete structures. The FRP bars are made from longitudinal fibres, usually glass, carbon and basalt, and from a thermoset or a thermoplastic resin. The fibres bear the load and the resin protects the fibres and transfers the loads to the fibres. Usually these bars have an orthotropic behaviour because of the manufacture. The process of the manufacture called pultrusion. The bars can used as main reinforcement and as stirrups also, but with using thermoset resin the bars cannot be bent after the manufacture procedure. With thermoplastic resin the bars can formed after the pultrusion as well with adding heat to the bar, however, the strength of the bar will be lower. Significant field for using FRP bars are the MRI rooms in hospitals, tramlines, where no magnetic material can be used. Also an alternative reinforcement can be the FRP bars in concrete roads and bridges where the electrolytic corrosion can be significant.

Synthetic macro polymer fibres became a well-used material in concrete structures at the second part of the 20th century. Similar to the steel fibres, this reinforcement must be added into the concrete until it will be equally mixed. The average length of the fibres is from 40 mm up to 60 mm and their material is usually polymer (olefin, polypropylene etc.). The fibres can increase the residual flexural strength of the concrete. In the literature a considerable amount of publication can be found about how the synthetic fibres can increase the shear capacity of the concrete elements (Li et al., 1992; Juhász and Schaul, 2015). The main territory of using synthetic fibres are the precast industry the industrial floors, the tunnels (shotcrete or TBM) and the tramlines- concrete railways.

Both of these synthetic reinforcements can increase the reinforced concrete elements' shear capacity, however there is no standard for the calculation method. In this article the formulas and recommendations will be presented which can help in the shear design of a synthetic reinforced concrete beams.

Fig 1: Principal compressive stress trajectories in a simple supported beam (Wight and Macgregor, 2012)

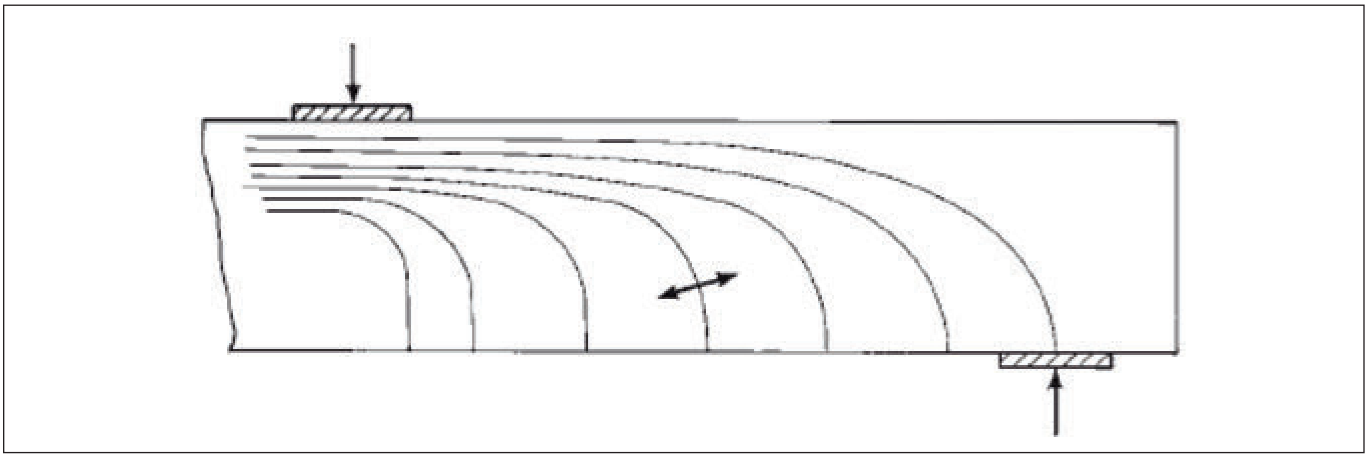

2. SHEAR IN CONCRETE STRUCTURES

The shear stresses are special tension stresses which always perpendicular to the direction of the principal compressive stress trajectories. These trajectories in a simply supported beam can be seen in fig 1. The crack pattern in a beam where only main reinforcements are follows the trajectory lines.

In a reinforced concrete beam the shear resistance comes from a contribution of several different effects.

2.1 Effect of the un-cracked compressive concrete zone

In reinforced concrete beams the depth of the compressive zone highly determines the shear resistance of the element. This part of the beam is un-cracked, therefore, the vertical forces can be transferred here.

2.2 Aggregate interlock

In the tensile zone, shear forces transfer across a crack by mechanical interlock, when the shear displacement is parallel to the direction of the crack (fig 2). Huge amount of scientific research tried to determine the contribution of the aggregate interlock to the full shear resistance. Some researchers questioned the existence of the effect (Völgyi et al. 2016) and some of them determined the contribution can be even 50% (Taylor, 1970). The vast majority of the articles locate the contribution between 33 and 50 % but with increasing the crack width this value can be reduce as well (Walraven, 1981).

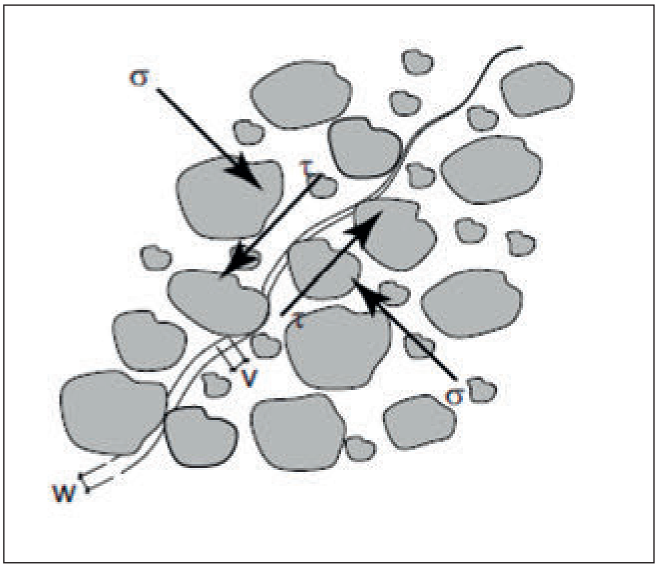

Fig 2: Mechanism of aggregate interlock (***fib*** Bulletin 40, 2007)

2.3 DOWEL ACTION

The dowel action is a combination of the tensile resistance of the concrete near to the flexural reinforcement and the bending and transverse shear resistance of the main reinforcement. According to the literature this shear component has the less contribution in the full shear resistance (Kotsovos, 1999).

2.4 Shear reinforcement

Shear links (stirrups), bent main reinforcement and fibre reinforcement can also take a contribution of a shear resistance of reinforced concrete beams. The bars bridge the two parts of the crack and can transfer the shear forces between the upper and the downer part of the crack. The most efficient bars are perpendicular to the crack. The fibre reinforcement can also increase the shear resistance by bridging the cracks. These small fibres with a randomly distribution can be effective independently of the place of the shear crack.

As it can see the determination of the shear resistance requires a lot of attention, the contribution of the different effects can change in beams with different geometry, main or shear reinforcements. The current standards try to simplify the shear mechanism, and summarize the different effect in a simple formula, which can be used for every reinforced concrete beam. One of the oldest explanations for reinforced concrete beams behaviour is the truss analogy. It says that the behaviour of a simply supported concrete beams is similar to a truss: the tension is carried by the flange members and the shear is carried out by the inclined compressed concrete trusses and by the shear reinforcement. This analogy is the base of the formulas in many standards, they calculate the shear resistance for the concrete and for the shear reinforcement as well. Some standards define the angle of the concrete truss in a specific value (Eurocode) and some of them give the opportunity of the determination to the designer. However, in a reinforced concrete beam these two effects can exist parallel, the codes allow to use only one of them (the concrete shear resistance or the reinforcement's shear resistance). Due to this the formulas have significant safety.

3. SHEAR DESIGN OF FRP REINFORCED CONCRETE BEAMS

The shear behaviour of the FRP reinforced concrete beams are similar to the traditional steel bar reinforced beams, because the mechanism is the same, just the material parameters are different. However, this different material parameters and material behaviours can change the contribution some of the shear components. The FRP bars' material behaviour can be considered as perfectly linear-elastic: the materials stress-strain relationship is linear up to the failure there is no plastic part of the diagram. This means the material's failure can occur without any visible sign, which make the proper design necessary. The elastic modulus of these bars is from 50 MPa (glass) to 220 MPa (carbon). From the shear components the effect of the compressive concrete zone changes most significantly. In FRP reinforced concrete (FRP RC) beams the area of the compression zone after cracking is smaller than the traditional RC structures because of the low elastic modulus. However, in case of traditional RC structures the depth of the neutral axis decreased significantly after the yield of the steel bars. This phenomenon is not happening in case of FRP bars because of the material behaviour, the depth of the neutral axis is monotone increasing after the first crack (fig 3).

Because of the low elastic modulus the cracks are larger in case of concrete beams with FRP bars than RC structures in the same load level, the effect of the aggregate interlock is smaller. Also because of t+P bars have a really low transversal stiffness, the dowel action is negligible (Kanakubo and Shindo, 1997). The effect of the shear reinforcement depends on the tensile strength of the material which is usually the yield strength of the steel bars. In case of FRP the maximal elongation and the bond between the bar and the concrete is more significant because of the linear- elastic material behaviour. Because of this usually the standards use the strain limit for FRP bars: the strains in the bars must be under a defined value.

The codes and the guidelines contain separate chapters for shear design of FRP bar reinforced concrete structures. These formulas usually the modification of the formulas for traditional RC structures, with taking into consideration the mentioned phenomenon.

3.1 ACI 440.1R (American Concrete Institute 440 Committee, 2015)

The formulas in the ACI recommendation are modifications for the shear formulas for RC structures according to the ACI 2005, but with using the maximum strain limit. The formula for concrete's shear resistance contains the effect of the FRP bars in the part of the calculating the depth of the compressive zone. The formula for concrete shear resistance with FRP main reinforcement is the following:

$$V_{cf} = 0.4\sqrt{f_c'}b_w c$$

where $c = k \cdot d$ for rectangular cross section

$$k = \sqrt{2\rho_f n_f + (\rho_f n_f)^2} - \rho_f n_f$$

where $\rho_f = \frac{A_f}{b_w d}$

A_f is the area of the FRP reinforcement

In the presented equations the b_w is the width of the cross section, d is the effective depth, and n_f is the ratio of the elastic modulus of the FRP and the concrete.

The contribution of the FRP stirrups is similar to the steel ones, but defining the tensile strength of the FRP bar as 0.004 E_f. The code defines also the minimum reinforcement ratio for FRP stirrups, as 0.35/0.004 E_f.

3.2 Italian National Research Council (CNR)

The Italian design specification (CNR-DT 204/2006) recommends a formula as a modification of CNR 2006 national de-

Fig 3: Depth of the neutral axis in terms of the longitudinal reinforcements' strain (*fib* Bulletin 40, 2007)

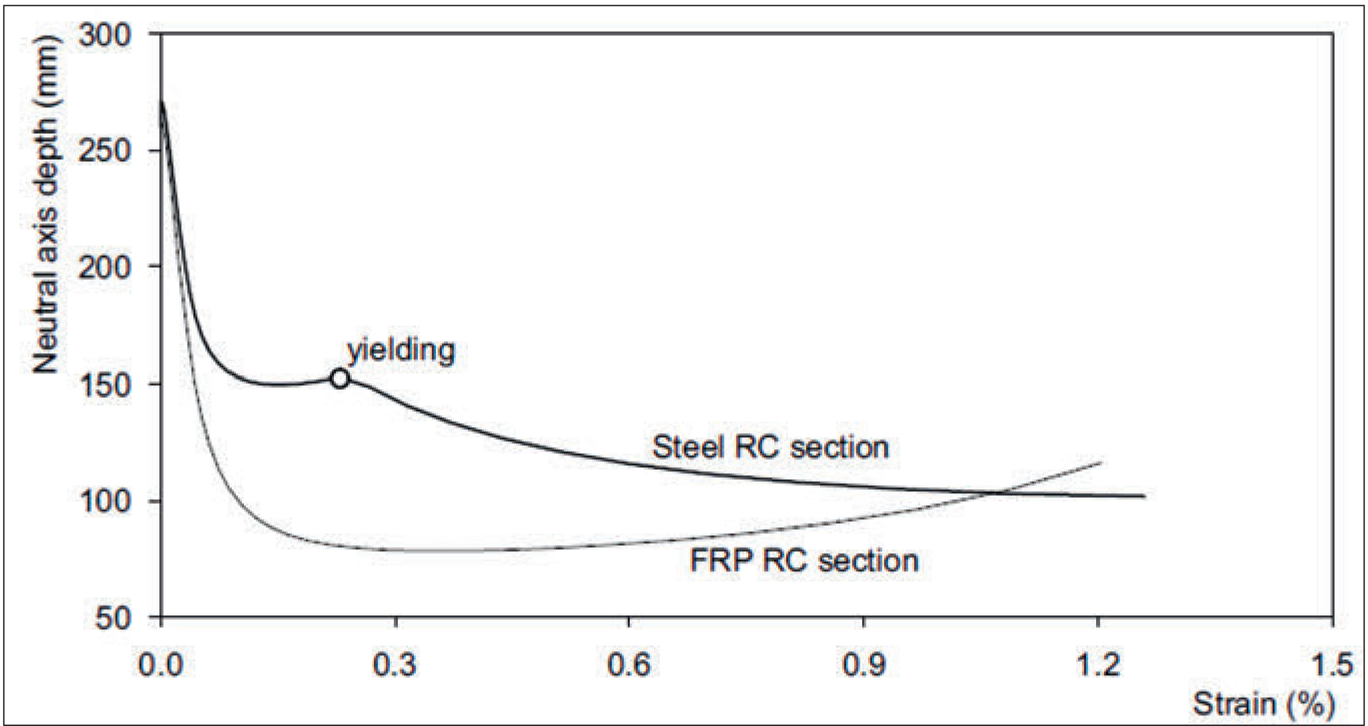

sign code, which based on Eurocode 2. The contribution of the concrete is modified by taking into consideration the FRP bars' axial stiffness as:

$$V_{cf} = 1.3 * \left(\frac{E_f}{E_s}\right)^{0.5} * \tau_{Rd} k(1.2 + 40\rho_f) b_w d$$

where ρ_f is the reinforcement ratio

The contribution of the FRP stirrups is similar to the steel shear links however there is a stress limit for the FRP bars, which is 50% of their design strength.

3.3 Design approach of Guadagnini et al. (2003) (Modification of EN 1992-1)

This recommendation based on the Eurocode 2 (European Committee for Standards, 2004) shear formula for calculating the shear resistance of the concrete with taking into consideration the ratio of the elastic modulus of the FRP and the steel bars.

$$V_{cf} = 0.12(1 + \sqrt{\frac{200}{d}})(100 \cdot \frac{A_f}{b_w d} \cdot \frac{E_f}{E_s} \cdot \phi_s \cdot f_{ck})^{1/3} b_w d$$

where E_f is the elastic modulus of the FRP, E_s is the elastic modulus of the steel bars, f_{ck} is the characteristic value of the concrete's compressive strength.

The formula for FRP stirrups uses the strain limit as well, it defined the maximum strain as 0.45%. The minimum reinforcement ratio for FRP stirrups can be calculated according Guadagnini et al. (2003) as:

$$0.08\sqrt{f_c'} \cdot \frac{1}{0.0045 \cdot E_f}$$

4. SHEAR DESIGN OF SYNTHETIC FIBRE REINFORCED CONCRETE BEAMS

The fibre reinforcement is a well-used material for shear strengthening, several recent studies show promising results with using steel fibre reinforcement (SFRC) as shear reinforcement (Kovács and Juhász, 2013). The added fibres increase the fracture energy of the concrete which makes the structure more ductile, and raise the residual flexural strength of the material. Because it was mentioned that the shear crack is a special type of the tensile cracks, the randomly distributed fibres can bridge the crack, and can transfer loads between the two parts. Also the fibre reinforcement decreases the crack width which helps to the aggregate interlock to be more efficient. The fib MC 2010 (***fib***, 2013) the RILEM (Dupont and Vandewalle, 2003) recommendation and many literature gives design formulas for steel fibre reinforcement as shear reinforcement, but there is no guidelines for synthetic fibre reinforced concrete structures. However in the literature several recent articles show (Li et al., 1992; Juhász and Schaul, 2015), that synthetic fibre reinforcement (SYFRC) can used as shear reinforcement as well. According to Yazdanbakhsh et al. (2015) the fib and the RILEM formulas can lead to proper results with SYNFRC as well, and with these the synthetic fibre reinforced concrete shear resistance can be calculated.

4.1 *fib* MC2010 (*fib*, 2013)

The Model Code 2010 (***fib***, 2013) defines the fibre reinforced concrete beam with longitudinal reinforcement by adding the effect of the fibre reinforcement to the concrete's shear resistance:

$$V_{frc} = 0.18(1 + \sqrt{\frac{200}{d}})(100 \cdot \frac{A_f}{b_w d} \cdot (1 + 7.5\frac{f_{Ftuk}}{f_{ctk}}) \cdot f_{ck})^{1/3} b_w d$$

where f_{ctk} is the characteristic value of the concrete's tensile strength

$$f_{Ftu}(w_u) = f_{Fts} - 0.5 * f_{R3} + 0.2 f_{R1} \tag{1}$$

In equation (1) the w_u=1.5mm and the f_{Fts}=0.45f_{R1}. The f_{R1} and f_{R3} values are the residual tensile stress values at Crack Mouth Opening Distance (CMOD) stage 0.5 mm and 2.5 mm reprehensively. These values can measure from three point bending beam tests according to RILTEM TC 162 (2003)

4.2 RILEM

The formula (Dupont and Vandewalle, 2003) was developed at the beginning of the 21th century to present a simple tool with a huge amount of safety for SFRC structures. During the years the formula modified, but the original one gives better correlation for synthetic fibre reinforced concrete beams

The shear resistance of a SYFRC beam can be calculated by summarize the shear capacity of the concrete and the added shear resistance by the fibres.

$$V_c = 0.15 \cdot \sqrt[3]{3(\frac{d}{a})} \cdot k(100 \cdot \rho \cdot f_c')^{1/3}$$

$$V_{SYF} = \frac{1600 - d}{1000} \cdot 0.5\frac{d}{a} f_{e,3}$$

$$V_{frc} = V_c + V_{SYF}$$

where a is the shear span, ρ is the reinforcement ratio, $f_{e,3}$ is the equivalent flexural strength

5. SHEAR DESIGN OF SYNTHETIC FIBRE REINFORCED CONCRETE BEAMS WITH FRP BARS

The combination of using FRP bars as longitudinal reinforcement and synthetic fibre reinforcement as shear reinforcement can be an alternative solution for traditional reinforced concrete where the conditions require the non-corrosively of the reinforcement. In the standards, guidelines or codes are not a design formula for these structures. However, according to the mentioned literature the shear resistance of a synthetic fibre reinforced concrete beam with longitudinal FRP reinforcement and without stirrups can be estimate as follows:

$$V_{frc,f} = 0.12(1 + \sqrt{\frac{200}{d}})(100 \cdot \frac{A_f}{b_w d} \cdot \frac{E_f}{E_s} \cdot \phi_s \cdot (1 + 7.5\frac{f_{Ftuk}}{f_{ctk}}) \cdot f_{ck})^{1/3} b_w d \tag{2}$$

However, this equation must be verified by laboratory tests, it can be a good opportunity to predict analytically the shear resistance of a non- corrosive reinforced concrete beam. The formula takes into consideration the ratio of the FRP and steel material, and the additional shear capacity from synthetic fibre reinforced concrete as well. The base of Eq. (2) is the shear resistance formula for FRP reinforced concrete beams according to Guadagnini at all and the ***fib*** MC2010 shear resistance formula for steel fibre reinforced concrete beams.

6. CONCLUSIONS

The shear failure of reinforced concrete beams is one of the most complex failure modes, where inclined crack disconnect the upper and the lower part of the beam. The shear resistance of reinforced concrete beams depends on several different effects such as effect of the compressed concrete zone the aggregate interlock, the dowel effect and the effect of the shear reinforcement. The contribution of these effects depends on many parameters, such as beam geometry, reinforcement ratio type of shear reinforcement, and also has an impact on each other.

Standards, codes and guidelines specify the shear resistance for steel reinforced concrete beams and steel fibre reinforced concrete beams as well. For non- corrosive materials, such as FRP bars or synthetic fibre reinforced concrete elements the literature recommend formulas to calculate the shear resistance. These formulas are basically the modification of the shear capacity equations for traditional steel reinforced concrete.

With merging the different formulas for FRP reinforced concrete beams and for SYFRC beams the shear capacity of the synthetic fibre reinforced concrete beam with longitudinal FRP reinforcement can be estimate according to Eq (2). The formula summarizes the effect of the FRP bars to the concrete's shear resistance, and the additional shear capacity of synthetic fibre reinforcement.

Structures with FRP bars and with synthetic fibre reinforcement are more and more frequent in modern constructions, the development of a proper analytical model for shear resistance became necessary.

With this overview and our future work we intend to contribute in the development of a proper and precise analytical model for shear capacity of concrete beams with non- metallic reinforcement.

7. REFERENCES

ACI (2015): ACI 440.1R-15: Guide for the Design and Construction of Concrete Reinforced with FRP Bars

Advisory Committee on Technical Recommendations for Construction (2006): "CNR-DT 204/2006: Guide for the Design and Construction of Fibre-Reinforced Concrete Structures"

Balázs, G. L. (2010), „A historical review of shear", in fib Bulletin 57 "Shear and punching shear in RC and FRC elements", ISBN 978-2-88394-097-0, pp. 1-10

European Committee for Standards: (2004)" Eurocode 1992-3: Design of Concrete Structures – Part 3" 6.2. Shear

Dupont D. and Vandewalle L. (2003): "Shear capacity of concrete beams containing longitudinal reinforcement and steel fibers" in ACI Special Publ. **216** pp. 79–94.

fib (2013): "*fib* Model Code for Concrete Structures 2010", Ernst & Sohn Wiley, ISBN 978-3-433-03061-5

fib Task Group 9.3. (2007): "fib Bulletin 40 – FRP reinforcement in RC structures", Sprint-Digital-Druck, ISBN 978-2-88394-080-2

Guadagnini, M., Pilakoutas, K. and Waldron, P. (2003): "Shear Performance of FRP Reinforced Concrete Beams", Journal of Reinforced Plastics and Composites, **22**(15), pp. 1389-1408.

Juhász, K.P, Schaul, P. (2015):"Shear behaviour of synthetic fibre reinforced concrete beams reinforced with FRP rebars" Proceedings of 11th CCC Congress, Hainburg, 2015, pp.42-46.

Kanakubo, T., and Shindo, M. (1997): "Shear Behaviour of Fiber-Mesh Reinforced Plates", Third International Symposium on Non-Metallic (FRP) Reinforcement for Concrete Structures, Sapporo, Japan, pp. 317-324.

Kotsovos, M. D., and Pavlovic, M. N. (1999): "Ultimate Limit State Design of Concrete Structures -A New Approach", Thomas Telford, Ltd., London, UK.

Kovács G. and Juhász K.P. (2014): "Synthetic and steel fibres in prestressed, precast long span beams", in: Proceedings of CCC 2014, Concrete Offers for Period of Economic Recovery. Liberec, Czech Rep. 2014.

Li V.C, Ward R, Hamza A.M. (1992): "Steel and synthetic fibers as shear reinforcement" ACI Material Journal **89** pp. 499–508.

Rilem TC. 162-TDF (2003): "Test and design methods for steel fibre reinforced concrete, σ-ε design method" (ed.: Chairlady L. Vandewalle). Mater Structures **36** pp. 560–567.

Taylor, H. P. J. (1970): "Investigation of the Forces Carried Across Cracks in Reinforced Concrete Beams in Shear by Interlock of Aggregate", 42.447, Cement and Concrete Association, London, UK.

Vecchio, F.J. and Collins, M.P. (1986): "The Modified Compression-Field Theory for Reinforced Concrete Elements Subjected to Shear" ACI Journal, Title no.83-22.

Völgyi, I. and Windisch, A., (2016): "Contribution of aggregate interlock to the shear resistance of RC beams", in press

Wight, J.K., and Macgregor, J.G. (2012):Reinforced concrete : mechanics and design - 6th edition. ISBN-13: 978-0-13-217652-1

Walraven, J. C. (1981): "Fundamental Analysis of Aggregate Interlock, Journal of the Structural Division", Proceedings of the American Society of Civil Engineering **107** (No. ST11), pp. 2245-2269.

Yazdanbakhsh, A., Altoubat, S. and Rieder K.A. (2015):"Analytical study on shear strength of macro synthetic fiber reinforced concrete beams" in Engineer Structures **100**, pp. 622-632.

Péter Schaul (1989), Civil Engineer, PhD student (Department of Construction Materials and Technologies, Budapest University of Technology and Economics). His main fields of activities are experimental investigation and modelling of FRC and FRP structures, finite element modelling of concrete structures. Structural engineer at JKP Static Ltd. schaul.peter@epito.bme.hu

György L. Balázs (1958), Civil Engineer, PhD, Dr.-habil., professor of structural engineering, head of Department of Construction Materials and Technologies and Deputy Dean of the Civil Engineering Faculty of Budapest University of Technology and Economics (BME). His main fields of activities are experimental investigation and modelling of RC, PC, FRC structures, HSC, fire resistance of concrete. He is chairman of several commissions and task groups of fib. He is president of Hungarian Group of ***fib***, Editor-in-chief of the Journal "Concrete Structures". He was elected as President of ***fib*** for the period of 2011-2012. balazs.gyorgy@epito.bme.hu

POSSIBILITY OF PRODUCING GREEN, SELF-COMPACTING, HIGH PERFORMANCE CONCRETE (GSCHPC) – REVIEW

Mohammed Abed – Rita Nemes

The trend of producing green concrete, utilizing the waste of construction with maintaining a sustainable environment is one of the most critical challenges in the construction industry. The possibilities in concrete technology are developing in two main directions: green concrete (i.e. using recycled or waste raw material and decreased cement content, or limitation of raw material transport distance) and high performance concrete (i.e. with high strength and high durability). This paper reviews and discusses some of the most recent novelties of using recycled concrete aggregate and supplementary materials instead of a specific amount of natural aggregate and cement respectively, as raw material for producing green concrete with special properties and specifications. The intent herein is an intensive literature review of the possibility of producing green, self-compacting, high performance concrete GSCHPC, by using recycled aggregate and different supplementary materials. The advantages in the utilization possibilities in making improvements through: (I) green concrete (GC) to reduce the usage of raw materials, (II) high performance concrete (HPC) to reduce the needed amount of concrete (III) self-compacting concrete (SCC) to reduce the construction mistakes and environment noise pollution. The results proved that, different waste materials effect the mechanical properties, the durability and the microstructural properties of concrete, depending on the dosage of these materials the mixing and some other factors.

Keywords: recycling, sustainability, supplementary materials, green concrete, GC, HPC, SCC, compressive strength, durability

1. CHALLENGES

It has been observed that concrete is the second material, which is used by people on our planet after freshwater (it is one of the most widely used building material with a global consumption rate approaching 25 gigatons (Gt) per year). This is a good and simultaneously also a bad information; good because of the fact, that thanks to concrete we are able to build solid and sustainable structures making our life easier and better, bad because making concrete is connected with huge energy consumption and high emission of greenhouse gases (Błaszczyński and Król 2015; Long, Gao and Xie 2015).

One of the frequent phenomenon today in a large part of the world is the demolition of concrete structures such as; old and deteriorated buildings and traffic infrastructure, followed by their substitution with new ones. There are a lot of justifications and reasons for this situation such as; changes of purpose, structural deterioration, rearrangement of a city, expansion of traffic directions and increasing traffic load, natural disasters, wars…etc (Malešev, Radonjanin and Marinković 2010; Guo et al. 2014).

The most common method of managing this material is through disposal in landfills. In this way, gigantic deposits of construction wastes are created, what consequently becomes a special problem of human environment pollution. For this reason, in developed countries, laws have been brought into force to restrict the amount of such waste in the form of prohibitions or special taxes are existing for creating landfill areas (Tabsh and Abdelfatah 2009; Butler, Tighe and West 2013).

The amount of waste materials has gradually increased with the increasing of population and urban development. Various strategies have been followed, separately or in combination to improve the sustainability of concrete, to develop green or more ecological concrete (Kubissa et al. 2017), solving the increasing waste storage problem, and the protection of limited natural resources of aggregates (Mohammadhosseini and Yatim 2017). According to (Guo et al. 2014) the advantages of recycled materials include reducing environmental pollution, reducing landfilling and preserving natural resources.

We are in the era of prosperity and progress, and as one of the requirements of this era is the compliance under the banner of clean technology. The major targets which are related to cleaner technologies in order to produce concrete (Suhendro 2014):

- Reduced CO_2 emission,
- Optimized mix design,
- Reduced energy consumption or fuel derived from fossil in cement manufacturing process,
- Reduced the substances that can endanger health or the environment such as the use of several types of chemicals in concrete mixtures., with fly ash in higher portion or the usage of other waste,

- Using new cement replacement materials, such as inorganic polymers, alkali-activated cement, magnesia cement, and sulfoaluminate cements.
- Utilizing the possibilities of using recycled cement/concrete and the use of alternative aggregates,
- Increasing the durability of concrete to extend its service life and to reduce long-term resource consumption,
- Selecting low impact construction methods,
- Other significant contribution policies.

There is no doubt that cleaner and more efficient management of various forms of waste generation is receiving more attention in order to maintain sustainability in green construction. The utilization of waste materials is one of the fundamental issues of waste management strategies in several parts of the world (Mohammadhosseini and Yatim 2017).

2. GREEN CONCRETE

The construction industry is one of the most industries that affected by the ongoing sustainability debate, primarily in order to the obvious environmental impact resulting from the production of building materials, the constructions of buildings and structures and the subsequent use thereof. (Mueller, et al. 2017).

Green concrete (environmental friendly concrete) is defined as a concrete which uses waste material as at least one of its components, or its production process does not lead to environmental destruction, or it has high performance and life cycle sustainability without destructing natural resources (Suhendro 2014).

Green concretes, also termed as eco-concretes, with reduced cement content may provide an alternative for improving concrete sustainability independently from the used supplementary materials. However to evaluate the sustainability of these new types of concretes, not only the ecological impact due to the composition may be considered, but in particular also their technical performance, i.e. their mechanical, physical and chemical properties, have to be taken into account (Mueller, et al. 2017).

Carbon dioxide is being produced from two main sources: natural and anthropogenic. The natural source was here on earth from the beginning, but our planet was dealing with it very well. The anthropogenic source is the real problem (Błaszczyński and Król 2015).

About 10% of total man-made CO_2 which is emitted into the atmosphere (which is believed to be the main driver of global climate change), did not come from the polluting vehicles on the highways or forest fires, but from cement manufacturing process in cement factories and its transportation (Long, Gao and Xie 2015).

Global warming gas is discharged when the raw the materials of cement, limestone and clay is crushed and heated in a furnace at high temperature (ca.1500°C). Each year, approximately 1.89 billion tons of cement (which is a major component of concrete) has been produced worldwide (Suhendro 2014).

The footsteps of the researchers for producing more sustainable and greener concrete are mainly through utilizing waste materials, either construction or industrial waste. There are many researches for using waste materials for producing green concrete. Mainly these investigations deal with the influence of using recycled materials instead or as a proportion of aggregate or cement. *Fig. 1* below shows the trend of utilization of waste materials for producing green concrete.

2.1 Less natural stone

In recent years, concrete made with recycled aggregate is considered as one of the most promising solution to reduce the amount of construction and demolition waste that may end up in landfills. The amount of construction and demolition waste has increased considerably in line with increased construction activities and due to the demolition and restoration of old buildings (Jitender and Sandeep 2014).

Since waste is gradually increasing with the increase of population and increasing of urban development, the research work on the recycling of waste construction materials has become one of the key requirements of today's concrete (Malešev, Radonjanin and Marinković 2010).

Fig. 1: The trend of utilization of waste materials for producing green concrete

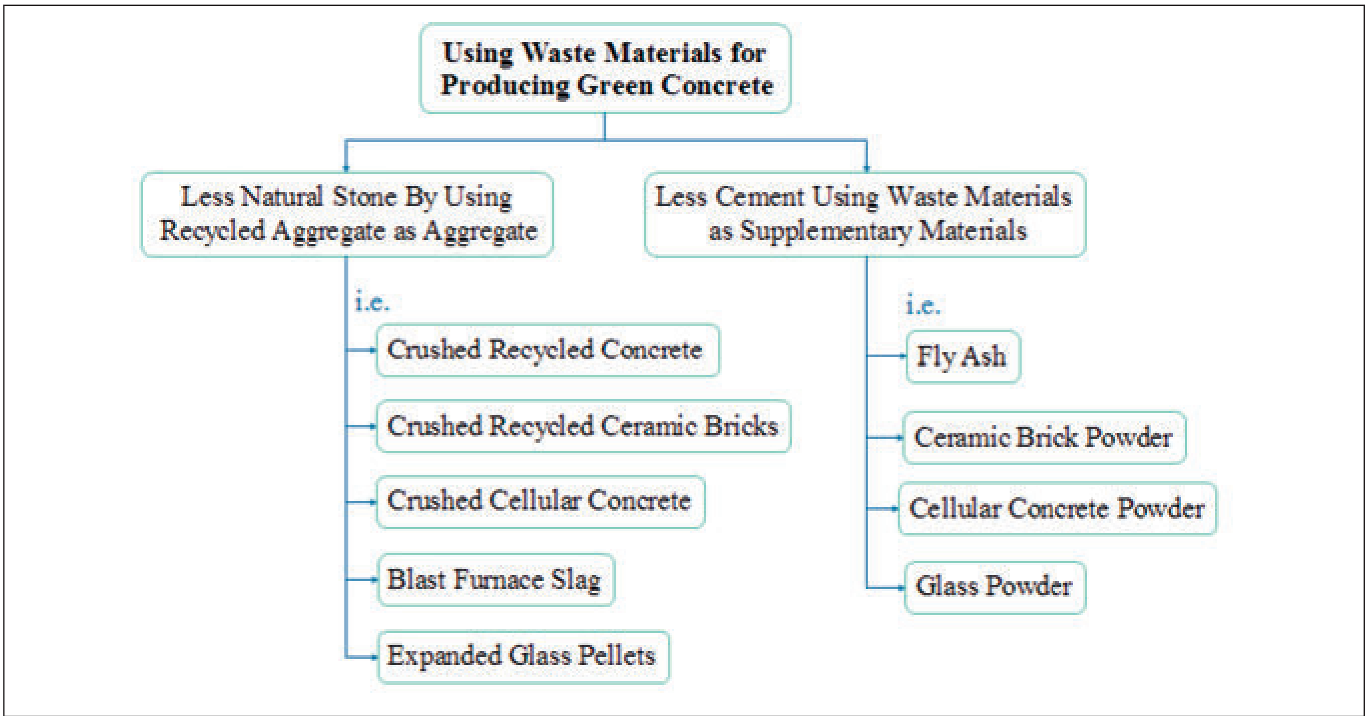

The volume of aggregate in concrete is the largest part of concrete mixture (approximately 70% of its total volume). This was a catalyst to increase the attention of using recycled aggregate as a proportion of natural aggregate to preserve a more sustainable environment (Jitender and Sandeep 2014).

A wide range of recycled aggregates have been steadily introduced in several civil engineering and construction applications as a partial replacement of natural aggregates due to their environmental benefits and meanwhile easiness to obtain them at a lower cost than "virgin" aggregate (Jitender and Sandeep 2014).

A large difficulty is that, most of the results, which were found by researchers, are not comparable due to the heterogeneity of the used recycled aggregates, water/cement ratios and types of cements (Thomas, et al. 2013).

2.1.1 Crushed recycled concrete

Reuse of aggregates from demolished concrete structures was introduced into practice many years ago. From the beginning, two main environmental aspects have been considered: solving the increasing waste storage problem and protection of limited natural resources of aggregates (Malešev, Radonjanin and Marinković 2010).

Many studies applied the concept of utilizing concrete waste as a recycled aggregate for producing new concrete, with using different replacement ratios of natural and recycled aggregate, starting with 10% up till 100%. There are many crushing methodologies used to crush concrete waste to different particles sizes, producing two types of aggregate; fine aggregate (under 4 mm in diameter) and coarse aggregate (over 4 mm). *Fig. 2* shows the methodology (Fan, et al. 2016) for crushing concrete waste to produce fine and coarse aggregate simultaneously.

Comparative analysis have been presented for many experimental results by researchers to show the effect of using recycled aggregates (fine, coarse, or both) on the properties of fresh and hardened concrete, offering results regarding the properties such as, mechanical, durability, macrostructural, and microstructural.

The basic properties of concrete with recycled concrete aggregate is mainly affected by the properties of the recycled aggregate, i.e. a certain amount of mortar or cement paste from the original concrete remains attached to stone particles in recycled aggregate when the concrete waste is crushed is the main reason for the lower quality of some properties of recycled aggregate concrete compared to those with natural aggregate (Malešev, Radonjanin and Marinković 2010).

Table 1 shows the most important properties of recycled concrete aggregate and concrete made with recycled aggregate based on available experimental evidence from researches, which used different percentages of recycled aggregate and investigated their effect on the properties of concrete.

It is important to notice that the decrease of water absorption depends on the porosity of cement matrix in the recycled concrete, the workability not affected by the recycled aggregate quantity but by the shape of the aggregate: If they have the same water content, the compressive and tensile strength depend mainly on the quality of recycled aggregate, and the bond between recycled aggregate concrete and the reinforcements is not affected, since it is realized through new cement paste. According to these tests results, the performance of recycled aggregate concretes, even with the total replacement of coarse natural aggregate with coarse recycled aggregate, is mainly satisfactory, not only in terms of the mechanical properties, but also the other requirements which are related to mixture proportion design and production of this concrete type. Nevertheless, due to the remarkable decrease of modulus of elasticity and shrinkage deformation; it is not recommended to apply this type of concrete for structural elements since large deformations can be expected. The effect of the

Fig. 2: A methodology of crushing concrete waste for producing fine and coarse aggregate simultaneously by Fan et al. (2016)

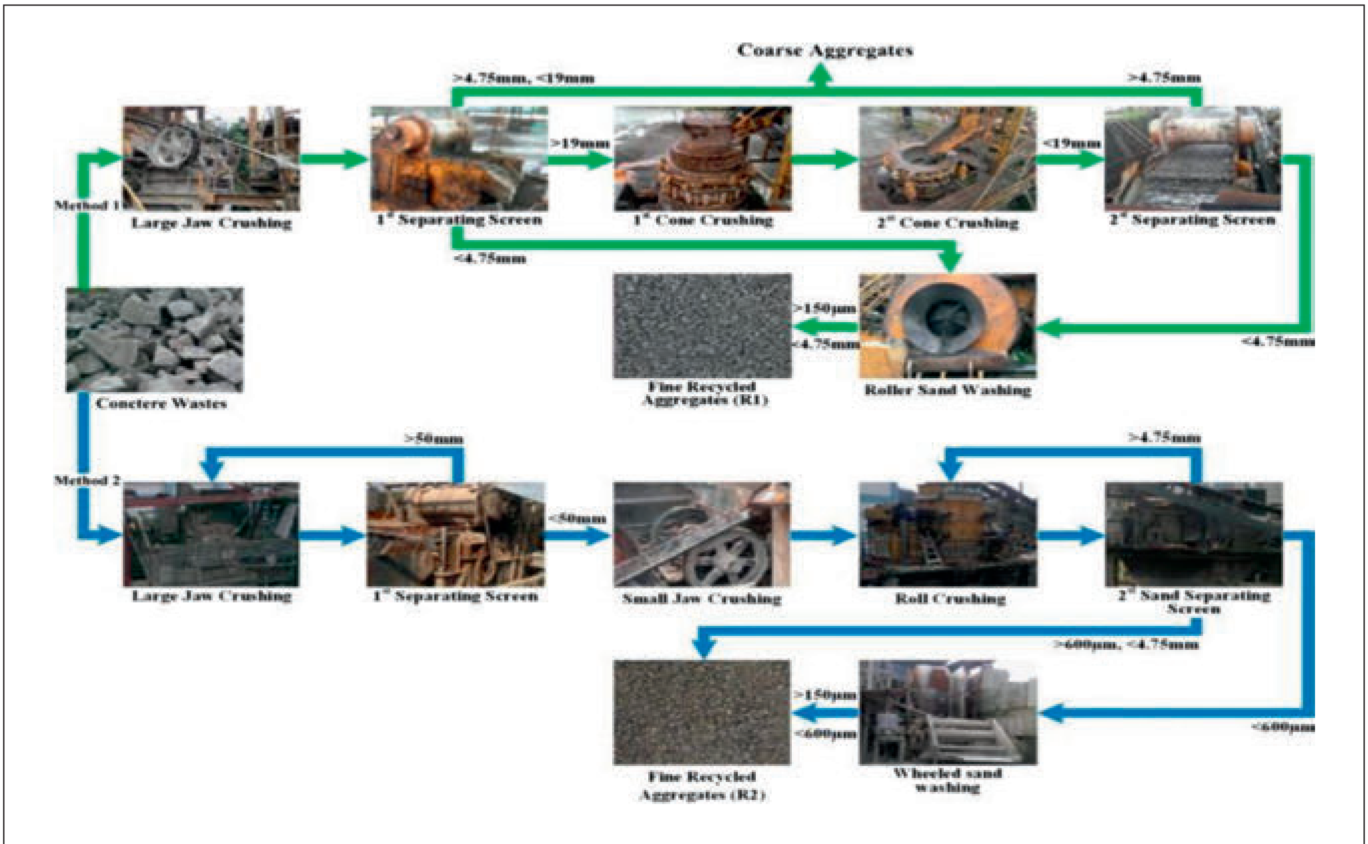

Table 1: *The effect of recycled concrete aggregates in concretes*

Properties	Effect of increasing the recycled aggregate	(Malešev, Radonjanin and Marinković 2010)	(Rahal 2007)	(Evangelista and Brito 2007)	(López-Gayarre, et al. 2009)	(Pavlu, Boehme and Hajek 2014)	(Ajdukiewicz and Kliszczewicz 2002)	(Jitender and Sandeep 2014)	(Tabsh and Abdelfatah 2009)	(Butler, Tighe and West 2013)	(Gómez-Soberón 2002)	(Olorunsogo and Padayachee 2002)	(Poon, et al. 2004)	(Topcu and Şengel 2004)
water absorption	**increase**	√			√			√	√	√	√		√	√
density	**decrease**	√		√				√		√	√			
specific gravity	**decrease**			√	√			√			√			√
abrasion resistance	**decrease**			√						√	√	√		
crushability	**increase**							√	√					√
workability	**not affected**	√			√	√							√	√
compressive strength	**decrease**	√	√	√	√	√	√	√	√				√	√
concrete tensile strength	**decrease**	√		√		√	√	√	√					√
wear resistance	**decrease**	√							√	√	√	√		
modulus of elasticity	**decreases**	√	√	√	√			√						
shrinkage	**increase**	√					√				√			
bond with reinforcement	**not affected**	√					√							

porosity is one of the major factors, which has to be taken into consideration during the design and production of durable concrete. The following four steps summarize the design considerations to minimize the pore content: (I) recycled concrete should be water saturated, (II) by small water/cement ratio plasticizer should be applied, (III) detect the airspace-volume in recycled aggregate and (IV) use an optimal duration of vibration (Pankhardt, Nehme, 2002).

2.1.2 Crushed recycled ceramic bricks

Using crushed ceramic bricks either as fine or course aggregate is studied by many researchers, they found that it is accepted with specific amount of replacement, depending on the type of the structure and the type of targeted concrete. The density of crushed brick concrete is lower than natural aggregate concrete, often under 2000 kg/m^3, so it is a lightweight concrete. The lower dead load, especially structures in bending results lower material consumption. *Fig. 3* shows concrete specimen with 100% crushed recycled ceramic bricks.

Debieb and Kenai (2008) studied the possibility of using crushed brick as coarse and fine aggregate for new concrete by partially replacing the natural sand, coarse aggregates or both with crushed brick aggregates. Their test results indicated that it is possible to manufacture concrete containing crushed bricks (course and fine) with characteristics similar to those of natural aggregates concrete if the percentage of recycled aggregates is limited to 25% and 50% for the coarse and fine aggregates, respectively.

Kenéz at al. (2014a) found in case of partial crushed brick aggregate concrete that the higher amount of natural sand as fine aggregate increase the compressive strength, but only to a limit. It is favorable, because in case of normal crushing process about 60% of the original material under 4 mm diameter is produced.

The using of crushed ceramic brick in concrete has an other advantage; this is the internal curing effect (Suzuki at al. 2009). The brick particle has high water absorption capacity and the water absorption rate is high, but the water loss is slow. As such, curing became good, but resulted in short time fresh concrete workability.

Adamson, Razmjoo and Poursaee (2015) studied the impact of partial replacement of natural coarse aggregates with crushed brick on the durability of concrete, and they found that the natural coarse aggregates could be replaced by crushed bricks, without significant change in the durability, when steel is not present as reinforcement. Moreover (Kenéz at al. 2014b) conclude that with appropriate concrete technology we can arrive to high performance concrete with 50 MPa compressive strength.

Table 2 summarizes the results of the effect of using crushed bricks as aggregate on the properties (compressive strength, flexural strengths, Porosity, water absorption, water permeability and shrinkage) of the concrete with those of

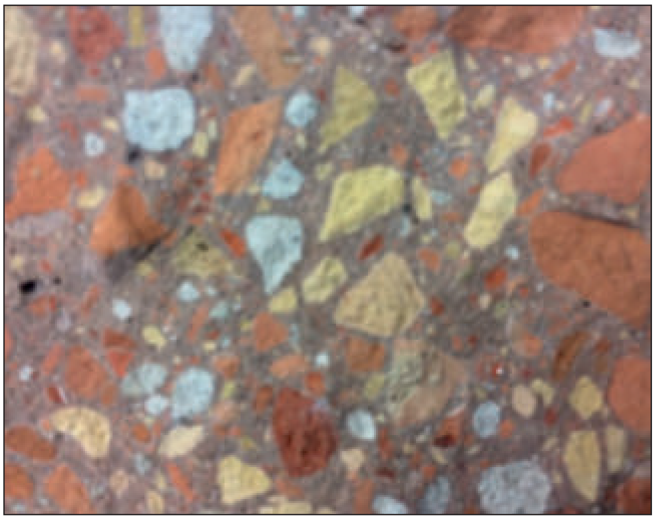

Fig. 3: Concrete specimen with 100% crushed recycled ceramic bricks

concretes mixed with natural aggregates. (Debieb and Kenai 2008; Adamson, Razmjoo and Poursaee 2015; Jankovic, Nikolic and Bojovic 2012; Vieira, et al. 2016; Jian, Qiang and Yiwang 2011; Kannan et al. 2017; Nemes, Török 2014)

2.1.3 Crushed cellular concrete

Crushed cellular concrete (similar to crushed ceramic brick) can be used as lightweight aggregate. (Fenyvesi, Jankus, 2015) found that the bond between cement matrix and cellular concrete aggregate is good, the density of the concrete with crushed cellular concrete aggregate is under 1800 kg/m^3, and the compressive strength is under 30 MPa. It is an environmentally friendly possibility, but first of all for internal usage and concretes for new masonry or ceiling elements.

2.1.4 Blast furnace slag

Blast furnace slag is obtained by quenching molten iron slag arising from a blast furnace in water or steam, to produce a glassy, granular product, which is dried. Blast furnace slag is a byproduct and using it as aggregate in concrete might prove an economical and environmentally friendly solution in local regions. The demand for aggregates is increasing rapidly, as the demand of concrete. Thus, it is becoming more important to find suitable alternatives of aggregates in the future. The results showed that it has properties, which are similar to natural aggregates and it would not cause any harm if incorporated into concrete. They show that, the usage of blast furnace slag as coarse aggregate in concrete has no negative effects on the short term properties of hardened concrete (Hiraskar, Patil 2013).

2.1.5 Expanded glass pellets

Under several different names are manufacture pellet products from industrial waste material having high glass content by recycling technologies. The waste glass materials may have organic and inorganic impurities. Waste materials of high glass content are ground to an appropriate particle diameter. Homogenization is carried out with a blowing agent dosed according to the amount of impurities in the raw materials. Granulation process is carried out by adding melting point reducer and viscosity modifying agents. The granulate is heat cured and coated to decrease its water absorption. Firing is carried out in a rotary furnace. The product is a lightweight artificial gravel with a diameter of 1 to 25 mm. This product has good bond capability if embedded in gypsum, cement or resin matrix. The obtained concretes are typical lightweight concretes, the achievable compressive strength is around 60 MPa. The use of expanded glass pellets is favourable from economical and environmental point of view (Józsa, Nemes 2002; Nemes, Józsa 2006).

2.2 Less cement

Cement primary is the most expensive component of concrete mixture and major ingredient among the concrete mixture ingredients, the production emits carbon dioxide. Partial or full replacement of cement is considered a sustainable solution toward decreasing the environmental impact of cement production and will also contribute to sustainable concrete.

The typical supplementary cementations materials are the silica fume (or silica slurry) and metakaolin. Usage of these supplementary materials leads to increasing compressive strength and durability (water absorption, water tightness, air permeability, chloride ion migration, freeze/thaw resistance, damage by acidic solutions, abrasion resistance) of concrete (Borosnyói, 2016). These materials have puzzolanic reaction, which in combination with cement can achieve a reaction with CH from cement. The C-S-H from supplementary material is similar to C-S-H from cement only. The industrial production, morphological properties and the influences of metakaolin to

Table 2 The effect of crushed ceramic brick aggregate in concrete

Properties	Effect of increasing the recycled crushed ceramic aggregate concrete
water absorption capacity	increase
density	decrease
segregation	increase
compressive strength	decrease
flexural tensile strength	decrease
modulus of elasticity	decrease
shrinkage	increase
water permeability	increase
workability	increase
resistance to chloride penetration	decrease
resistance to freeze/thaw tests	increase
bond with reinforcing	not affected
corrosion of the reinforcing steel bars	increase

concrete properties are summarized by (Kopecskó, Mlinarik 2014). In case of partial supplementary material use instead of cement, the introduction of water-binder ratio is necessary, instead of the original water-cement ratio: water/(cement + *k* * SCM). The value of *k* is in relationship with the water-cement ratio and the compressive strength of concrete. Lot of types of metakaolin and silica fumes has defined this k value (Borosnyói, Szijártó, 2016). There is a maximum value of metakaolin or silica fume dosage, because of these materials use the portlandit from cement matrix (Mlinárik, Kopecskó, 2013 and 2017). If we combine silica fume and metakaolin no better properties can be achieved than the usage of only one of them (Borosnyói, 2015).

Originally silica fume is a by-product of producing metal alloys, but the good quality silica powder is produced directly for concrete technology using high energy consumption. Metakaolin can also be a by-product of manufacturing bricks, but the main part of the used metakaolin is produced directly for SCM. The temperature of producing metakaolin is 650-800°C, it is lower than the temperature of cement production.

Many waste materials and industrial by-products have been used as supplementary materials partially instead of cement for this purpose; they show variant possibilities of improvements. Some of these materials are fly ash, perlite, blast furnace slag, ceramic brick powder and cellular powder. It is important to increase the strength of concrete with SCM but there is a need of longer curing time (Nehme, 2015).

2.2.1 Fly ash

Fly ash has been commonly used as mineral supplementary material to partially replace Portland cement in normal, high performance, and high-strength concrete. Increased usage of industrial by-products leads to a decrease of CO_2 emission and energy consumption (Hu 2014).

Hu 2014; Nath and Sarker (2011) investigated the impact of using fly ash on the properties of Portland cement and they conclude their findings by the positive contribution of fly ash on the compressive strength and durability properties, also they conducted the microstructural analysis and found that using fly ash accelerate the puzzolanic activity to produce more C–S–H gel. All of these improvements that fly ash provided, depend mainly on the optimum amount of the used fly ash.

Yazıcı (2008) showed that using fly ash with optimum amount as a supplementary material for cement does not only improve the properties of normal concrete but also offers self-compaction and high performance of concrete.

There are no big differences between the chemical components of fly ash types (depending on the resource of fly ash) however there is some disparity on the fly ash impact on the properties of concrete. *Table 3* shows the chemical components of cement and fly ash.

The compressive strength, drying shrinkage, absorption and rapid chloride permeability of the fly ash and control concrete specimens were determined by (Kou, Poon and Chan 2008; Nath and Sarker, 2011). Especially in case of high strength concrete they found that fly ash reduces the absorption, decreases drying shrinkage, and give better resistance to chloride ion penetration.

As showed above; the positive effect of fly ash as a partial replacement of cement on the durability of concrete is recognized through numerous researches; however, the extent of improvement depends on the properties of the fly ash. The activation of fly ash strongly depends on relative surface. The relative surface can be increased effectively with grinding (Mucsi, 2016). Eventually the quality of fly ash is very different and long time storage decreases the possibility of the hydraulic reaction.

2.2.2 Ceramic brick powder

Kannan et al. (2017) showed that high performance concrete mixtures incorporating up to 40% ceramic waste powder as large partial replacement of cement can be produced with high strength and excellent durability performance, and they recommended to producing high performance concrete because it is an excellent source for recycling large quantities of ceramic waste powder, *Fig. 4* shows the chemical analysis of ceramic brick powder.

Kulovana et al. (2016) tested Portland cement with ceramic brick powder. Blended Portland cement-ceramic powder binder containing up to 60% fine-ground waste ceramics from a brick factory is used in concrete mix design as an environmentally friendly alternative to the commonly used Portland cement. The experimental analysis of basic physical characteristics, mechanical and fracture-mechanical properties, durability properties and hydrothermal characteristics shows that the optimal amount of ceramic powder in the mix is 20 % of the mass of blended cement. The decisive parameters in that respect are compressive strength, liquid water transport parameters and resistance to de-icing salts, which are not satisfactory for higher ceramics dosage in the blends.

Fig. 4: Chemical analysis of ceramic brick powder (Kannan et al. 2017)

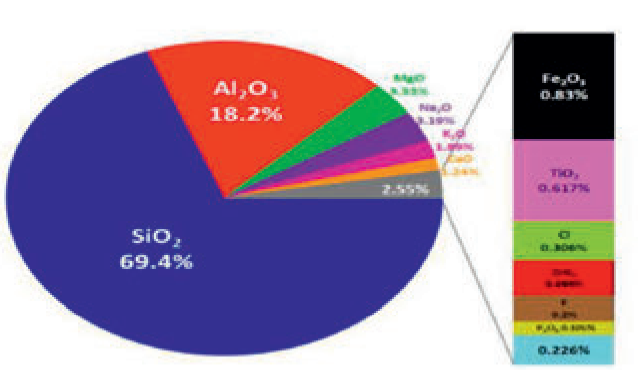

Table 3: The chemical components of cement and fly ash (Nath and Sarker, 2011).

Parameter	SiO_2	Al_2O_3	Fe_2O_3	SiO_2+Al_2O_3 +Fe_2O_3	CaO	MgO	SO_3	K_2O	Na_2O	P_2O_5	Chloride	Loss on ignition
Cement (%)	21.10	4.70	2.70	28.50	63.60	2.60	2.50	-	0.50	-	0.01	2.00
Fly ash (%)	50.50	26.57	13.77	90.84	2.13	1.54	0.41	0.77	0.45	1.00	-	0.60

In the case of other parameters studied, the limits for the effective use of ceramic powder are higher: 40% for effective fracture toughness and specific fracture energy, 60% for frost resistance and chemical resistance to $MgCl_2$, NH_4Cl, Na_2SO_4, HCl and CO_2. In our own previous studies, we found that the addition of brick powder to the cement slightly reduced the strength but increased the frost resistance (Gyurkó et al. 2017).

2.2.3 Cellular concrete powder

With increasing the materials that prove its efficiency to use as supplementary materials for cement the cellular concrete exists as one of the modern alternative of these materials. Cellular concrete has same chemical composition as concrete. A fine powder has become a by-product when the masonry elements are manufactured. This cellular concrete powder was studied for the impact as a specific amount on cellular concrete on some properties of concrete and they found that it increased the 28 days compressive strength, enhance the resistance in aggressive environment by frost resistance and in freeze thaw tests (Gyurkó et al. 2017).

2.2.4 Glass powder

Waste glass utilization could be the application in concrete as a supplementary cementations material (SCM). Laboratory tests were carried out on cement paste specimens, in which waste glass powder (WGP) addition was used as a SCM. Cement was substituted with WGP at levels of 20% or 30% per mass. It was demonstrated that the WGP addition is applicable in view of drying shrinkage with total deformation of up to 2.5‰ in the period of 592 days. The WGP addition contributes to a slowdown in the rate of hydration of the cement paste, so the early age shrinkage cracking tendency becomes more favorable, which can be seen in the longer cracking time result during the ring tests (Kara at. al.2014).

3. HIGH PERFORMANCE SELF-COMPACTING CONCRETE

High performance concrete (HPC) is defined by ACI as follows: "HPC is a concrete meeting special combinations of performance and uniformity requirements that cannot always be achieved routinely using conventional constituents and normal mixing".

As one of the great innovations in concrete technology self-compacting concrete (SCC). SCC is a new category of high-performance concrete, which is in the process of casting without imposing additional vibrating forces, and only gravity is necessary to completely fill the mold cavity to form a uniform dense concrete, it is a really significant forward step in the direction of sustainably developed concrete. SCC has the following advantages to use: (Pandaa and Balb 2013; Boudali et al. 2016; Kou and Poon 2009)

- To ensure high flowability, which has a low resistance to flow.
- To maintains a homogeneous deformation through restricted sections, such as closely spaced reinforcements, because its viscosity is moderate.
- To shorten the construction period.
- To reduces noise due to a vibration.
- To ensure compaction in the structure especially in confined zones where vibrating compaction is difficult to perform, and
- To eliminate noise due to vibration especially at concrete production plants.
- To reduce construction costs and improve the construction environment.
- To improve the productivity of casting congested sections and to ensure that concrete entirely fills restricted areas with minimum or no consolidation.

The most significant disadvantage of SCC is that it is more expensive than conventional concrete based on concrete material costs due to the reduction in aggregate content and using high volume of cement, which using supplementary materials will contribute so far to mitigate this disadvantage, provide excellent alternative leading to the reduction of clinker consumption contribute in preserving the environment, and giving high performance SCC with very good properties.

Boudali et al. (2016), Pandaa and Balb (2013), Kou and Poon (2009) showed that recycled aggregate could be used for SCC and give very good and accepted properties specially if it is mixed with supplementary materials, and they investigated many properties that proved the efficiency of using recycled aggregate and supplementary materials.

El Mir and Nehme (2017) investigated the usage of some of supplementary cementations materials as a filler in SCC. Their results indicated that supplementary cementations material had a significant puzzolanic effect on the concrete microstructure, resulting in a positive impact on the compressive strength of concrete. Furthermore, it enhanced the durability properties of SCC mixtures.

3. A NEW RESEARCH FIELD

Although significant amount of research has been done on concrete using different types of recycled aggregates including recycled concrete aggregate, a lack of information can still be observed regarding using recycled aggregate with supplementary materials for producing self-compacting and high performance concretes. In the furtherance, as (Ajdukiewicz and Kliszczewicz, 2002) mentioned in their research that the green high performance concrete is the future of concrete development.

Not all the possibilities that can be used for producing green concrete are exclusive for only the normal concrete; they would be used for all other types of concretes. Since the researchers already have studied the possibility of using either the recycled aggregate or supplementary materials on a lot of types of concretes, study is to be carried out regarding of the ability and feasibility of using supplementary materials and recycled aggregate for producing green self-compacting, high performance concrete GSCHPC and making a comprehensive investigations on its properties and optimum dosage of materials.

5. CONCLUSIONS

A wide range of recycled aggregate has been steadily introduced in a range of civil engineering and construction applications as partial replacement of natural aggregates in concrete. Although the use of recycled aggregate had a negative effect on some of mechanical properties of concrete, it is clear that the usage of additional supplementary materials will be able to mitigate this detrimental effect and contribute to improving the properties of concrete. The conclusion can be summarized as the following points:

- We can not be generalize the previous researches result values concerning the recycled aggregate concrete, because it is dependent mainly on the characteristics of the original concrete before crushing.

- By using supplementary materials with optimum dosage we can overcome the deteriorations caused by using the recycled aggregate.
- The effectiveness of the waste materials make them a challenge for producing new concrete types and emerging a number of concrete types together to get new specifications for the new concretes.
- The effectiveness of supplementary materials for improving the concrete properties varies depending in their chemical composition and the used dose.

6. ACKNOWLEDGEMENT

Authors are grateful to the Hungarian Scientific Research Fund (OTKA) for the financial support of the OTKA K 109233 research project.

7. REFERENCES

Adamson, M., A. Razmjoo, and A. Poursaee (2015) "Durability of concrete incorporating crushed brick as coarse aggregate." Construction and Building Materials, pp. 426-432.

Ajdukiewicz, Andrzej , and Alina Kliszczewicz (2002) "Influence of recycled aggregates on mechanical properties of HS/HPC." Cement and concrete composites 24, no. 2 pp. 269-279.

Ajdukiewicz, Andrzej , and Alina Kliszczewicz (2002) "Influence of recycled aggregates on mechanical properties of HS/HPC." Cement & Concrete Composites 24 pp. 269–279.

Błaszczyński, Tomasz, and Maciej Król (2015) "Usage of Green Concrete Technology in Civil Engineering." Procedia Engineering 122 pp. 296-301.

Borosnyói, Adorján (2015) "Development of compressive strength of HPC with the use of supplementary cementing material (SCM) combination" Építőanyag – Journal of Silicate Based and Composite Materials, Vol. 67, No. 3 pp. 110–115.

Borosnyói, Adorján (2016) "Long term durability performance and mechanical properties of high performance concrtes with combined use of supplementary cementing materials " Construction and Building Materials 112 pp. 307-324.

Borosnyói, Adorján – Szijártó, Anna (2016) "Analysis of metakaolin as supplementary cementing material by the k-value concept" ("Metakaolin vizsgálata cement kiegészítő anyagként a k-érték elve szerint") Építőanyag – Journal of Silicate Based and Composite Materials, Vol. 68, No. 2, pp. 40–44.

Boudali, S, D.E. Kerdal, K. Ayed, and B. Abdulsa (2016) "Performance of self-compacting concrete incorporating recycled concrete fines and aggregate exposed to sulphate attack." Construction and Building Materials, pp. 705-713.

Butler, Liam, Susan Tighe, and Jeffrey West (2013) "Guidelines for selection and use of coarse recycled-concrete aggregates in structural concrete." Transportation Research Record: Journal of the Transportation Research Board, no. 2335 pp. 3-12.

Debieb, Farid , and Said Kenai (2008) "The use of coarse and fine crushed bricks as aggregate in concrete." Construction and Building Materials 22, no. 5 pp. 886–893.

El Mir, Abdulkader, Nehme Salem G. (2017) "Utilization of industrial waste perlite powder in self-compacting concrete." Journal of Cleaner Production, pp. 507-517.

Evangelista, L, J de Brito (2007) "Mechanical behaviour of concrete made with fine recycled concrete aggregates." Cement & Concrete Composites 29 pp. 397–401.

Fan, Cheng-Chih , Ran Huang, Howard Hwang, and Sao-Jeng Chao (2016) "Properties of concrete incorporating fine recycled aggregates from crushed concrete wastes." Construction and Building Materials 112 pp. 708–715.

Fenyvesi, O; Jankus, B (2015) Opportunities in recycling AAC waste as aggregate for lightweight concrete Építőanyag (ISSN: 0013-970X) (eISSN: 2064-4477) 67: (2) pp. 66-70.

Gómez-Soberón, José MV (2002) «Porosity of recycled concrete with substitution of recycled concrete aggregate An experimental study.» Cement and concrete research 32, no. 8 pp. 1301-1311.

Guo, Y.C. , J.H. Zhang, G.M. Chen, and Z.H. Xie (2014) «Compressive behaviour of concrete structures incorporating recycled concrete aggregates, rubber crumb and reinforced with steel fibre, subjected to elevated temperatures.» Journal of Cleaner Production, pp. 193-203.

Gyurkó, Zoltán, Szijártó, Anna, Nemes, Rita (2017) «Increasing freeze-thaw resistance of concrete by additions of powdered cellular concrete and clay bricks.» International Conference on Analytical Models and New Concepts in Concrete and Masonry Structures AMCM'2017

Hiraskar K.G., Chetan Patil (2013) "Use of Blast Furnace Slag Aggregate in Concrete" International Journal Of Scientific & Engineering Research, Volume 4, Issue 5, May 2013

Hu, Chuanlin (2014) «Microstructure and mechanical properties of fly ash blended cement pastes.» Construction and Building Materials 73 pp. 618–625.

Jankovic, Ksenija , Dragan Nikolic, and Dragan Bojovic (2012) «Concrete paving blocks and flags made with crushed brick as aggregate.» Construction and Building Materials 28, no. 1 pp. 659–663.

Jian, Yang , Du Qiang, and Bao Yiwang . «Concrete with recycled concrete aggregate and crushed clay bricks.» Construction and Building Materials, 2011: 1935-1945.

Jitender , Sharma, and Singla Sandeep (2014) «Influence of Recycled Concrete Aggregates on Strength Parameters of Concrete» SSRG International Journal of Civil Engineering (SSRG-IJCE), 2014: 20-24.

Józsa Zs., Nemes R. (2002) "Bond of a New Recycling Glass Lightweight Aggregate" In: Balázs, G. L., Bartos, P. J. M., Cairns, J., Borosnyói, A. (Ed.) Bond in Concrete – from research to standards: Proceedings of the 3rd International Symposium 2002. 835 p. Budapest, Hungary, 2002.11.20-2002.11.22. pp. 420-427.

Kannan, Dima M., Sherif H. Aboubakr, Amr S. EL-Dieb, and Mahmoud M. Reda Taha (2017) «High performance concrete incorporating ceramic waste powder as large partial replacement of Portland cement.» Construction and Building Materials, 2017: 35-41.

Kara P; Borosnyói A; Fenyvesi Olivér (2014) Performance of waste glass powder (WGP) supplementary cementitious material (SCM): Drying shrinkage and early age shrinkage cracking ÉPÍTŐANYAG (ISSN: 0013-970X) (eISSN: 2064-4477) 66: (1) pp. 18-22.

Kenéz, Á, Kovács, É, Rácz, A. Fenyvesi, O. (2014a) "Industrial waste reusing for concrete aggregate " ("Ipari hulladékok újrahsznosítása beton adalékanyagként") in proceeding Török Á, Puzder T, Cserny T (Eds) Meddő? Hulladék? Nem! Haszonanyag! Mérnökgeológia-kőzetmechanika kiskönyvtár; 17. pp. 111-118.

Kenéz, Á, Kovács, É, Rácz, A. Fenyvesi, O. (2014b) "Construction lightweight aggregate concrete for precast bridge elements" ("Szerkezeti könnyűbeton előregyártott hídszerkezeti elemekhez") in proceeding Köllő Gábor (Ed.) XVIII. Nemzetközi Építéstudományi Konferencia Csíksomlyó, Romania, 2014.06.12-2014.06.15. Erdélyi Magyar Műszaki Tudományos Társaság (EMT), 2014. pp. 149-152.

Kopecskó, K, Mlinarik, L (2014) «Metakaolin in concrete» Metakaolin a betonban, Beton XXII. (3-4) 2014: p 8-21.

Kou, S.C., and C.S. Poon (2009) «Properties of self-compacting concrete prepared with coarse and fine recycled concrete aggregates.» Cement & Concrete Composites, 2009: 622-627.

Kou, Shi Cong , Chi Sun Poon, and Dixon Chan (2008) «Influence of fly ash as a cement addition on the hardened properties of recycled aggregate concrete.» Materials and Structures 41 (2008): 1191–1201.

Kubissa, Wojciech, Simon, Tamas, Jaskulaki Roman, Reiterman Pavel, Supera Marcin (2017) «Ecological High Performance Concrete.» Procedia Engineering, 2017: 595-603.

Kulovana, T;Vejmelkova, E, Keppert, M, Rovnanikova, P, Kersner, Z; Cerny, R (2016) "Mechanical, durability and hygrothermal properties of concrete produced using Portland cement-ceramic powder blends" Structural Concrete 2016/17-1 pp. 105-115

Long, Guangcheng, Yu Gao, and Youjun Xie (2015) «Designing more sustainable and greener self-compacting concrete.» Construction and Building Materials 84 (2015): 301–306.

López-Gayarre, F, P Serna, A Domingo-Cabo, M A Serrano-López, and C López-Colina (2009) «Influence of recycled aggregate quality and proportioning criteria on recycled concrete properties.» Waste Management 29 (2009): 3022–3028.

Malešev, Mirjana, Vlastimir Radonjanin, and Snežana Marinković (2010) «Recycled Concrete as Aggregate for Structural Concrete Production.» Sustainability 2, no. 5 pp. 1204-1225.

Mlinárik, L, Kopecskó, K. (2013) "Impact of metakaolin - a new supplementary material - on the hydration mechanism of cements" Acta Technica Napocensis - Civil Engineering & Architecture 56:(2) pp. 100-110.

Mlinárik, L, Kopecskó, K. (2017) "The influence of combined application of two SCMs on the corrosion and acid attack durability of mortars" Periodica Polytechnica-Civil Engineering Paper 9352. 9 p.

Mohammadhosseini, Hossein, and Jamaludin Mohamad Yatim (2017) «Microstructure and residual properties of green concrete composites incorporating waste carpet fibers and palm oil fuel ash at elevated temperatures.» Journal of Cleaner Production 144 pp. 8-21.

Mucsi, G. "Mechanical activation of power station fly ash by grinding – A review" (2016) Építőanyag – Journal of Silicate Based and Composite Materials, Vol. 68, No. 2, pp. 56-61.

Mueller, Harald S, Michael Haist, Jack S Moffatt, and Michael Vogel (2017) «Design, Material Properties and Structural Performance of Sustainable Concrete.» Procedia Engineering 171 pp. 22-32.

Nath, P, and P Sarker (2017) «Effect of Fly Ash on the Durability Properties of High Strength Concrete.» Procedia Engineering 14 pp. 1149–1156.

Nehme Salem Georges (2015) “Infuence of supplementary cemneting materials on conventionel and self compacting concrete Part 1. –Literature review” (“Kiegészítőanyagok hatása a szokványos és az öntömörödő betonokra (1. rész. Szakirodalmi áttekintés)”) Építőanyag – Journal of Silicate Based and Composite Materials, Vol. 67:(1) pp. 28-33.

Nehme Salem Georges (2015) Kiegészítőanyagok hatása a szokványos és az öntömörödő betonokra (1. rész. Szakirodalmi áttekintés) Építőanyag – Journal of Silicate Based and Composite Materials, Vol. 67:(1) pp. 28-33.

Nehme Salem Georges (2015)Kiegészítôanyagok hatása a szokványos és az öntömörödô betonokra 2. rész. Laboratóriumi vizsgálatok Építőanyag – Journal of Silicate Based and Composite Materials, Vol. 67:(2) pp. 72-78.

Nemes, R., Józsa Zs. (2006) “Aspects of Mix Design of Lightweight Aggregate Concrete” Concrete Structures: Annual Technical Journal: Journal of The Hungarian Group of *fib* 7: pp. 82-87.

Nemes, R, Török B. (2014) “Bond of steel reinforcement in different lightweight aggregate concretes” (“Betonacél tapadása különböző könnyű adalékanyagok alkalmazása esetén”) Építőanyag – Journal of Silicate Based and Composite Materials, Vol. 66, No. 1, pp. 7–12.

Olorunsogo, F T, Padayachee N (2002)»Performance of recycled aggregate concrete monitored by durability indexes.» Cement and Concrete Research 32, no. 2: 179–185.

Pandaa, K C, and P K Balb (2013) «Properties of self compacting concrete using recycled coarse aggregate.» Chemical, Civil and Mechanical Engineering Tracks of 3rd Nirma University International Conference on Engineering (NUiCONE 2012), 2013: 159-164.

Pankhardt, Kinga, Nehme, Salem G. (2002) “Strength and deformation of recycled concrete” in: Proceedings fib (1) (Osaka) Session 8. pp. 59-68.

Pavlu, Tereza, Luc Boehme, and Petr Hajek (2014) «Influence of recycled aggregate quality on the mechanical properties of concrete.» Komunikacie/Communications 16, no. 4 (2014): 35-40.

Poon, S C, Z H Shui, L Lam, H Fok, and S C Kou (2004) «Influence of moisture states of natural and recycled aggregates on the slump and compressive strength of concrete.» Cement and concrete research 34, no. 1 (2004): 31-36.

Rahal, Khaldoun (2007) «Mechanical properties of concrete with recycled coarse aggregate.» Building and Environment 42 (2007): 407–415.

Russell HG. (1999) ACI Defines High-Performance Concrete. Concert Internet 1999;21(2):56–57.

Schoon, Joris , Klaartje De Buysser, Isabel Van Driessche, and Nele De Belie (2013) «Feasibility study on the use of cellular concrete as alternative raw material for Portland clinker production.» Construction and Building Materials 48 (2013): 725–733.

Suzuki M, Meddah M. S, Sato R. (2009) Use of porous ceramic waste aggregates for internal curing of high-performance concrete, Cement and Concrete Research Institute (2009) 39. pp. 373-381.

Suhendro, Bambang (2014) «Toward green concrete for better sustainable environment.» Procedia Engineering 95 (2014): 305-320.

Tabsh, Sami W., and Akmal S. Abdelfatah (2009) «Influence of recycled concrete aggregates on strength properties of concrete.» Construction and Building Materials, 2009: 1163-1167.

Thomas, C, J Setién, J A Polanco, P Alaejos, M Sánchez de Juan (2013) «Durability of recycled aggregate concrete.» Construction and Building Materials 40 (2013): 1054–1065.

Topcu, Ilker Bekir, and Selim Şengel (2004) «Properties of concretes produced with waste concrete aggregate.» Cement and concrete research 34, no. 8 (2004): 1307-1312.

Vieira, T, A Alves, J de Brito, J R Correia, R V Silva (2016) «Durability-related performance of concrete containing fine recycled aggregates from crushed bricks and sanitary ware.» Materials and Design 90 (2016): 767–776.

Yazıcı, Halit (2008) «The effect of silica fume and high-volume Class C fly ash on mechanical properties, chloride penetration and freeze–thaw resistance of self-compacting concrete.» Construction and Building Materials 22 (2008): 456–462.

Mohammed Abed (1991) civil engineer (MSc). PhD candidate at the Department of Construction Materials and Technologies, Budapest University of Technology and Economics. Main fields of interests: recycled concrete aggregate, non-destructive testing of concert, high performance concrete, supplementary cementations materials. abed.mohammed@epito.bme.hu

Rita Nemes (1978) civil engineer (MSc), postgraduate diploma in concrete technology, PhD, associate professor at the Department of Construction Materials and Technologies, Budapest University of Technology and Economics. Main fields of interest: non-destructive testing of concrete, supplementary cementing materials for concrete, bond in concrete, fibre reinforced concrete, lightweight concrete, shrinkage of concrete, durability measurement, waste materials as aggregates. Member of the Hungarian Group of ***fib*** and the Scientific Society of Silicate Industry. nemes.rita@epito.bme.hu

FIRE BEHAVIOUR OF CONCRETE – INFLUENCING PARAMETERS

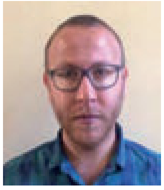
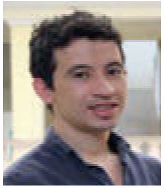

Naser Alimrani – Abdelmelek Nabil – György L. Balázs – Éva Lublóy

Concrete can be exposed to elevated temperatures during fire or when it is close to furnaces and reactors. The behaviour of a concrete structural member exposed to fire is dependent, in part, on physical, thermal, and mechanical deformation properties of concrete of which the member is composed. These deterioration processes influence the durability of concrete structures and may result in undesirable structural deterioration or even failure. In present paper we intended to give an overview of the different parameters and their influence on the behaviour of concrete at elevated temperatures or on fire.

Keywords: concrete, high temperature, fire, colour change, cement type, w/c, type of aggregate

1. INTRODUCTION

Concrete can be exposed to elevated temperatures during fire or when it is close to furnaces and reactors. The behaviour of a concrete structural members exposed to fire is dependent, on physical, thermal, and mechanical deformation properties of concrete of which the member is composed. The deterioration processes influence the durability of concrete structures and may result in undesirable structural failures. Therefore, preventative measures such as choosing the right materials should be taken to minimize the harmful effects of high temperature on concrete. The high temperature behaviour of concrete is greatly affected by material properties, such as the properties of the aggregate, the cement paste and the aggregate-cement paste bond, as well as the thermal compatibility between the aggregate and cement paste.

2. BEHAVIOUR OF CONCRETE IN FIRE

2.1 Physical behaviour (colour changes)

It is generally agreed (Short et al., 2001; Colombo and Felicetti, 2007) that concrete containing siliceous aggregates when heated between 300 °C and 600 °C it will turn red; between 600 °C and 900 °C, whitish-grey; and between 900 °C and 1000 °C, a buff colour is present. The colour change of heated concrete results from the gradual water removal, dehydration of the cement paste and transformations occurring within the aggregate, respectively. The most intense colour change, the appearance of red colouration, is observed for siliceous river-bed aggregates containing iron. This colouration is caused by the oxidation of mineral components. While siliceous aggregates turn red when heated, the aggregates containing calcium carbonate get whitish. Due to calcination process $CaCO_3$ turns to lime and give pale shades of white and grey (*Fig. 1*) (Hager, 2013b).

In general two approaches can be adopted when the colour change of concrete is analysed (Hager, 2013b). First, the external surface of the element can be examined. This involves the observation of an element's outer walls (in particular, the cement paste). The other possibility is to observe the surface with visible aggregates (sample cored or sawn out from the element) (Short et al., 2001; Colombo and Felicetti, 2007). When it is necessary to evaluate the condition of concrete after a fire, colour change is a physical property of concrete that can be used as an assessment method (Hager, 2013a).

2.2 Thermal behaviour

Thermal properties that govern temperature dependent properties in concrete structures are thermal conductivity, specific heat (or heat capacity) and mass loss (Kodur, 2014).

The density of concrete shows only slight temperature

Fig. 1: Colour change of heated concrete (Hager, 2013a)

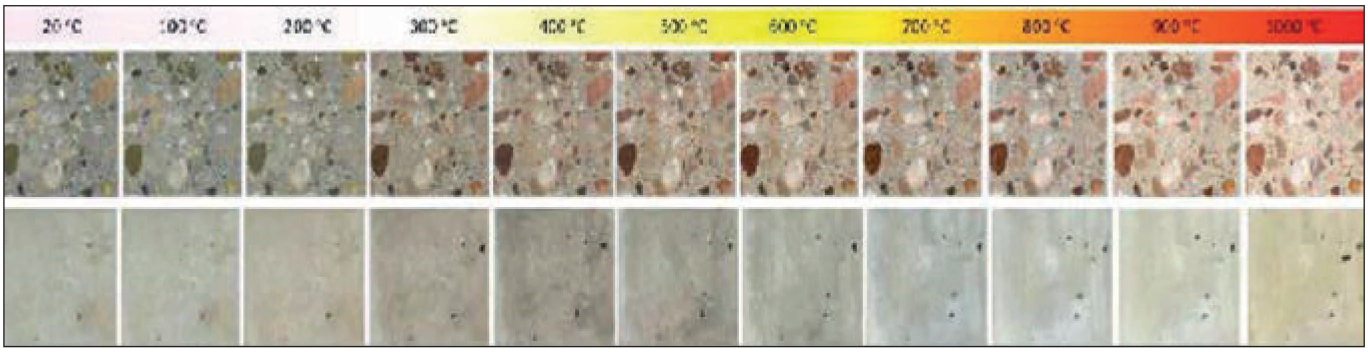

dependence, which is mostly due to moisture losses during heating. However limestone concretes show a significant decrease of density at about 800 °C due to the decomposition of the calcareous aggregate. The thermal conductivity of concrete depends on the conductivities of its constituents. The major factors are the moisture content, the type of aggregate and the mix proportions. The conductivity of any given concrete varies approximately linearly with the moisture content (Schneider, 1988).

2.3 Mechanical behaviour

The mechanical properties that are of primary interest in fire resistance design are compressive strength, tensile strength, elastic modulus and stress-strain response in compression. Mechanical properties of concrete at elevated temperatures have been extensively studied in the literature in comparison to thermal properties (Kodur, 2014).

Fig. 2: Stress-strain relationship for normal concrete derived in strain-rate controlled tests (Schneider, 1988)

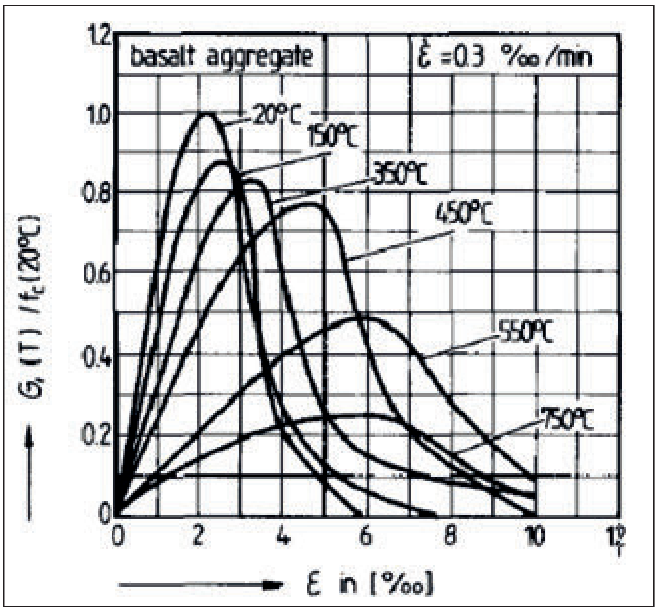

Table 1. The list of changes taking place in concrete during heating (Hager, 2013a)

Temperature range	Changes
20–200°C	slow capillary water loss and reduction in cohesive forces as water expands; 80–150°C ettringite dehydration; C-S-H gel dehydration; 150–170°C gypsum decomposition ($CaSO_4 \cdot 2H_2O$); physically bound water loss;
300–400°C	approx. 350°C break up of some siliceous aggregates (flint); 374°C critical temperature of water;
400–500°C	460–540°C portlandite decomposition $Ca(OH)_2 \rightarrow CaO + H_2O$;
500–600°C	573°C quartz phase change $\beta - \alpha$ in aggregates and sands;
600–800°C	second phase of the C-S-H decomposition, formation of β-C_2S;
800–1000°C	840°C dolomite decomposition; 930–960°C calcite decomposition $CaCO_3 \rightarrow CaO + CO_2$, carbon dioxide release; ceramic binding initiation which replaces hydraulic bonds;
1000–1200°C	1050°C basalt melting;
1300°C	total decomposition of concrete, melting.

Changes in mechanical properties that occur during heating are the result of changes taking place in concrete. Those material factors include physico-chemical changes in the cement paste and aggregates as well as the incompatibilities between them listed in *Table 1*. Other factors affecting the material damage level are as follows: heating rate, maximum temperature, time of exposure to temperature, load applied during heating, moisture content of the material, etc. (Hager, 2013a).

The mechanical response of concrete is usually expressed in the form of stress-strain relations, which are often used as input data in mathematical models for evaluating the fire resistance of concrete structural members (Hager, 2013a).

Generally, because of a decrease in compressive strength and increase in ductility of concrete, the slope of stress-strain curve decreases with increasing temperature. The strength of concrete has a significant influence on stress-strain response both at room and elevated temperatures (*Fig. 2*).

3. INFLUENCING PARAMETERS

3.1 Test methods

The test method has an important influence on the evaluation of the properties of heated concrete. The most common way to study the influence of high temperature on the properties of concrete is to expose the material to high temperatures, cool it down to room temperature, and then carry out the test, such as compression or tensile tests. However, this method gives the "post fire" or "post exposure to the high temperature" properties of concrete. Nevertheless, we have to consider that the most appropriate procedure to test the mechanical properties at high temperature is to determine the properties of material at elevated temperature (tested "hot") (Hager, 2013a).

It should be noticed that the selection of the type of test to be carried out should be determined in function of the real conditions that are intended to simulate. Thus, the tests carried out at high temperatures allow assessing the behaviour of concrete under fire conditions, while the tests after heating and cooling of the concrete allow knowing the residual behaviour after fire (Santos and Rodrigues, 2016).

3.2 Heating rate

While tests could be carried out under varying temperature ranges, the usual practice for clarity and simplification is to carry out tests either at constant temperature (e.g. 300 °C) or at constant rates of heating (e.g. at 2 °C/minutes). As for cooling, it could be natural or forced (*fib*, 2007).

Heating rates, for example 2 °C/min for mechanical properties, while too slow to simulate fire conditions are applied by scientists – and recommended by RILEM Committee – in order to separate as far as possible the material effects from structural effects of heating a specimen with the size of e.g. 6 cm in diameter and 18 cm in length (Khoury et al., 1984). In this respect fast heating will introduce thermal and moisture gradients and hence thermal stresses within the specimen. Smaller sizes in specimens (and in powder form) are generally exposed to higher heating rates because the size limits the structural effects. The limitation in heating rate has been shown to provide more accurate indication of the material behaviour for some material properties (*fib*, 2007).

3.3 Type of cement

The incorporation of pulverised fly ash (PFA) and slag in Portland cements or blended cements can generally keep the mechanical properties of concrete at a higher level after heating to high temperature. Compared to PC, the residual compressive strength, splitting tensile strength, flexural strength and modulus of elasticity of PC blended with PFA increase by 1.2–270%, 1.1–80%, 4.5–200% and 3–38%, respectively, while the values for PC blended with slag are 1.5–510%, 1.2–43%, 1–180% and 1.3–117% higher, respectively. The values vary mainly with different temperatures, replacements and types of aggregates. In the research carried out by Wang (Wang, 2008) the bare PC paste had lost its compressive strength and modulus of elasticity completely at the temperature of 1050 °C. However, 18% of the compressive strength and 81% of the modulus of elasticity still remained for PC blended slag paste with the replacement rate of 80% at the same temperature. Furthermore, PCs blended with PFA and slag also exhibit a high resistance to spalling at high temperatures (Poon, Azhar, Anson, Wong, 2008; Heikal,-Didamony, Sokkary, Ahmed, 2013; Mendes, Sanjayan, Collins, 2008; Xu, Wong, Poon, Anson , 2003)

Karakurt and Topcu (Karakurt, Topcu, 2013) found by using SEM analysis that thermal cracking did not occur in PFA, and slag blending samples and that the degradation of C–S–H decreased compared to the reference samples made of Portland cement. Moreover, the incorporation of slag significantly reduces the amount of portlandite in PC. This way the extent of portlandite dehydration due to high temperature is decreasing. As a result of the above three aspects, the total porosity and the average pore diameter of PCs blended with PFA and slag are smaller than those of bare PC at high temperatures (Poon, Azhar, Anson, Wong, 2008). This could explain the higher resistance of PCs blended PFA and slag to high temperature.

Khoury et al. (Khoury et al., 2001) tested ordinary Portland cement (OPC) – PFA cement pastes containing 30% PFA by weight under a series of temperatures till 650 °C. The relative residual compressive strength was 88% at 450 °C and 73% at 600° C, which was almost double than the residual strength shown by pure OPC pastes. In a recent research, Yu et al. (Yu et. al, 2001) studied the effects of PFA replacement level, water/binder ratio (W/B), and curing conditions on the residual properties of concrete at elevated temperatures. An increase in strength was observed at 250 °C. All PFA concrete specimens showed better performance up to 650 °C than OPC concrete specimens; however, after that there was no significant difference in the residual strength of all specimens. It was found that a high dosage of PFA enhanced the residual properties of concrete at elevated temperatures. The results were also verified by porosity analysis done by mercury intrusion porosimetry (MIP) technique.

Nasser and Marzouk (1979) found that the PFA improved the performance of concrete at elevated temperatures as compared to silica fume or pure OPC concretes. However, this improvement was more significant at temperatures below 600 °C. Moreover, it was discovered that PFA also reduced the surface cracking of concrete both at elevated temperatures and after post cooling in air or water.

An extensive experimental study was carried out by Lublóy et al (Lublóy et al, 2016) to analyze the post-heating characteristics of concretes subjected to temperatures up to 800 °C. Major parameters of the study were the slag content of cement (0, 16, 25, 41 or 66 m%) and the value of maximum annealing temperature. The results indicated that (I) the number and size of surface cracks as well as compressive strength decreased by the increasing slag content of cements due to elevated temperature; (II) the most intensive surface cracking was observed by using Portland cement without addition of slag. The increasing slag content of cement increased relative post-heating compressive strength. Tendencies of surface cracking and reduction of compressive strength were in agreement, i.e. the more surface cracks, the more strength reduction.

On the other hand, type of cement had little effect on strength temperature characteristics (Santos and Rodrigues, 2016). Type of cement seems to be of minor influence as far as concretes are considered. Mortars (mix proportion 1:3:0.5) made with different types of cement showed significant differences. (Schneider, 1988). That result leads to studies performed by Bamonte and Gambarova (2007) that showed that the residual modulus of elasticity depends on the type of concrete, up to 400 °C, being that dependency vanished for higher temperatures (Santos and Rodrigues, 2016).

The heating of cement paste results in drying. Water evaporates from the material. The order in which water is removed from heated concrete depends on the energy that binds the water and the solid. Thus, free water evaporates first, followed by capillary water, and finally by physically bound water. The process of removing water that is chemically bound with cement hydrates is the last to be initiated. The mechanical properties of cement paste are strongly affected by chemical bonds and cohesion forces between sheets of calcium silicate hydrate (C-S-H) gel. It is assumed that approximately 50 % of cement paste strength comes from cohesion forces (important C-S-H gel sheet area); therefore, the evaporation of water between C-S-H gel sheets strongly affects the mechanical properties of the cement paste (Hager, 2013a).

Heating the cement paste with a C/S ratio around 1.5 to temperature above 100 °C produces several forms of calcium silicates, in general highly porous and weak. When the C/S ratio is close to 1.0 and the temperature is above 150 °C, a 1.5 to 1.0 tobermorite gel can form. At temperature between 180 °C and 200 °C, other silicates such as xonolite and hillebrandite may be formed. As soon as cement paste is heated to temperature of 500–550 °C, the portlandite content rapidly drops, as it decomposes according to the following reaction: $Ca(OH)_2 = CaO + H_2O$. The portlandite decomposition reaction explains the observed increase in CaO content in cement paste at the temperature of approximately 550 °C (Piasta, 1989; Castellote et al., 20014). The CaO created in this reaction makes the elements made of the Portland cement practically redundant after cooling. The dehydration process of

Fig. 3: Effect of heating on cumulative pore of Portland cement paste heated to 200 °C, 400 °C, 600 °C and 800 °C (w/c=0.6, Hager, 2013 a)

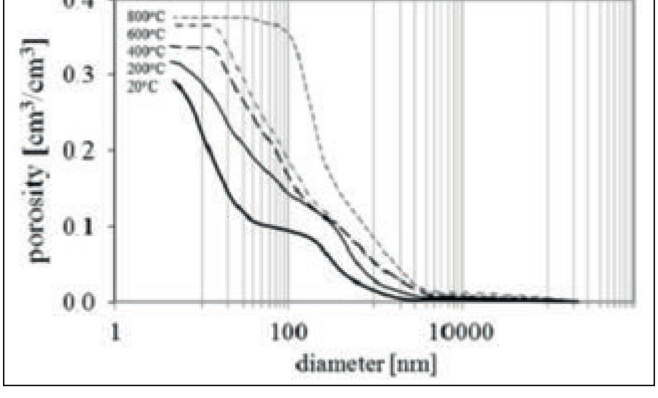

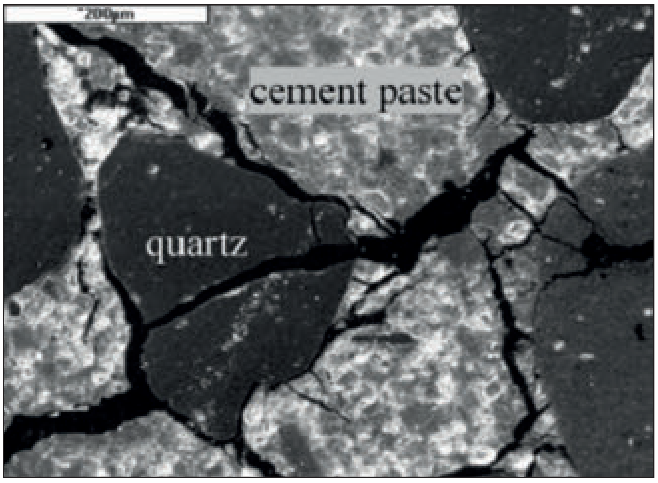

Fig. 4: The microstructure of concrete heated to 600 °C (SEM, 50x) concrete based on silicio-calcareous aggregates, f_c=75 MPa (Hager, 2013a)

the C-S-H gel reduces its volume, which in turn increases the porosity of the cement matrix. Moreover, during heating, the cement paste experiences a slight expansion up to temperature of approximately 200 °C (Piasta, 1989; Verbeck and Copeland, 1972, Khoury et al., 1985) although the intense shrinkage begins as soon as this temperature is exceeded. This significantly contributes to the porosity evolution of the cement paste. Due to heating total pore volume increases, as does the average pore size (*Fig. 3*) (Hager, 2013a).

The heating of concrete makes its aggregate volume grow, and at the same time it causes the contraction of the cement paste which surrounds it. As a result, the cement paste-aggregate bond is the weakest point in heated cementitious material. To a large extent, damage to concrete is caused by cracking, which occurs arising due to mismatched thermal strains between the coarse aggregates and the matrix. Fig. 4 shows an example of thermally damaged concrete, which is made of silico-calcareous aggregates, and heated to 600 °C. The SEM photo shows cracks crossing the cement paste and proceeding though the interfacial transition zone. Also, cracks passing through siliceous aggregate are present, indicating the tendency of some siliceous aggregates to break up at 350 °C (Khoury, 1992).

3.4 Type of aggregate

Aggregates occupy 70 to 80% of the volume of concrete and thus heavily influence its thermal behaviour. Type of aggregate is the main factor affecting the shape of the stress-strain curves. Concretes made with hard aggregates (siliceous, basaltic) generally have a steeper decrease of the initial slope with increasing test temperatures than those with softer aggregates (e.g., lightweight aggregates) (Schneider, 1988). Fig. 5 shows the stability and other changes of various aggregate types at elevated high temperatures (*fib*, 2007)**.**

A few reasons of why the aggregate is so important follow:

- It occupies some 60-80% by volume of concrete
- Variations in aggregate properties on heating can have a significant effect on the performance of concrete at elevated temperatures.
- Physico-chemical changes also occur in the aggregate depending upon the type of aggregate used, but aggregate differ greatly in their response to heat. A key factor in the behaviour of heated concrete is the chemical and physical stability of the aggregate. The choice of aggregate is, therefore, an important factor in determining the thermal properties, and thermal stability, of the concrete in fire.
- Restrains creep and shrinkage of the paste (*fib*, 2007).

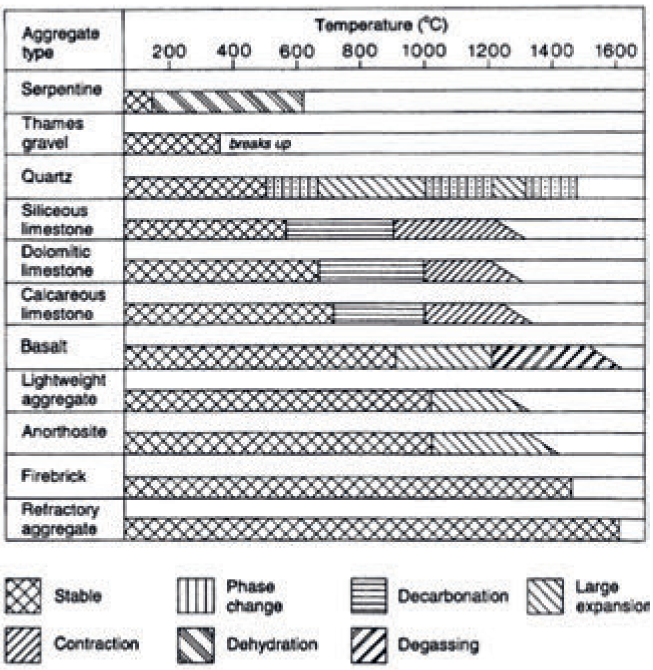

Fig. 5: Non-exhaustive examples of the large range of thermal stabilities and processes, those take place in aggregates during heating. Source (***fib*** 2007)

3.5 W/C ratio

Original strength and the water-cement ratio within the practical range of concrete application hardly influence the shape of stress-strain curves (*Fig. 6*) (Schneider, 1988).

The modulus of elasticity of heated concretes decreases in a similar way for all water-cement ratios. The relative values of modulus of elasticity seem to be independent of the water-cement ratio (see Fig. 6). For all three concretes the percentage drop in E value can be considered as quasi-identical. The increase in temperature generally leads to a consecutive fall in the modulus of elasticity value. However, the elasticity values depend to a large extent on whether the concrete is loaded during heating. It was reported that when constant loading of 20% of f_c is applied during heating, Young's Modulus may remain unchanged even up to 600 °C (Hager, 2013 a).

3.6 Aggregate/cement ratio

Aggregate-cement ratio has a significant effect on the modulus of elasticity and consequently also on the initial slope of the stress-strain curves. Mortars (high cement content!) indicate a lower initial slope than normal concretes; stress-strain curves of concrete indicate a somewhat greater curvature than those of mortars (Schneider, 1988).

From *Fig. 7* we can conclude the two main following results:

- Pure hydrated cement paste indicates contraction shrinkage at temperatures above 150-400 °C.
- The main factor affecting the thermal strain is the type of aggregate; the coarse aggregate fraction plays a dominant role (Schneider, 1988).

3.7 Supplementary materials

Dias et al. (1990) reported that although no initial signs of distress were visible on OPC pastes heated to 400 °C or above and cooled to room temperature, all specimens exhibited severe cracking to the point of disintegration after a few days. Above this temperature (400 °C) OPC pastes presented total

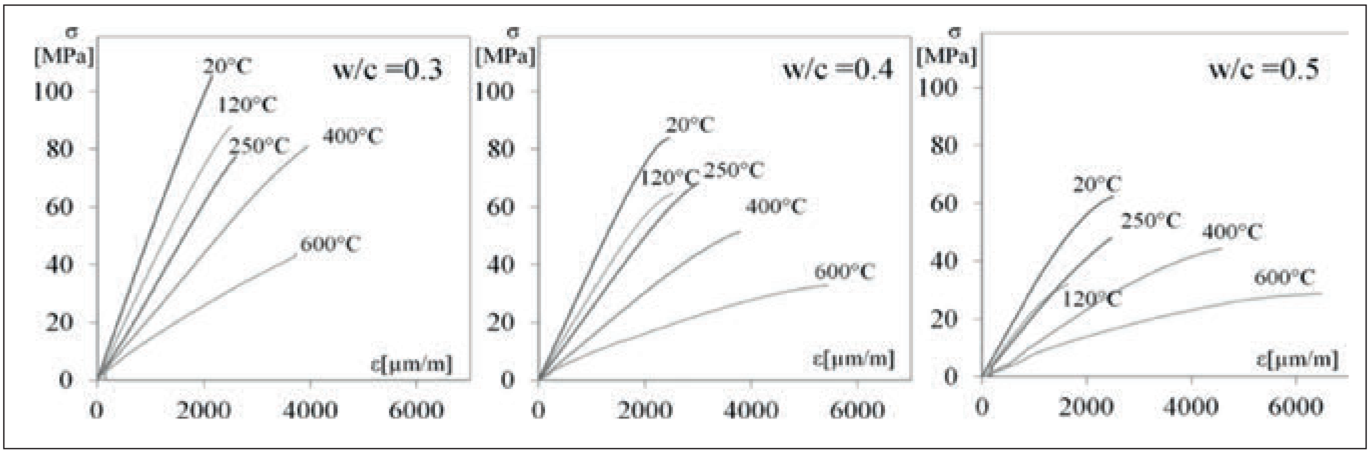

Fig. 6: The stress-strain diagrams for concretes with w/c ratio of 0.3, 0.4, and 0.5, obtained at temperature of 120 °C, 250 °C, 400 °C, 600 °C (tested "hot", Hager, 2013a)

strength loss due to dehydration of $CaOH_2$ and rehydration of CaO. However, dehydration of $CaOH_2$ and rehydration of CaO had no impact in pastes where OPC was partially replaced with ground granulated blast furnace slag, a by-product of the iron blast furnace industry. This is illustrated in *Fig. 8* (Mendes et al., 2012).

Poon et al. (2003) showed a comprehensive experiment comparing metakaolin (MK) and Fly Ash (FA) with different ratios compared to ordinary Portland cement (Poon et al., 2003). The mix proportions are given in *Table 2*. The results of the experiments shown in *Fig. 9*:

Fig. 7: Thermal strain of different concretes (Schneider, 1988)

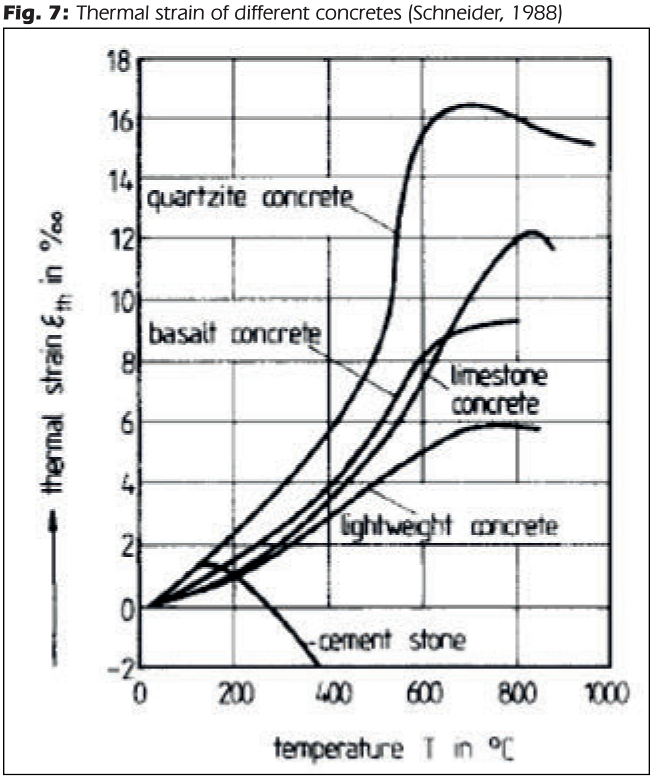

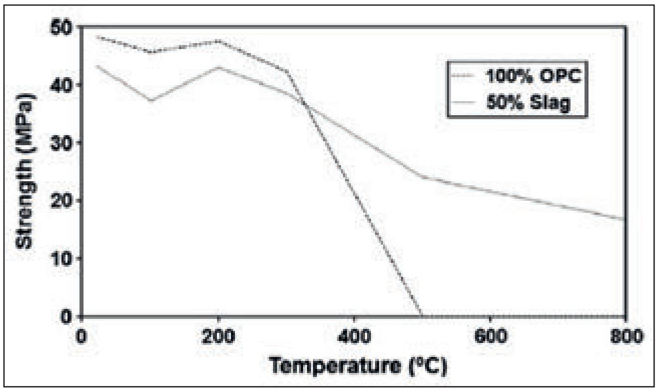

Fig. 8: Compressive strength of OPC and 50% slag pastes at different temperatures (Mendes et al., 2012)

- The MK concrete showed a distinct pattern of strength gain and loss at elevated temperatures. - After gaining an increase in compressive strength at 200 °C, it maintained higher strengths as compared to the corresponding SF, FA and pure OPC concretes up to 400 °C.
- Within the range 400–800 °C, MK concretes suffered more loss and possessed lower residual strengths than the other concretes (Poon et al., 2003).
- Explosive spalling was observed particularly between 450 and 500 °C. The spalling frequency increased with the higher MK content. The vapour pressure build-up by dense pore-structure seems to be the obvious reason for such spalling.
- The MK concrete with 5% cement replacement showed better performance than the corresponding pure OPC and SF concretes at all tested temperatures. No spalling was observed in this concrete (Poon et al., 2003).

Table 2. Mix proportions of concrete mixtures (Poon et al., 2003)

Mix	SF (%)	FA (%)	MK (%)	W/B	Batched quantities (kg/m³)					28 days compressive strength (MPa)
					Water	Cement	Fine agg.	Coarse agg.	SP[a]	
Normal strength concrete (NSC)										
NS-CC[b]	–	–	–	0.50	195	390	768	917	–	35.8
NS-MK5	–	–	5	0.50	195	370	710	1067	–	40.7
NS-MK10	–	–	10	0.50	195	351	620	1154	0.2	47.6
NS-MK20	–	–	20	0.50	195	312	618	1149	0.5	58.4
NS-FA20	–	20	–	0.50	195	312	615	1143	–	39.3

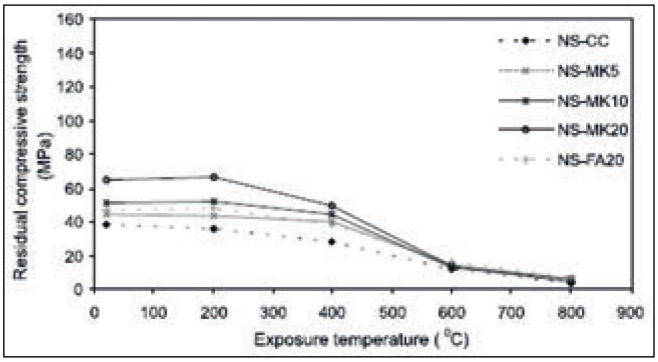

Fig. 9: Residual compressive strength of NSCs (Poon et al., 2003)

4. CONCLUSIONS

The present work presents the influence different parameters on the behaviour of concrete at elevated temperatures or on fire. The following conclusions may be drawn:

- The behaviour of a concrete exposed to fire is dependent, in part, on physical, thermal, and mechanical deformation properties of concrete.
- The extent of cement paste deterioration is mainly related to the rate of water absorption. Type of cement seems to be of influence as far as concretes are considered.
- Type of aggregate is the main factor affecting the shape of the stress-strain curves. Concretes made with hard aggregates (siliceous, basaltic) generally have a steeper decrease of the initial slope with increasing test temperatures than those with softer aggregates (e.g. lightweight aggregates).
- Supplementary materials have no significant effect on the mechanical properties of concrete certain range of temperatures; however they have an obvious effect on the normal compressive strength.

5. ACKNOWLEDGEMENTS

Authors acknowledge the support by the Hungarian Research Grant NVKP_16-1-0019 "Development of concrete products with improved resistance to chemical corrosion, fire or freeze-thaw".

6. REFERENCES

Castellote, C., Alonso, M. Andrade, C., Turrillasa, C. and Campoc, J. (2004), "Composition and microstructural changes of cement pastes upon heating, as studied by neutron diffraction", *Journal Cement and Concrete Research* 34, 1633–1644.

Colombo, M., Felicetti, R. (2007), "New NDT techniques for the assessment of fire-damaged concrete structures", *Fire Safety Journal* 42 (6–7), 461-472.

Dias, WPS, Khoury, G.A., Sullivan, P.J.E. (1990), "Mechanical properties of hardened cement paste exposed to temperatures up to 700 °C (1292F)", *ACI Materials J.*, 1990; 87 (2):160–6.

fib (2007), "Fire design of concrete structures, materials, structures and modelling", *fib* Bulletin 38, International Federation for Structural Concrete

Lublóy, É., Kopecskó, K., Balázs, G.L, Szilágyi, I. M., Madarász, J.,(2016), "Improved fire resistance by using slag cements", *Journal of Thermal Analysis and Calorimetry* 125:(1) pp. 271-279.

Hager, I. (2013a), "Behaviour of cement concrete at high temperature". *The Journal of Polish Academy of Sciences. Vol 61, Issue 1, Mar 2013. Poland*

Hager, I. (2013B), "Colour change in heated concrete", *Fire Technology*, 50, 945–958

Heikal, M., El-Didamony, H., Sokkary, T.M., Ahmed, I.A. (2013), "Behavior of composite cement pastes containing microsilica and fly ash at elevated temperature", *Constr Build Mater* 2013;38:1180–90.

Karakurt, C, Topcu, I.B. (2012), "Effect of blended cements with natural zeolite and industrial by-products on rebar corrosion and high temperature resistance of concrete", *Constr Build Mater* 2012;35:906–11

Mendes A, Sanjayan J, Collins F. (2008), "Phase transformations and mechanical strength of OPC/slag pastes submitted to high temperatures", *Mater Struct*. 2008;41:345–50.

Kodur, V. R. (2014), "Properties of Concrete at Elevated Temperatures", *Civil Engineering Volume* Hindawi Publishing Corporation ISRN, Article ID 468510, 15 p.

Khoury, G.A., et al. (2001), "Fire Design of Concrete Materials Structures and Modelling", *Proceedings of the 1st fib Congress, Osaka, Japan, Oct. 2001.*

Khoury, G.A., Sullivan, G.P.E., and Grainger, B.N. (1985), "Strain of concrete during first heating to 600 °C under load", *Magazine of Concrete Research* 37 (133) 195–215.

Khoury, G.A. (1992), "Compressive strength of concrete at high temperatures: a reassessment", *Magazine of Concrete Research* 44 (161), 291–309.

Khoury, G.A., Sullivan, P.J.E. and Grainger, B.N. (1984), "Radial temperature distributions within solid concrete cylinders under transient thermal states", *Magazine of Concrete Research*, Vol. 36, No. 128, Sept. 1984

Mendes, A., Sanjayan, J. G., Gates, W. P., Collins, F. (2012), "The influence of water absorption and porosity on the deterioration of cement paste and concrete exposed to elevated temperatures, as in a fire event", *Cement and Concrete Composites*, Elsevier 34 (2012) 1067–1074.

Nasser, K.W., Marzouk H.M. (1979), "Properties of mass concrete containing fly ash at high temperatures, *ACI J.* 76 (4) (1979) 537–551.

Piasta, J. (1989), "Heat deformation of cement phases and microstructure of cement paste", *Materials and Structures* 17 (102) 415–420 (1989).

Poon, C-S., Azhar S, Anson M, Wong Y-L. (2001), "Comparison of the strength and durability performance of normal- and high-strength pozzolanic concretes at elevated temperatures", *Cem and Concr Res* 2001;31:1291-300.

Poon, C-S., Azhar, S, Anson, M, Wong, Y-L. (2003), "Performance of metakaolin concrete at elevated temperatures", *Cement and Concrete Composites*, Elsevier 25 (2003) 83–89.

Santos, C. C., Rodriguesb, J.P. C. (2016), "Calcareous and granite aggregate concretes after fire", *Journal of Building Engineering* 8 (2016) 231–242

Schneider., U. 1988. "Concrete at high temperatures—a general review," *Fire Safety Journal*, vol. 13, no. 1.

Short, N.R., Purkiss, J.A., and Guise, S.E. (2001), "Assessment of fire damaged concrete using color image analysis", *Construction and Building Materials 15, 9–15.*

Verbeck, G. and Copeland, L.E. (1972), "Some physical and chemical aspects of high pressure steam curing", *Menzel Symposium on High Pressure Steam Curing ACI SP-32*, 1–131 (1972).

Wang, H.Y. (2008), "The effects of elevated temperature on cement paste containing GGBFS", *Cem and Concr Compos* ;30:992–9.

Xu, Y., Wong, Y.L., Poon, C-S., Anson, M. (2003), "Influence of PFA on cracking of concrete and cement paste after exposure to high temperatures", *Cem and Concr Res.* 2003;33:2009–16.

Yu, X., Wong, Y.L., Poon, C.S., Anson, M. (2000), "Damage to PFA concrete subject to high temperatures", *Proceedings of International Symposium on High Performance Concrete-Workability, Strength and Durability, Hong Kong, 2000 pp.1093–1100.*

Naser Alimrani (1989), PhD student at the Department of Construction Materials and Technologies, Budapest University of Technology and Economics. His main fields of research interest are: fire design and behaviour of concrete at elevated temperature.
alimrani.naser@epito.bme.hu

Abdelmelek Nabil (1992), PhD student at the Department of Construction Materials and Technologies, Budapest University of Technology and Economics. His main fields of research interest are: fire design and behaviour of concrete at elevated temperature.
abdelmelek.nabil@epito.bme.hu

György L. Balázs (1958), Civil Engineer, PhD, Dr.-habil., professor of structural engineering, head of Department of Construction Materials and Technologies and Deputy Dean of the Civil Engineering Faculty of Budapest University of Technology and Economics (BME). His main fields of activities are experimental investigation and modelling of RC, PC, FRC structures, HSC, fire resistance of concrete. He is chairman of several commissions and task groups of ***fib***. He is president of Hungarian Group of ***fib***, Editor-in-chief of the Journal "Concrete Structures". He was elected as President of ***fib*** for the period of 2011-2012.
balazs.gyorgy@epito.bme.hu

Éva Lublóy (1976), Dr.-habil, PhD, Senior lecturer in structural engineering, at the Budapest University of Technology and Economics. Her main fields of interest are: fire design, behaviour of constructions materials at elevated temperature. Member of the Hungarian Group of ***fib***.
lubloy.eva@epito.bme.hu

SHEAR STRENGTH OF FRC BEAMS WITH REDUCED SHEAR REINFORCEMENT


Kálmán Koris – István Bódi

During the design of reinforced concrete beams at least a minimum amount of shear reinforcement must be applied according to the detailing rules of EC2. However, the assembly of shear reinforcement is usually a time and labour-intensive process which may reduce the effectiveness of the mass production of prefabricated concrete elements. A possible way to improve the overall performance of concrete members is to use fibre reinforced concrete. The objective of our research was to find out, whether the use of appropriate fibre reinforcement could partially or fully replace the conventional shear reinforcement in prefabricated beams for building construction. Analytical and numerical analysis was carried out on different prefabricated prestressed floor beams to compare their behaviour for shear. Analysed beams were made of steel fibre reinforced concrete, with or without lightened conventional shear reinforcement. The effect of fibre dosage on the shear and bending capacity of FCR beams was investigated and quantified by numerical analysis. Results of numerical analysis were verified by test results, and they were also compared to results of analytical calculations. The amount of steel fibre reinforcement needed to be able to replace conventional shear reinforcement was determined for the examined beam. The mixed application of steel fibre reinforcement and lightened conventional reinforcement was also analysed and evaluated.

Keywords: prefabrication, prestressing, steel fibre reinforced concrete, shear strength, bending strength

1. INTRODUCTION

In connection with the structural engineering, the applied materials, structural solutions and construction techniques depend on many different factors like function and location of the building, architectural, structural, building installation and environmental requirements, available building materials, professional capacity of the building contractors, climatic conditions, available construction time, financial opportunities, as well as others. Current tendencies in Hungary show a significant shortage of labour in the construction industry which requires the application of less labour-intensive structural solutions in the prefabrication industry, too. The application of materials like high strength and/or fibre reinforced concrete for prefabricated structural members is a promising way to reduce the demand for labour of reinforcement assembly and speed up the construction process. According to the detailing rules of EN 1992-1-1 standard a certain minimum amount of shear reinforcement must be applied for the design of reinforced concrete beams. The applied shear reinforcement can be, however, decreased below the required minimum, or it may be even completely neglected by the application of proper fibre reinforcement. The objective of our research was to find out whether the use of fibre reinforced concrete mixture could partially or fully replace the conventional shear reinforcement in prefabricated beams for industrial halls.

The concept of using fibres as reinforcement is not new, they have been used as reinforcement since ancient times. Fibres are usually used to increase ductile behaviour of concrete, control cracking due to plastic and drying shrinkage, reduce bleeding of water and permeability of concrete, and produce a better resistance against dynamic impacts (Balázs, 1999). Generally, fibres do not increase the flexural strength of structural members, however, shear strength can be significantly improved as tensile strength of the concrete is increased by the application of fibre reinforcement (Balázs, Kovács, 1997; Balázs, Kovács, Erdélyi, 1999; Dulácska, 1999; Kovács, Balázs, 2003; Kovács, Balázs, 2004).

The present research was preceded by previous studies. To find the fibre type that is best suited to the objective set in terms of performance, workability and efficiency an extensive experimental program was carried out at the Laboratory of Materials and Structures, Budapest University of Technology and Economics (Kovács, 2014). Another experimental program was also carried out at the Structural Laboratory of Budapest University of Technology and Economics between 2014-2015. In this experimental program the shear strength of small span, prefabricated, prestressed beams without conventional shear reinforcement, but with variable fibre type and content were tested (Koris et al. 2015). During the current research we focused on the shear capacity of larger span (12-25 m) prefabricated, prestressed FRC beams without or with lightened shear reinforcement. Within the frames of the research, both analytical and numerical approaches were used. Results of analytical and numerical calculations were compared to available test results.

2. ANALYTICAL APPROACH

2.1 Tested beam specimens

In frames of the present research four different prefabricated, prestressed FRC floor beams were studied (*Fig. 1*). Beam types

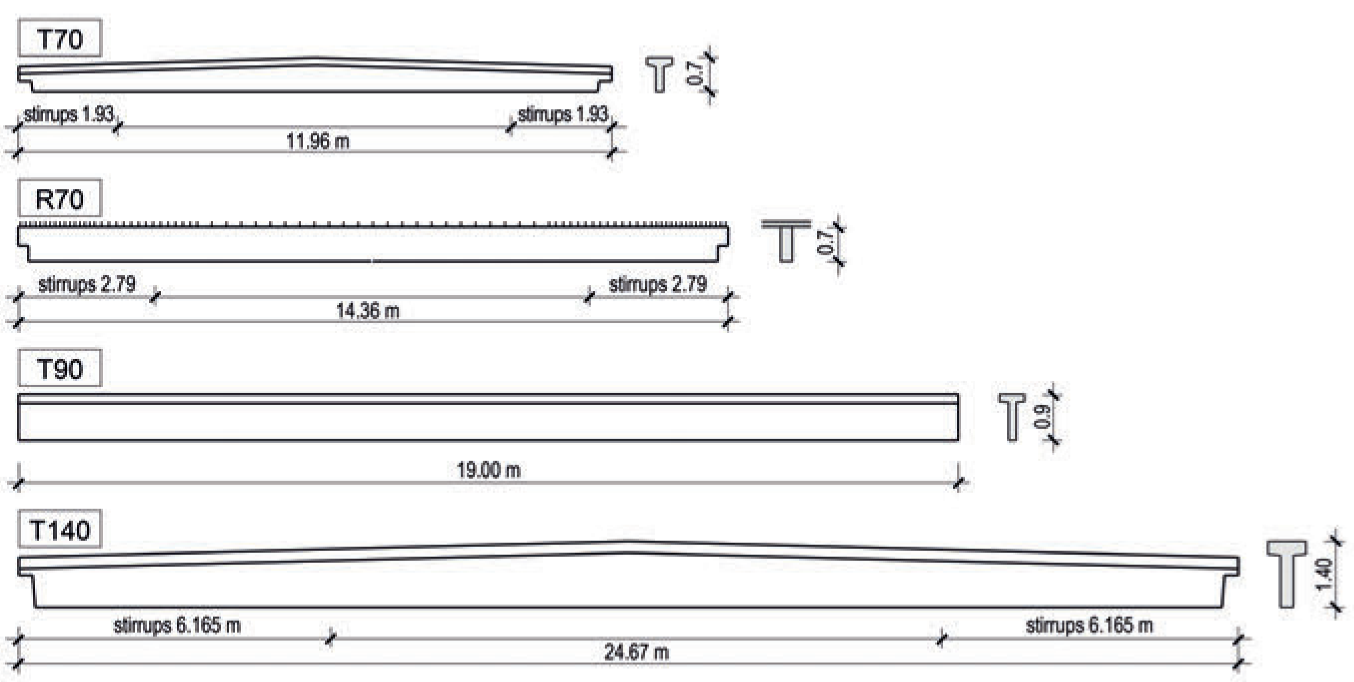

Fig. 1*: Side view and cross-section of tested beams*

T70 and T140 have T section of variable height, beam type T90 has constant height and beam type R70 has rectangular cross-section. This latter beam works together with a 15 cm thick in-situ reinforced concrete slab in the final state. Conventional shear reinforcement (closed stirrups) was completely neglected for beam type T90 and 30 kg/m^3 Dramix steel fibres were applied in this element. Other three beam types include stirrups at their ends, and they were manufactured using 20 kg/m^3 Dramix steel fibre dosage. All beam types except T90 had notched ends. Typical shapes, cross-sections and main dimensions of analysed beams are illustrated in *Fig. 1*. Concrete grades, as well as the applied longitudinal reinforcement of different beams are shown in *Table 5*.

2.2 Calculation of the shear strength of FRC beams

Since the EN 1992-1-1 standard (EC2) does not provide guidance on the detailed analysis of fibre reinforced concrete structures, therefore the effect of fibre reinforcement on shear strength was considered on the basis of the *Steel Fibre Concrete Directives from German Committee on Reinforced Concrete* (DAfStb-Richtlinie Stahlfaserbeton, 2012), which also conforms to the Eurocode standard system. According to the DAfStb directives, steel fibre reinforced concrete beams can be classified into the strength classes L1 and L2 based on the characteristic bending-tensile strength that can be measured after the cracking of the concrete. The L1 performance class delivers the characteristic post-cracking bending-tensile strength of concrete in serviceability limit state, while class L2 stands for post-cracking bending-tensile strength in ultimate limit state. Classification of fibre reinforced concrete is performed by four point bending test on at least 6 beam specimens (*Fig. 2*).

The characteristic post-cracking bending-tensile strength that belongs to class L1 or L2 can be calculated from the *F* force belonging to δ_{L1}=0.5 mm or δ_{L2}=3.5 mm displacement according to the measured force-displacement diagram (*Fig. 3*). The values of average post-cracking bending-tensile strength for L1 and L2 classes can be obtained as:

Fig. 2*: Test arrangement for the determination of characteristic post-cracking bending-tensile strength*

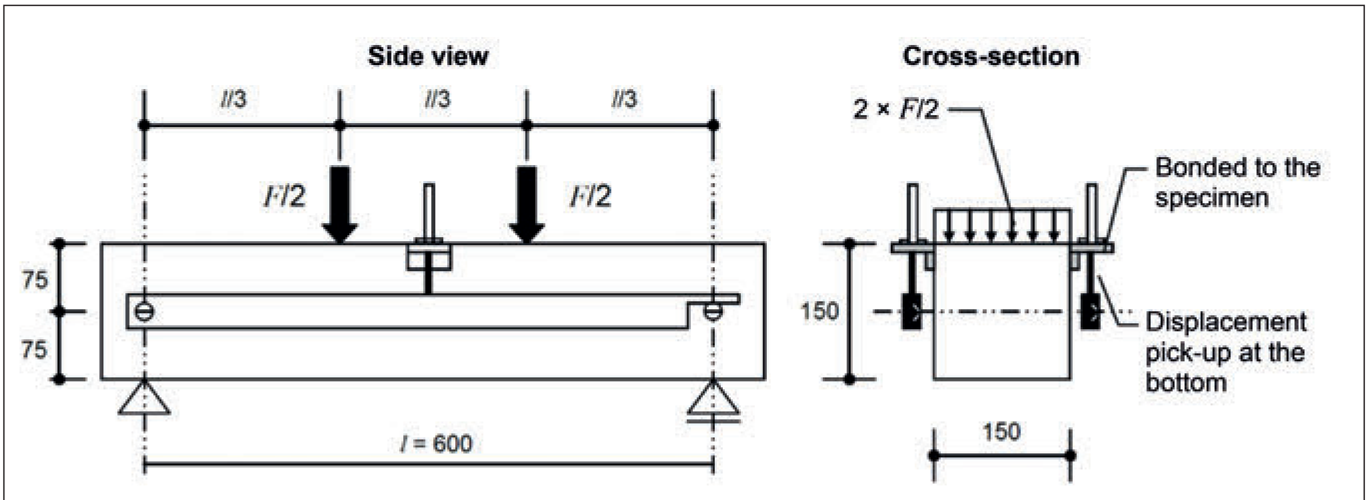

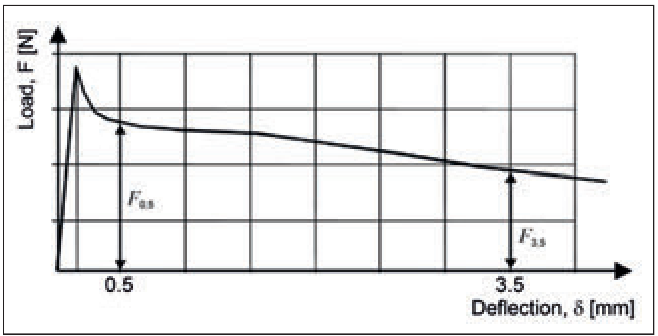

Fig. 3: Measured force-displacement diagram for the determination of characteristic post-cracking bending-tensile strength

$$f^{\mathrm{f}}_{\mathrm{cflm,L1}} = \frac{1}{n}\sum_{i=1}^{n}\frac{F_{0.5,\mathrm{i}}\cdot l}{b_{\mathrm{i}}\cdot h_{\mathrm{i}}^{2}} \qquad \text{and} \qquad f^{\mathrm{f}}_{\mathrm{cflm,L2}} = \frac{1}{n}\sum_{i=1}^{n}\frac{F_{3.5,\mathrm{i}}\cdot l}{b_{\mathrm{i}}\cdot h_{\mathrm{i}}^{2}}$$

where b, h and l specify the size of the specimen, i is the number of the specimen, while $F_{0.5,\mathrm{i}}$ and $F_{3.5,\mathrm{i}}$ are the loads belonging to the 0.5 mm and 3.5 mm deflections, respectively. The characteristic value of post-cracking bending-tensile strength – as the measure of the performance class – can be determined by the following form:

$$f^{\mathrm{f}}_{\mathrm{cflk,Li}} = e^{\left(Lf^{f}_{cflm,Li} - k_s \cdot Ls\right)} \leq 0.51 \cdot f^{\mathrm{f}}_{\mathrm{cflm,Li}}$$

where:

$Lf^{\mathrm{f}}_{\mathrm{cflm,Li}} = 1/n \cdot \sum ln\left(f^{\mathrm{f}}_{\mathrm{cfl,Li,i}}\right)$ is the mean value of the logarithmic measurement results,

$$Ls = \sqrt{\frac{\sum\left[Lf^{\mathrm{f}}_{\mathrm{cflm,Li}} - ln\left(f^{\mathrm{f}}_{\mathrm{cfl,Li,i}}\right)\right]^{2}}{n-1}}$$

is the standard deviation of logarithmic measurement results, and k_s is the value of the conversion factor between the mean value and the characteristic value (5% fractile) of post-cracking bending-tensile strength at 75% confidence level (*Table 1*).

The shear strength of fibre reinforced concrete beams can be calculated from the $f^{\mathrm{f}}_{\mathrm{cf0,u}}$ post-cracking centric tensile strength of the concrete. In case of ultimate limit state (class L2) the centric tensile strength may be determined from the bending-tensile strength using a β_s=0.37 conversion factor:

$$f^{\mathrm{f}}_{\mathrm{cf0,u}} = \beta_s \cdot f^{\mathrm{f}}_{\mathrm{cflk,L2}}$$

Table 1: The k_s factor for the conversion between the mean and characteristic values as a function of the number of specimens (DAfStb-Richtlinie Stahlfaserbeton, 2012)

Number	Number of specimens n	Conversion factor k_s
1	6	2.336
2	9	2.141
3	12	2.048
4	15	1.991
5	20	1.932
6	25	1.895
7	100	1.760
8	∞	1.645

The size of structural element as well as the fibre orientation must be considered for the calculation value of post-cracking centric tensile strength:

$$f^{\mathrm{f}}_{\mathrm{cfR,i}} = \kappa^{f}_{G}\cdot\kappa^{f}_{F}\cdot f^{\mathrm{f}}_{\mathrm{cf0,u}}$$

where $\kappa^{f}_{G} = 1{,}0 + A^{\mathrm{F}}_{\mathrm{ct}}\cdot 0{,}5 < 1{,}70$ is the factor for the consideration of structural element size, that is the cross-sectional area under tension ($A^{\mathrm{F}}_{\mathrm{ct}}$) and κ^{f}_{F} is the factor that takes fibre orientation into account. In general cases the fibre orientation factor can be taken as 0.5, while for flat, horizontal structural members like floor slabs its value is 1.0. The design value of centric tensile strength is:

$$f^{\mathrm{f}}_{\mathrm{cfd,i}} = \frac{\alpha^{f}_{c}\cdot f^{\mathrm{f}}_{\mathrm{cfR,i}}}{\gamma^{f}_{ct}}$$

where α^{f}_{c} =0.85 is the coefficient taking account the long term effects on the compressive strength and γ^{f}_{ct} =1.25 is the partial safety factor. The additional shear strength that is provided by the steel fibres can be calculated from the design centric tensile strength:

$$V_{Rd,cf} = f^{\mathrm{f}}_{\mathrm{cfd,i}}\cdot b_w \cdot h$$

where b_w is the web thickness and h is the overall height of the beam.

The additional shear strength provided by the fibres can be summarised with the shear strength of concrete to obtain the total shear strength of the concrete cross section. The shear resistance of the member without shear reinforcement is satisfactory if the following criterion is fulfilled (Gödde et al. 2010):

$$V_{Rd,c} + V_{Rd,cf} \geq V_{Ed}$$

where $V_{Rd,c}$ is the design shear resistance of the member without shear reinforcement calculated according to EC2, and V_{Ed} is the design value of the applied shear force.

The performance class of an FRC beam is influenced by several factors, like the grade of concrete, type, size, amount and orientation of applied fibres, concrete casting method, etc. (Rosenbusch, 2003). The effect of these factors can be determined by the evaluation of test results described above. However, in our situation, the performance class of the tested beams was not determined by the manufacturer, only the amount and type of applied fibres were known. Therefore, the performance class was approximately determined based on the empirical data available in the relevant literature. *Table 2* illustrates the considerable performance class values as a function of the fibre type, fibre slenderness (λ=fibre length/

Table 2: Considerable performance classes depending on the fibre type, fibre slenderness and fibre content

Performance class [N/mm²]	Fibre content [kg/m³]				
	Wire fibres			Sheet metal strips	Steel swarf
	λ = 45	λ = 65	λ = 80		
1.0	30	20	15	60	80
1.5	40	30	25	> 100	> 100
2.0	50	40	30	> 100	> 100
2.5	> 70	50	40	> 100	> 100
3.0	> 85	60	50	> 100	> 100

Table 3: The effect of applied concrete grade on the performance class

Performance class	Concrete grade		
	C25	C35	C45
0	1.1	1.3	1.5
1	1.6	1.9	2.3
2	2.1	2.6	3.0
3	2.6	3.2	3.8

fibre diameter) and fibre volume in case of C25/30 concrete grade (Schwarz, 2002).

The effect of applied concrete grade on the performance class was considered by interpolating or extrapolating the empirical data from *Table 3* (Schwarz, 2002).

In our case the studied beams were made of grade C40/50 or C50/60 concrete with 20 kg/m³ or 30 kg/m³ Dramix fibre dosage. The slenderness of the applied 45 mm long and 1 mm thick steel fibres was λ = 45mm / 1mm = 45. Plotting the corresponding data from *Table 2* we may determine the regression function that describes the connection between performance class values and the fibre volume (*Fig. 4*). The regression function can be written as following:

$$L = -0{,}0003 \cdot V^2 + 0{,}0663 \cdot V - 0{,}7184$$

where L is the value of performance class (that is the characteristic value of post-cracking bending-tensile strength) and V is the fibre volume. According to the procedure described above the values of centric tensile strength were determined for the tested beams, considering the appropriate concrete grades and fibre volumes (*Table 4*).

2.3 Analytical verification of the tested beams

Compliance of the tested beams was verified by analytical calculations according to EN 1992-1-1 standard. Loads acting on the beams were assumed to adapt to the actual design situation. During the calculation most of the variables (e.g. cross-sectional properties, internal forces, stresses) were treated as functions thus changing height of the beams (T70, R70 and T140) could be also considered. Initial prestress in the tendons was calculated from the 110 kN tensioning force that was applied by the manufacturer for the construction of the members.

The distribution of prestress in the tendons was determined

Fig. 4: Connection between the applied fibre volume and the performance class in case of C25/30 concrete, steel wire fibres and λ=45 fibre slenderness

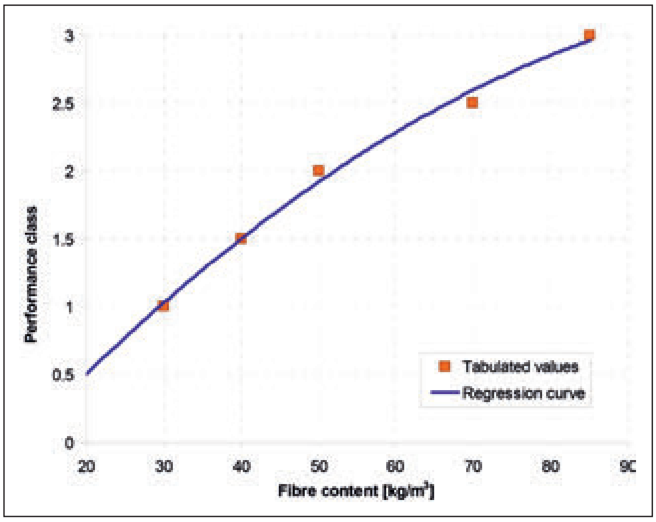

Table 4: Determination of centric tensile strength for the tested beams

Beam type	Concrete grade	Fibre volume [kg/m³]	Performance class (L2) [N/mm²]		Centric tensile strength [N/mm²]
			C25/30	Actual concrete	
T70	C40/50	20	0.488	0.631	0.233
R70	C40/50	20	0.488	0.631	0.233
T90	C50/60	30	1.001	1.564	0.579
T140	C50/60	20	0.488	0.736	0.272

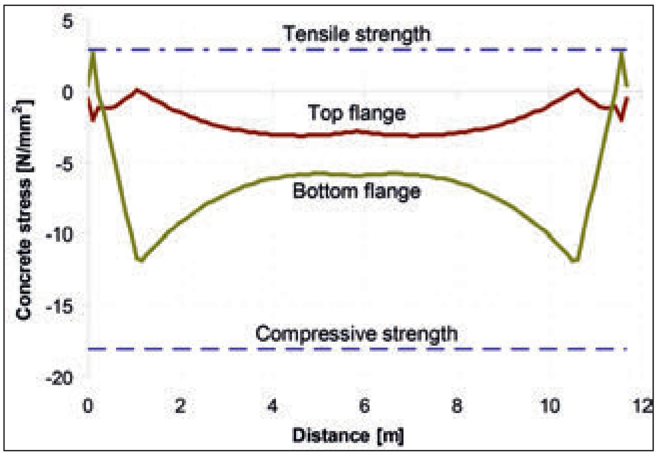

Fig. 5: Distribution of concrete stresses in initial state (t=0) in beam type T70

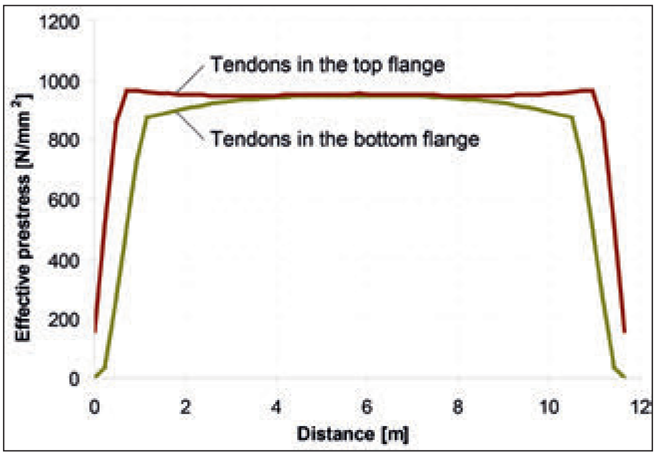

Fig. 6: Effective prestress in different tendons in final state (t=∞) in beam type T70

in initial state (after releasing the tendons, t=0), and concrete stresses were verified (*Fig. 5*). The loss of prestressing force due to shrinkage, creep and relaxation was calculated and the distribution of effective prestress was determined in final state (t=∞). *Fig. 6* illustrates the distribution of effective prestress in beam type T70. Bending moment resistances of different beams were verified considering the calculated effective prestress values. In case of beam type R70 a 15 cm think in-situ concrete (grade C30/37) slab was also taken into account for the determination of bending moment resistance. The corresponding detailing rules of EC2 were neglected during the verification of shear strength because of the reduced (or completely missing) shear reinforcement, but at the same time the effect of fibre reinforcement was considered (see chapter 2.2).

Serviceability limit states (including stress limitation, deflection control and crack width control) as well as transition states (lifting, transportation) were also verified. The ends of the beams (anchorage region of the tendons) were verified for transverse tension taking into account the shear utilization of the stirrups. Results of the analytical calculations are briefly introduced in the following chapter.

2.4 Results of the analytical approach

Most important results of the analysis are summarized in *Table 5*. According to the comprehensive study of the beams, we may conclude that despite the reduced (or neglected) shear reinforcement the tested members meet the requirements in most design situations. However, we encountered some problems with the shear strength, as well as with the transverse tensile strength at the ends of the beams. *Fig. 7* illustrates the distribution of design shear force and shear resistance along the beam type T70. The end of the beam is satisfactory for shear, but there are regions along the length where design shear force slightly exceeds the shear resistance. Shear strength of the concrete, the fibres and the shear reinforcement together would be able to provide appropriate resistance. However, EC2 does not allow the summary of concrete and steel strength values in a shear design situation as an approximation to the safe side.

In order to have satisfactory structural elements also for shear and transverse tension, the concrete grade, the diameter or spacing of the stirrups and/or the applied fibre volume may be modified. For the studied beams the concrete grade and the amount of stirrups was left unchanged but an increased fibre volume was assumed (for beam types T70, R70 and T90 40 kg/m^3, and for the beam T140 60 kg/m^3 Dramix fibres were considered). According to the calculations, all beam types were satisfactory for shear and transverse tension with the increased fibre volume. *Fig. 8* illustrates the distribution of design shear force and shear resistance along the beam type T70 with fibre volume increased to 40 kg/m^3. Results of the analysis showed that the application of the right type and amount of fibres can partially replace the conventional shear reinforcement in prefabricated floor beams. If we want to completely neglect the stirrups from the beams, the fibre volume must be significantly increased to have equivalent shear strength (see also the numerical results in chapter 3). However, concrete mixing and casting in case of such high fibre volumes is still a challenge for the domestic concrete industry.

3. NUMERICAL ANALYSIS

The effect of applied steel fibre volume on the shear strength of prestressed beams was analysed using the ATENA v5.1.1 nonlinear finite element software. This software allows the consideration of both conventional and fibre reinforcement, as well as geometric and material nonlinearity for the calculation of structural behaviour. The numerical analysis with the ATENA software is a rather time-consuming process; therefore,

Table 5: *Results of the analytical calculations*

			Type of beam			
			T70	R70	T90	T140
Shape of the cross-section				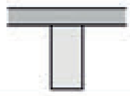	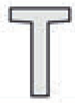	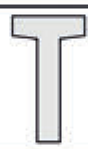
Total length	L [m]		11.96	14.36	19.00	24.67
Heigh (at midspan)	h [m]		0.70	0.70	0.90	1.40
Concrete grade (prefabricated girder)			C40/50	C40/50	C50/60	C50/60
Dramix fibre volume [kg/m^3]			20	20	30	20
Longitudnial reinforcement	Bottom		2Ø16 + 2×3Fp93	3×4Fp93	-	4×4Fp93
	Top		2Ø16 + 2×Fp52	4×Fp52	-	2×Fp52
Design load [kN/m]			25.34	38.28	18.97	32.92
Concrete stresses at t=0 time			satisfactory	satisfactory	satisfactory	satisfactory
Bending moment capacity at midspan	M_{Ed} [kNm]		425.11	934.23	798.58	2381.20
	M_{Rd} [kNm]		638.26	1333.86	1105.30	2812.68
	Verification		satisfactory	satisfactory	satisfactory	satisfactory
Shear capacity at the end of the beam	V_{Ed} [kN]		144.72	263.69	174.04	385.09
	$V_{Rd,c}$ [kN]	Notched beam end	41.57	98.13	-	61.25
		Full cross-section	82.84	184.83	154.35	242.23
	$V_{Rd,cf}$ [kN]	Notched beam end	3.29	6.45	-	5.14
		Full cross-section	6.50	13.25	21.45	19.58
	$V_{Rd,s}$ [kN]		149.62	336.66	-	413.71
	Verification		satisfactory	satisfactory	satisfactory	satisfactory
Stress limitation	Max. concrete stresses		satisfactory	satisfactory	satisfactory	satisfactory
	Max. steel stresses		satisfactory	satisfactory	satisfactory	satisfactory
Deflection of midspan	y_d [mm]		15.4	23.5	72.2	16.0
	y_{adm} [mm]		46.6	56.6	73.4	97.5
	Verification		satisfactory	satisfactory	satisfactory	satisfactory
Crack width	w_d [mm]		crack free	0.16	0.04	crack free
	w_{adm} [mm]		0.20	0.20	0.20	0.20
	Verification		satisfactory	satisfactory	satisfactory	satisfactory

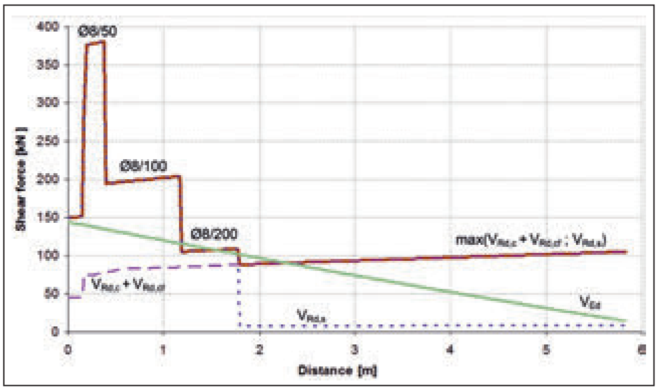

Fig. 7: Distribution of the design shear force and shear resistance in beam type T70 (fibre content 20 kg/m^3)

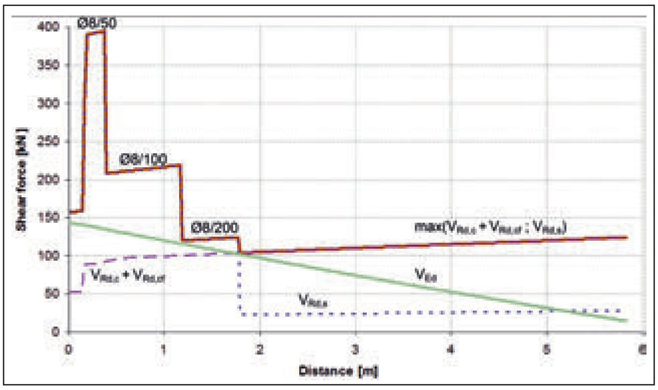

Fig. 8: Distribution of the design shear force and shear resistance in beam type T70 (fibre content 40 kg/m^3)

we modelled only one of the four beam types (T90). The numerical analysis intended to compare the shear strength of prestressed FRC beams with different amount of steel fibres and also to compare these values to the shear strength of a beam containing the amount of stirrups required by the EN 1992-1-1 standard. In addition to the shear analysis, the bending strengths of beams with different fibre volumes were also determined and compared, using the same numerical model (Karimi, 2016).

The analysed T90 beam was already introduced in chapter 2.1. This is a 19.00 m long prestressed T beam with a constant height of 90 cm. The longitudinal reinforcement of the beam was designed to conform the criteria of EC2 to bending and to serviceability limit states as well. Concrete grade used in numerical modelling was C50/60, the steel grade was S500 and the tensile strength of prestressing tendons was 1860 N/mm^2. Shape of the cross-section and the applied longitudinal reinforcement is shown in *Table 5*. In the numerical model fork support was applied according to the usual construction solution. The analyzed beam was symmetrical so it was possible to analyze only the symmetrical half, and thus the running time could be speeded up. In the calculations, the *CC3DNonLinCementitious2* material model built into ATENA was used to describe concrete behaviour. The beam was modelled by tetrahedral and brick elements, the average mesh size was 0.1 m (0.2 m mesh with 0.5 length coefficient). The finite element mesh applied for shear analysis is displayed in *Fig. 9*. To have constant shear force distribution on the beam, a concentrated force was applied 2.25 m from the support (*Fig. 9*). The load was applied in 20 kN steps to the structure. Bending strength analysis was performed on the same numerical model, but with four symmetrically arranged concentrated forces (on both sides 3.00 and 7.00 m from the support) for a constant bending moment in the middle section.

Concrete has a high capability to develop cracks. In order to evaluate the structure's load bearing capacity, knowing the cracking behaviour is very important. Using fibres in concrete proved to be effective in preventing primarily the crack propagation of the FRC structure. ATENA software offers a fracture-plastic model for concrete. Fracture-plastic model combines constitutive models for tensile (fracturing) and compressive (plastic) behaviour. The model can be used to simulate concrete cracking, crushing under high confinement (such as steel fibre reinforcement), and crack closure due to crushing in other material directions. One of the fundamental crack analysis parts is the crack bridging. In case of cyclic loading of a fibre reinforced concrete the crack bridging depends on two parts, fibre bridging and aggregate bridging. Lots of experiments have been done in order to predict the location of the first crack in a composite structure like fibre reinforced concrete. In ATENA software the widely known AKC-model (Aveston, Cooper and Kelly, 1971) is used to predict the stress and strain for the concrete containing fibres. The model is characterized by the elastic modulus, ultimate strain, fracture energy and volume of the concrete matrix, as

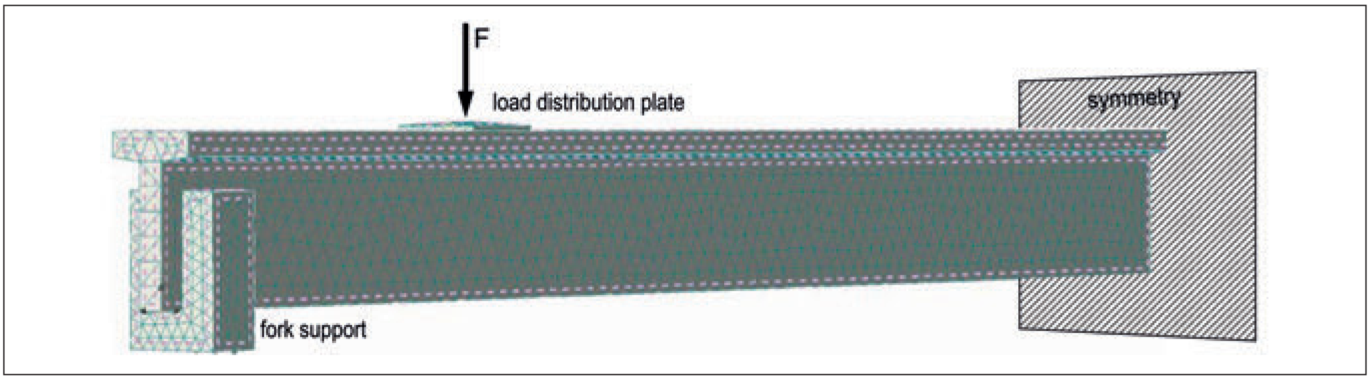

Fig. 9: Finite element mesh of the numerical model for shear analysis

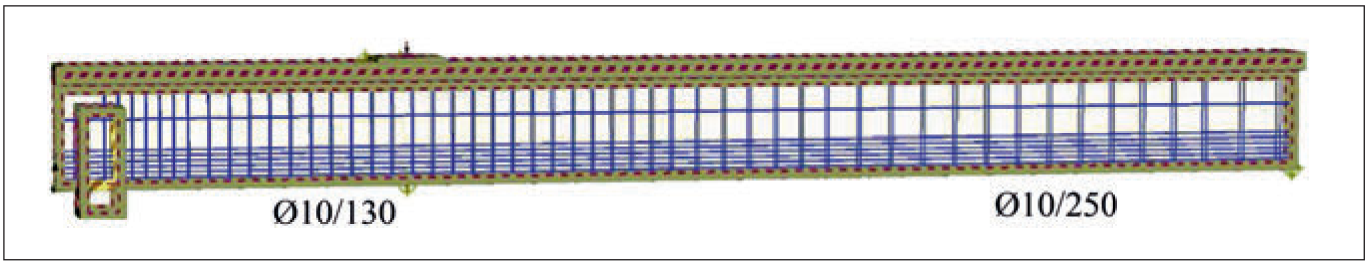

Fig. 10: Applied reinforcement in the numerical model in case of full shear reinforcement according to EC2

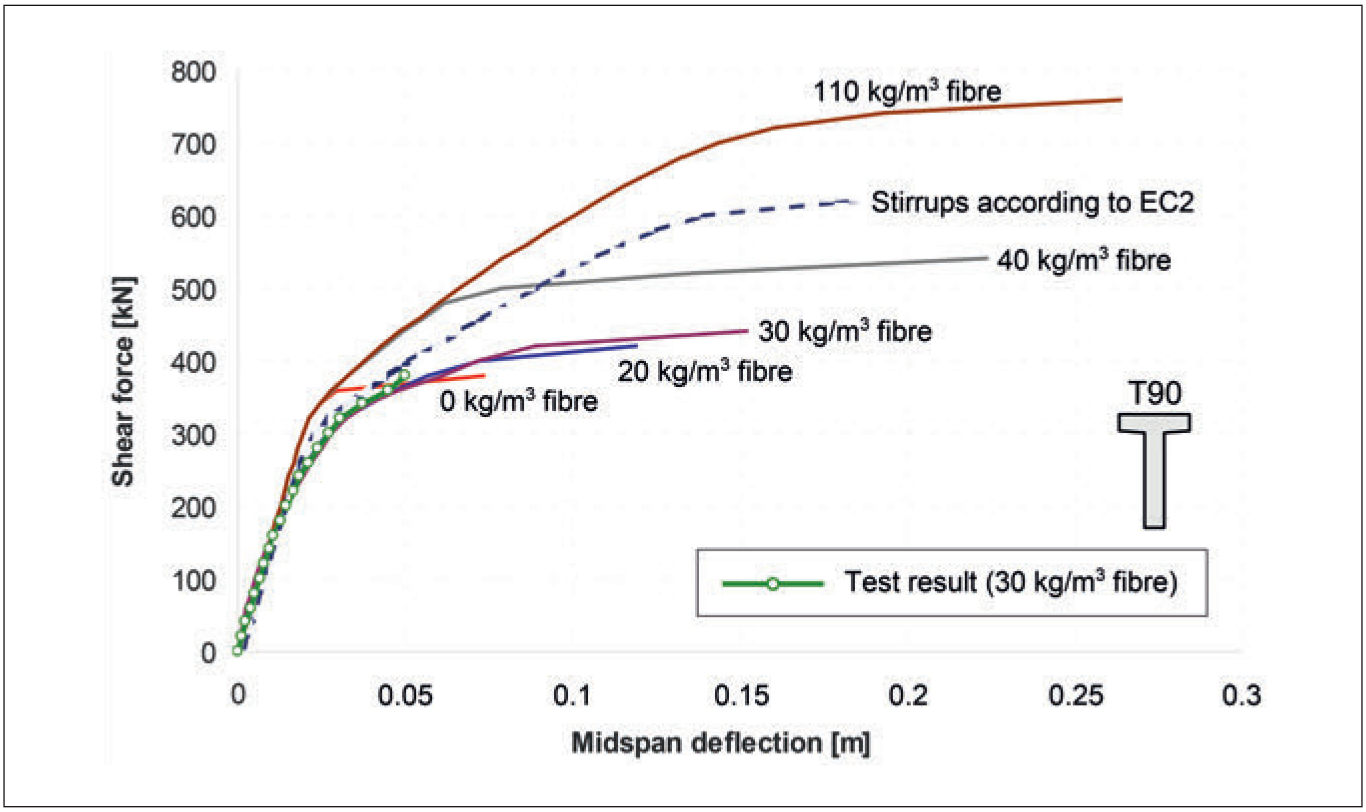

Fig. 11: Shear force–deflection diagrams of beams with different fibre volumes

well as the elastic modulus, ultimate strain and volume of the fibres. In the numerical model the amount of applied fibres was entered as a certain reinforcement ratio. Fibres were defined in 7 directions (direction of the 3 axes and 4 directions pointing to the middle of the octants). This modelling is not perfect in terms of the influence of fibre bond, but it definitely gives the general response including the strain hardening.

The beam was analysed in 6 different situations. In the first case stirrups fulfilling the requirements of EN 1992-1-1 standard were applied in the beam (*Fig. 10*). In five more cases the beam was modelled without stirrups, but with variable fibre contents (0, 20, 30, 40, 110 kg/m^3).

During the numerical analysis the shear force–deflection diagrams and the corresponding shear capacities were determined for each shear reinforcement type. The results of the shear strength are shown in *Fig. 11*. Based on these results, the shear capacity of the beam increases by increasing the amount of fibre reinforcement, however, it is clear that the 30 kg/m^3 fibre content applied in the test beam is not able to provide the same shear resistance as the conventional stirrups according to EC2. It can be seen from *Fig. 11* that only a significantly higher fibre dosage (about 75 kg/m^3) than the typically applied 20-40 kg/m^3 can provide the shear strength that is equivalent to the shear strength of stirrups. The mixing and casting of concrete with such high fibre contents can be difficult using the existing technologies in Hungary. Thanks to the crack bridging effect of the steel fibres, the ductility of the beam significantly increases by the increase of fibre dosage. *Fig. 12* illustrates the distribution of shear cracks in ultimate limit state in case of different fibre

Fig. 12: Distribution of shear cracks in ultimate limit state in case of different fibre volumes

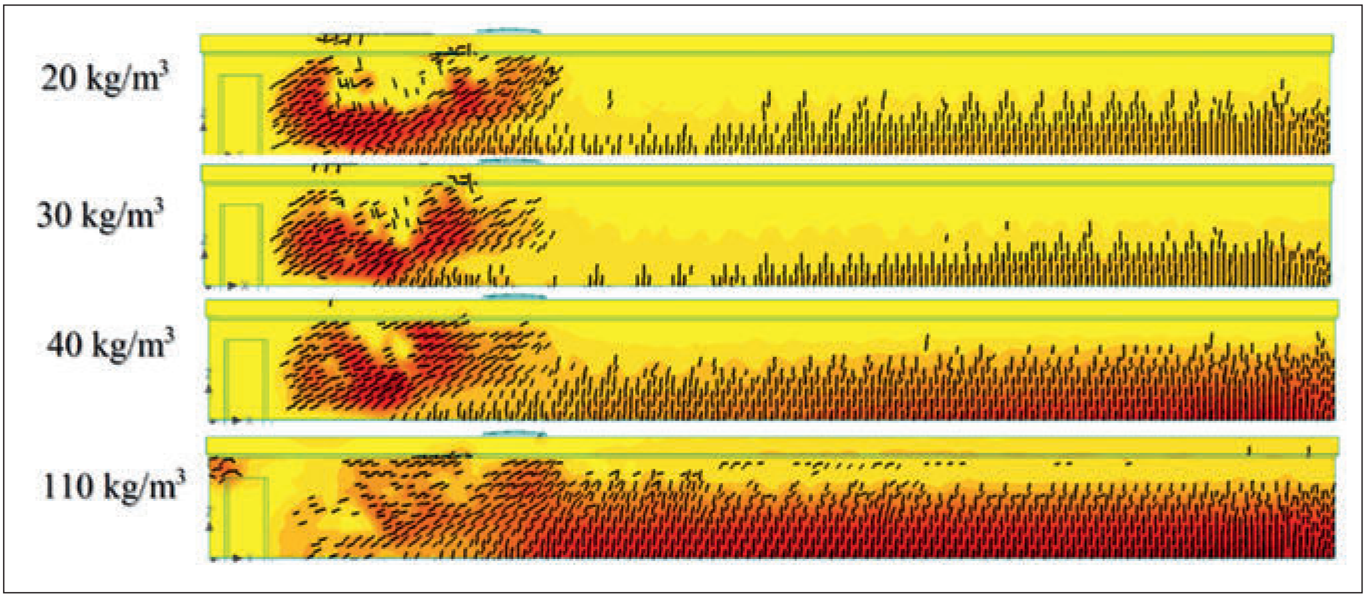

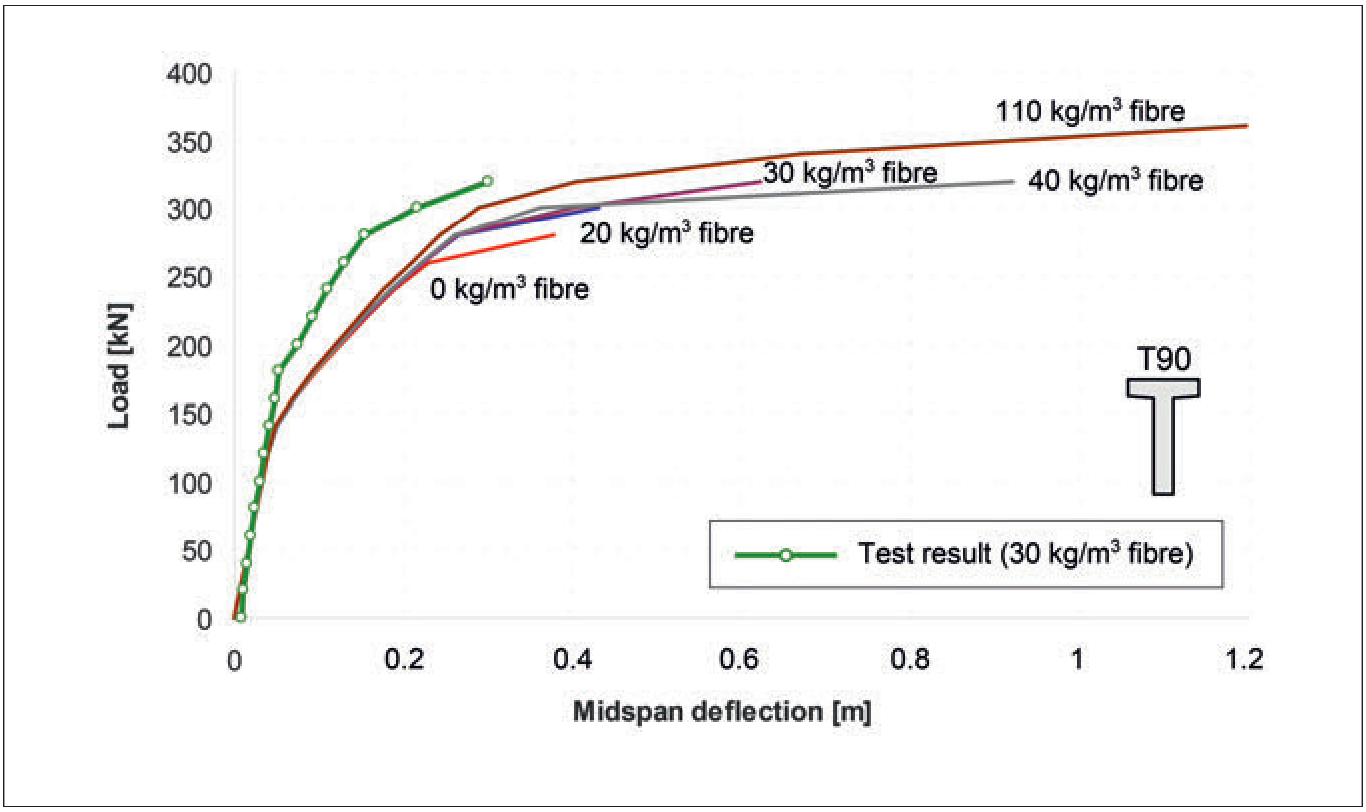

Fig. 13: Bending load–deflection diagrams of beams with different fibre volumes

volumes. The figure shows that the number and spacing of cracks increase as we increase the amount of fibres, because due to the tensile strength of the fibres, the larger part of the beam is engaged in the load bearing. This of course enables the increase of shear strength and a more ductile behaviour.

It was also observed during the numerical modelling, that while shear strength can be efficiently increased by the application of proper fibre dosage, the bending moment resistance does not increase considerably even if the amount of fibres is significantly increased. Calculated load–deflection diagrams for bending are shown in *Fig. 13*. If we increase the fibre dosage from 20 kg/m^3 to 110 kg/m^3 for the analysed T90 beam, the bending capacity is increased by 20% only, while the increase in shear capacity is 81%. Of course, the ductility for bending will be considerably higher by increasing the fibre dosage, which could be an important advantage in certain design situations. *Fig. 14* illustrates the distribution of bending cracks in ultimate limit state in case of different fibre volumes. It may be seen from the figure that the number of cracks increases in case of higher fibre volumes so a larger part of the beam is involved in the load bearing, but the crack pattern does not significantly change in the middle cross-section that is most used for bending. That means there is no significant difference in the bending moment resistance between the different versions.

4. CONCLUSIONS

We can conclude that steel fibre reinforcement significantly increases the shear strength, and slightly increases the bending strength of prestressed concrete beams. However,

Fig. 14: Distribution of bending cracks in case of different fibre volumes

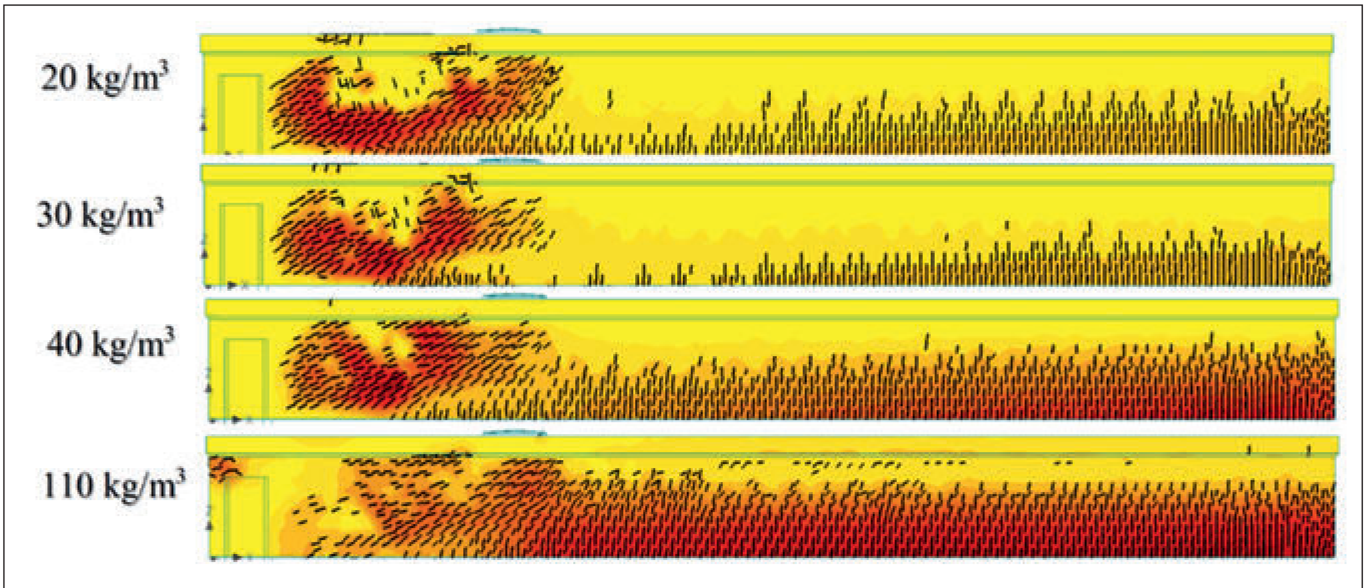

in case of the studied beam, only a significant amount of steel fibre reinforcement (75 kg/m^3 or greater) could replace the conventional shear reinforcement (closed stirrups). The mixing and casting of concrete with such high fibre content can be technologically problematic with the use of the currently available domestic pre-casting technologies. According to the analytical and numerical calculations, it could be a suitable and economical production alternative for prestressed concrete beams (that are not subjected to dynamic loads or fatigue) to provide the shear strength by the mixed application of about 40 kg/m^3 steel fibre content and conventional stirrups with lightened spacing at places that are most utilized for shear. As it is also shown by some foreign approaches (Grunert et al. 2004), a more economical production of such structural elements may be achieved if we completely neglect the stirrups from prestressed concrete floor beams by using high strength concrete (HSC) mixtures and by significantly increasing the fibre content, which of course requires the development of manufacturing technology, too.

5. REFERENCES

Aveston, J., Cooper, G. A., Kelly, A. (1971), „The Properties of Fibre Composites", *Conference Proceedings*, National Physical Laboratory (IPC Science and Technology Press Ltd, Paper I, p. 15.

Balázs, L. Gy., Kovács, I. (1997), „Increase in shear strength of beams by applying fiber reinforcement", *Proceedings, Symposium organized for the 65th birthday of Prof. G. Mehlhorn* „Materialmodelle und Methoden zur wirklichkeitsnahen Berechnung von Beton-, Stahlbeton- und Spannbetonbauteilen" (eds. F. Blaschke, G. Günther, J. Kollegger), ISBN 3-88122-903-5, Kassel, pp. 10-17.

Balázs, L. Gy. (1999), „Fibre reinforced concrete – from the research till the application" (in Hungarian), *Conference Proceedings*, Hungarian Group of *fib*, Budapest, ISBN 963-420-589-5.

Balázs, L. Gy., Kovács, I., Erdélyi, L. (1999), „Flexural behaviour of RC and PC beams with steel fibers", *Proceedings 3rd Int. Workshop on High Performance Fiber Reinforced Cement Composites*, (eds. H.W. Reinhardt and A.E. Naaman), Mainz, pp. 499-508.

Dulácska, E. (1999), „Design theory of steel fibre reinforced concrete and reinforced concrete" (in Hungarian), *Proceedings of the Conference: Fibre reinforced concrete – from the research till the application*, Hungarian Group of *fib*, Budapest, ISBN 963-420-589-5.

Gödde, L., Strack, M., Mark, P. (2010), „Structural elements made of steel fibre reinforced concrete and steel fibre strengthened concrete", (in German), *Beton- und Stahlbetonbau 105 (2010), Heft, 2* Ernst & Sohn Verlag für Architektur und technische Wissenschaften GmbH & Co. KG, Berlin, p. 78-91.

Grunert, J., P., Strobach, C., Teutsch, M. (2004), „Prestressed steel fibre reinforced SCC beams without steel reinforcement", (in German), *BFT International 2004/04*, Bauverlag BV GmbH, Gütersloh, p. 50-55.

Kovács, I., Balázs, L., Gy. (2003), „Structural behaviour of steel fibre reinforced concrete", *Journal of Structural Concrete*, 2003/2, pp. 57-63.

Kovács, I., Balázs, L., Gy. (2004), „Structural performance of steel fibre reinforced concrete", Book, Publ. Comp. of Budapest University of Technology and Economics, ISBN 963-410-822-3, 233. p.

Kovács, G. (2014), „Partial replacement of reinforcement with fibre reinforced traditional concrete. Report 1: Fibre comparison and selection", ASA Construction Ltd. – Consolis Group Material Development Centre, Budapest.

Koris, K., Bódi, I., Polgár, L., Mansour, K. (2015) „Experimental analysis of the shear capacity of prestressed FRC beams", *Proceedings of the 8th International Conference Fibre Concrete 2015 - Technology, Design, Application*, Prague, 529 p., ISBN:978-80-01-05683-7.

Karimi, R. (2016), „DEM and FEM analysis of fibre-reinforced prefabricated concrete beams", MSc Thesis at the Budapest University of Technology, Faculty of Civil Engineering, Budapest.

Rosenbusch, J. (2003), „Shear force capacity of steel fibre reinforced beams", (in German), *Dissertation*, Technische Universität Braunschweig, Department of civil engineering, 199 p.

Schwarz, P. (2002), „Steel fibre reinforced concrete - New design principles: Performance classes" (in German), *Concrete-Industrial-Floors*.

Dr. Kálmán Koris (1970) civil engineer, graduated in 1993 at the Budapest University of Technology and Economics, PhD, Senior assistant professor at the Department of Structural Engineering, Budapest University of Technology and Economics. Research fields: safety of reinforced concrete structures, analysis of prefabricated, prestressed concrete structures, strengthening of structures. Member of the standardization subcommittee "NAD MSZ ENV 1992 Eurocode 2, Design of concrete structures" and the Hungarian Chamber of Engineers. Member of the Hungarian Group of ***fib*** and the public body of the Hungarian Academy of Sciences. koris.kalman@epito.bme.hu

Dr. István Bódi (1954) civil engineer, post-graduate engineer in mathematics, PhD, Associate professor at the Department of Structural Engineering, Budapest University of Technology and Economics. Research fields: Reconstruction and strengthening of reinforced concrete and conventional structures, modelling of timber structure joints. Member of the ACI (American Concrete Institute), the ACI Subcommitte#423 „Prestressed Concrete" and the Hungarian Chamber of Engineers. President of the standardization committee Eurocode 5 - MSZ NAD (Timber Structures). Member of the Hungarian Group of ***fib***. Member of the „Schweizerische Arbeitsgemeinschaft für das Holz". bodi.istvan@epito.bme.hu

CRACK WIDTH OF CONCRETE MEMBERS WITH SKEW REINFORCEMENT

Dedicated to the 90th anniversary of Prof. Árpád Orosz at TU Budapest

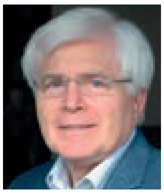

Andor Windisch, PhD, Prof. h.c.

In plane and spatial r.c. structural elements the direction of stress trajectories and of the mostly orthogonal reinforcement meshes are different. At dimensioning in addition to the choice of reinforcement directions and the evaluation of the amount of reinforcements in ULS, their control in SLS (crack width) are the fundamental task of the designer. The crack width control becomes more and more the governing requirement for the amount of rebars. The existing formulas in the codes are vague and impracticable.
The paper presents a theoretically sound and practical calculation model.

Keywords: crack width, skew reinforcement, efficiency factor

1. INTRODUCTION

At dimensioning of an orthogonal reinforcing mesh which is inclined to the principal stress/strain directions – in addition to the fulfilment of equilibrium and compatibility conditions – the control of the design crack width is a fundamental task. The question of the skew reinforcement is dealt since over 60 years by different researchers worldwide. Windisch (2000) gives an overview. During the last decades, especially due to the introduction of the partial safety factor-concept into the dimensioning, the control of crack width became the governing factor of the amount of reinforcement. Hence the crack control methods given in the codes and standards became more and more important. Nevertheless, the relevant methods in the model codes remained impractical and unchanged during the last 25 years. Based on a former paper (Windisch, 2000) of the author a theoretically sound and practical calculation model is presented herein.

2. MODEL CODE 2010

Chapter 7.6.4.4.3: Orthogonal reinforcement directions. Main provisions:
"If the cracks in a member reinforced in two orthogonal directions are expected to form at an angle which differs substantially (> 15°) from the direction of the reinforcement, the approximation by Eq. (7.6-8) and (7.6-9) may be used to calculate $l_{s,max}$ and w_d. The explanation is as follows:
When a more refined model is not available, the following expression for $l_{s,max}$ may be used:

$$l_{s,max,\theta} = \left(\frac{cos\theta}{l_{sx,k}} + \frac{sin\theta}{l_{sy,k}}\right)^{-1} \qquad \text{(MC2010 Eq. 7.6-8)}$$

Fig. 1: Figure 7.6-6 Basis for calculation of crack width for reinforcement deviation from the direction orthogonal to the crack.

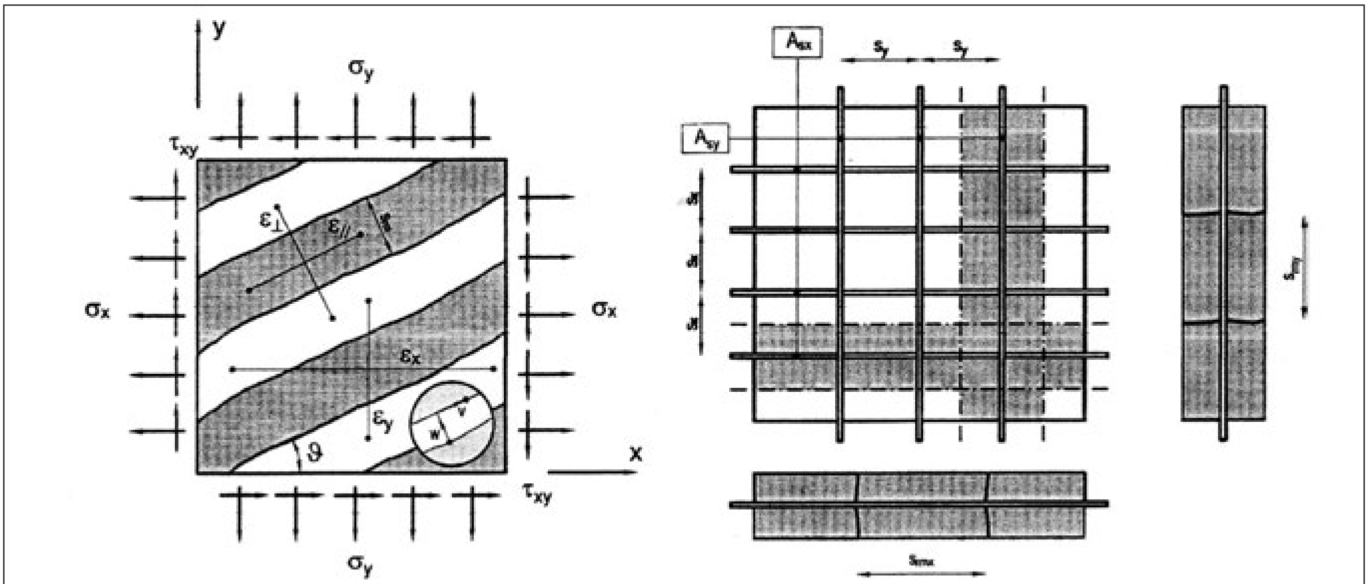

where

θ denotes the angle between the reinforcement in the x-direction and the direction of the principal tensile stress,

$l_{sx,k}$, $l_{sy,k}$ denote the max. crack spacings in the two orthogonal directions, calculated according to

$$l_{s,max} = k \cdot c + \frac{1}{4} \cdot \frac{f_{ctm}}{\tau_{bm}} \cdot \frac{\phi_s}{\rho_{s,ef}} \qquad \text{(MC2010 Eq. 7.6-4)}$$

The design crack width can then be calculated from:

$$w_d = 2 \cdot l_{s,max,\theta}(\varepsilon_\perp - \epsilon_{c,\perp}) \qquad \text{(MC2010 Eq. 7.6-9)}$$

where

$\varepsilon_\perp$ *and* $\epsilon_{c,\perp}$ represent the mean strain and the mean concrete strain, evaluated in the direction orthogonal to the crack (*Fig. 1:*Figure 7.6-6 of MC2010).

At derivation of Eq. (7.6-8) the tension chord model (Kaufmann, 1998) is extended to cracked panels. Instead of direct reference to the rebar's stress-strain characteristics and bond, relationships between the maximum steel stresses in the crack and average strains in x and y directions are established. In the concrete struts between the cracks (shaded areas in Fig. 7.6-6) compression softening is taken into account. After questionable approximations the Eq. (7.6-8) is presented. For more details see Kaufmann (1998). It should be noted that Eq. (7.6-4) refers to the slip length whereas Eq. (7.6-8) to the crack distance. The crack distance and the slip length are not interrelated to each other hence a certain incompatibility exists here.

The inapplicability of Eq. (7.6-9) can be revealed as both are "virtual" quantities (Bisch, 2016), i.e. incomprehensible, as in the ⊥-direction no reinforcement does exist: without steel stress and load transfer by bond no mean reinforcement strain can be calculated; it could be assumed that the mean strain could be calculated by FEM model using smeared crack philosophy. Nevertheless, what is then $\varepsilon_{c\perp}$? How can it be calculated? The support given in Kaufmann (1998) is rather confusing. Moreover, evaluation of test results (e.g. of Broms et al., 1965) showed that the mean strain ($\varepsilon = w/s$) is a poor characteristics of the cracking phenomenon.

3. THE EFFICIENCY FACTOR OF AN INCLINED REBAR

Windisch (1993, 2000) introduced and deduced the efficiency factor ψ of an inclined rebar, i.e. which runs at an angle α related to the direction of principal tensile stress (*Fig. 2*). It was shown that the stresses in the inclined rebars which fulfill the compatibility criterion

$$\Delta_\alpha = \frac{w_0}{2\cos\alpha} \qquad \text{and} \qquad s_\alpha = \frac{s}{\cos\alpha}$$

with

Δ_α slip in the crack, s_α crack distance, both independent of the angle α, are

$$\sigma_{s\xi} = \psi_\xi \cdot \sigma_{sn}\ ; \quad \sigma_{s\eta} = \psi_\eta \cdot \sigma_{sn}$$

where

ψ_ξ and ψ_η efficiency factors of the inclined rebars.

The steel stresses $\sigma_{s\alpha}$ for the different values of Δ_α and s_α were determined with a shooting technique, i.e. the boundary condition problem was converted into an initial-value problem. The rebar was modelled as an elastic steel rod which is elastically embedded in the concrete owing to the gripping action of the ribs. The forces in the concrete resulting from the embedment are calculated from the bond stresses, by applied the local bond stress-local slip relationship, similar to that in MC2010. The $\sigma_{s\alpha}$ values were calculated for different sets of rebar diameters, crack distances and crack widths/slip values. In order to simplify the evaluation and application of the results the efficiency factor of an inclined rebar was introduced:

$$\psi_\alpha = \frac{\sigma_{s\alpha}}{\sigma_{s0}} \qquad (3)$$

The values $\sigma_{s\alpha}$ and σ_{s0} correspond to the same values of (w, s). For practical purposes the following tri-linear function was defined:

$\psi = 1.0$ for $0° \leq \alpha \leq 10°$
$\psi = 1.0 - 0.01 \cdot (\alpha - 10)$ for $10° < \alpha \leq 30°$
$\psi = 0.8 - 0.015 \cdot (\alpha - 30)$ for $30° < \alpha \leq 70°$.

Fig. 2: Uniaxial tensile force taken by (a) parallel, and (b) inclined rebars

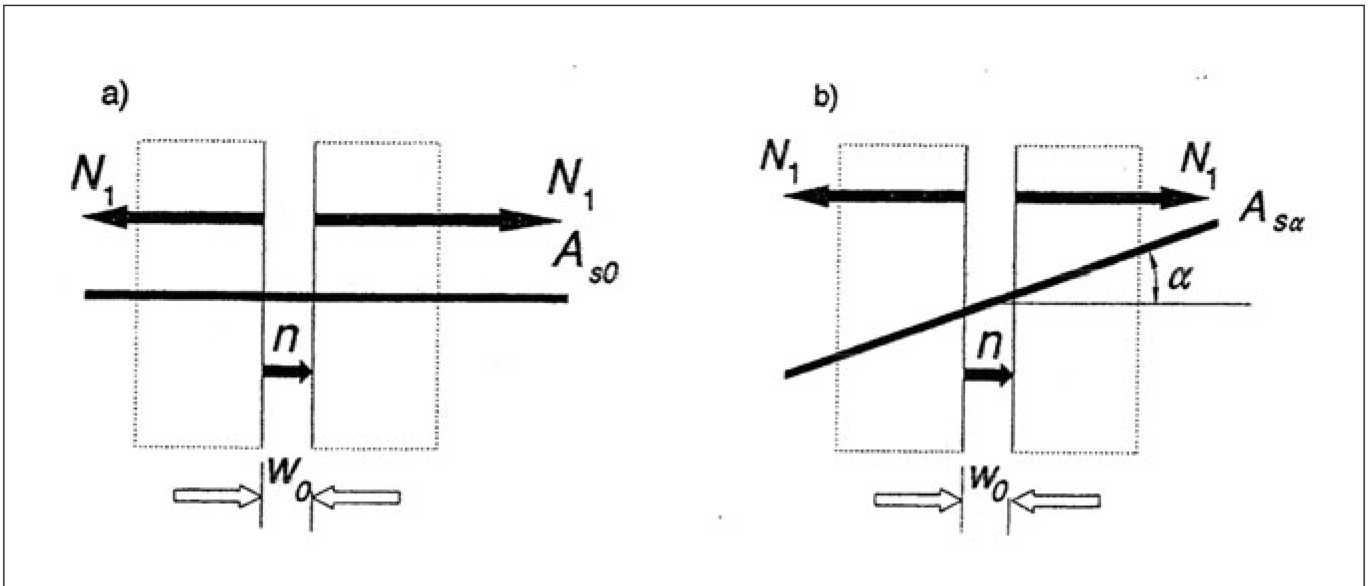

4. THE NEW DESIGN EQUATION FOR INCLINED ORTHOGONAL NETS

At derivation of design equations equilibrium, compatibility conditions and material laws must be considered. Equilibrium will be fulfilled along the primary crack running perpendicular to the principal tensile stress/strain direction. Along this primary crack the tensile forces are equilibrated by the inclined rebars forming an orthogonal net (ξ and η). The existence of tangential forces due to the forces in the inclined rebars, of concrete compressive stresses and of aggregate interlock will be discussed later.

Using the legend in *Fig. 3* the compatibility will be fulfilled within the crack: the slips of the inclined rebars are

$$w_\xi = \frac{w_n}{2\,cos\alpha}\;; \qquad w_\eta = \frac{w_n}{2\,sin\alpha} \tag{1}$$

with

w_n the crack width allowed for in the principal tensile direction.

The actual specific principal tensile force in the crack, N_n is balanced as

$$N_n = \frac{A_{s\xi}}{s_\xi}\,\sigma_{s\xi}\cdot cos^2\alpha + \frac{A_{s\eta}}{s_\eta}\,\sigma_{s\eta}\cdot sin^2\alpha \tag{2}$$

where

n direction of principal tensile stress
ξ, η directions of rebars in orthogonal net
α angle between n and ξ
s_ξ, s_η distance of the rebars in the orthogonal net

Windisch (1993, 2000) introduced and deduced the efficiency factor ψ of a "skew" rebar i.e. which runs at an angle α related to the principal tensile stress. It was shown that the stresses in the inclined rebars which fulfill the compatibility criterion are

$$\sigma_{s\xi} = \psi_\alpha\cdot\sigma_{sn}\;; \quad \sigma_{s\eta} = \psi_{90-\alpha}\cdot\sigma_{sn} \tag{3}$$

With

ψ_α and efficiency factors of the inclined rebars.
Substituting in (2) we get

$$\frac{A_{s\xi}}{s_\xi}\,\psi_\alpha\cdot\sigma_{sn}\cdot cos^2\alpha + \frac{A_{s\eta}}{s_\eta}\,\psi_{90-\alpha}\cdot\sigma_{sn}\cdot sin^2\alpha = \frac{A_{sn}}{s_n}\,\sigma_{sn} \tag{4}$$

A_{sn}/s_n and σ_{sn} are the rate of reinforcement running in the direction of the tensile principal stress and the steel stress in the crack in SLS, resp. which fulfill the required crack width. The task of crack control is reduced to an already solved problem: the determination of crack width in a rebar running in the direction of tensile trajectory.It is obvious that the (specific) forces in the inclined rebars (having a resultant perpendicular to the crack) yield (specific) force parallel to the crack:

$$Q_n = \frac{A_{s\xi}}{s_\xi}\,\sigma_{s\xi}\cdot cos\alpha\; sin\alpha - \frac{A_{s\eta}}{s_\eta}\,\sigma_{s\eta}\cdot sin\alpha\; cos\alpha \tag{5}$$

Depending on the crack distance and bond characteristics of the rebars a part or the whole force is transferred into and out of the concrete between two neighboring cracks. Depending on the boundary conditions these forces are balanced by these supports (causing a modification of the state of stress) or cause displacements. Special cases are slabs where the transverse forces (parallel to the middle plane) let induce stresses in the concrete compression zone which changes the state of stress. It is obvious that choosing the parameters of the inclined orthogonal reinforcement our target shall be to minimize the tangential forces.

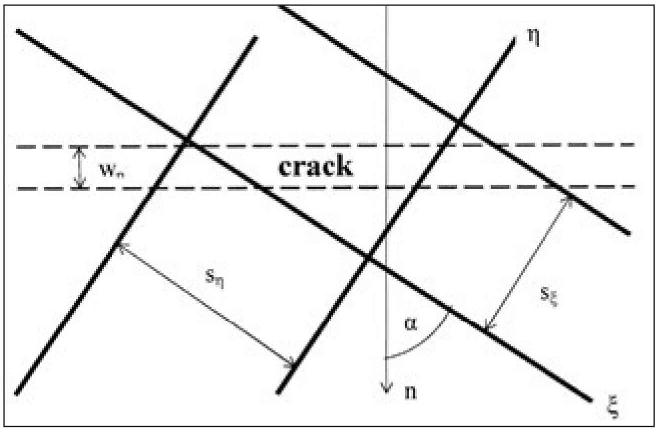

Fig. 3: Orthogonal net of rebars inclined to the crack, legend (not to scale!)

Short mention must be made here on kinking and dowel action of rebars and on aggregate interlock. In case of SLS the crack widths are up to 0.4 mm, whereas the diameters of the rebars are in the range from 5 mm to 32 mm and more. This means that self-adaption of the rebars to the direction of the principal tensile stress is hardly possible. Slight kinking is possible. The dowel forces may partly resist the force parallel to the crack. The contribution of aggregate interlock will be discussed in a next paper.

5. DIMENSIONING OF AN INCLINED ORTHOGONAL NET FOR A GIVEN CRACK WIDTH

Based on the model described in Chapter 4 the procedure of the dimensioning is as follows:

- Calculate the principal tensile stress (at cracking, $\sigma_{s,cr,n}$ and in SLS, σ_{sn}) and its direction
- Calculate the rate of reinforcement (A_{sn}/s_n) which fulfills the required crack width acc. to MC 2010. For A_{sn} choose the bigger diameter of the rebar in the orthogonal net to be applied.
- Choose the direction of the orthogonal net of rebars.
- Calculate $A_{s\xi}/s_\xi$ and $A_{s\eta}/s_\eta$ according to Eq. (4)
- In order to control the crack widths between the rebars, at choosing s_ξ and s_η consider the max. distances which depend on the rebar's diameter.
- If possible, choose a direction and/or $A_{s\xi}/s_\xi$ and $A_{s\eta}/s_\eta$ (two equations and three parameters!) where the force parallel to the crack (5) is minimum.

6. CONCLUSIONS

After a review of the relevant rules given in MC2010 a theoretically sound and practical method of dimensioning is presented herein based on the efficiency factors of the inclined rebars.

7. REFERENCES

Bisch, P. (2015), "Skew cracking" in Bulletin "SLS in Model Code 2010", in press

Broms, B. B., Lutz, L. A., (1965) "Effects of Arrangement of Reinforcement on Crack Width and Spacing of Reinforced Concrete Members". ACI Structural Journal Nov. 1965, No. 62-77 pp. 1395-1410. + Part II Report.

fib Model Code for Concrete Structures 2010, (2013) Ernst & Sohn, Oct. 2013, 434 p. ISBN: 978-3-433-03061-5

Kaufmann, W. (1998), "Strength and Deformations of Structural Concrete Subjected to In-Plane Shear and Normal Forces", IBK Bericht Nr. 234, Institut für Baustatik und Konstruktion, ETH Zürich, Birkhäuser Verlag, Juli 1998, 147 p.

Windisch, A. (1993), "Der Wirkungsgrad eines schräg zum Riß angeordneten Bewehrungsstabes", Bauingenieur 68, 1993, pp. 175-181, Springer Verlag

Windisch, A. (2000), "On the design of two-way reinforcements in R/C" Studi e Ricerche – Vol. 21, 2000, Italcementi S.p.A., Bergamo, pp. 283-302.

Windisch, A. (2016) "Crack control: an advanced calculation model – Part I: Review of classic tests". Concrete Structures, 2016, pp. 41-48.

Andor Windisch PhD, Prof. h.c. retired as Technical Director of Dywidag-Systems International in Munich, Germany. He made his MSc and PhD at Technical University of Budapest, Hungary, where he served 18 years and is now Honorary Professor. Since 1970 he is member of different commissions of FIP, CEB and fib. He is author of more than 120 technical papers. Andor.Windisch@web.de

CCC2017 Tokaj

31 Aug. – 1 Sept. 2017

The 12th Central European Congress on Concrete Engineering

Innovative materials and technologies for concrete structures

3rd Announcement and Call for Papers

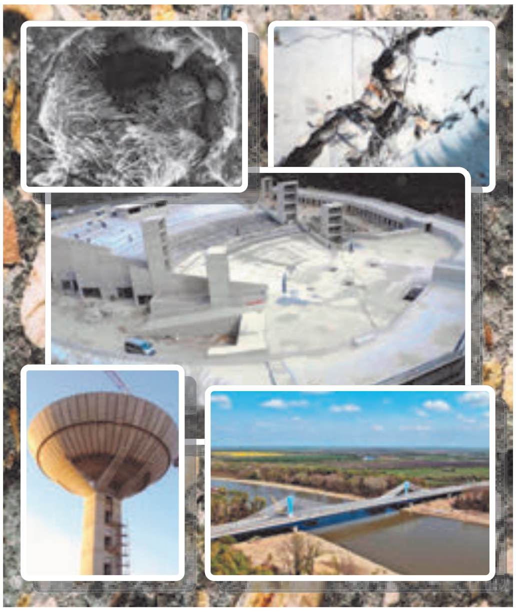

Host CCC Association
Hungarian Group of *fib*

Co-organisers:

www.fib.bme.hu/ccc2017.html

CONGRESS SECRETARIAT

CCC2017 Tokaj Congress Secretariat
Hungarian Group of *fib*
Budapest University of Technology and Economics
Department of Constructions Materials and Technologies
1111 Budapest, Műegytem rkp. 3.
Tel: +36-1-463-4068
Fax: +36-1-463-3450
e-mail: ccc2017@epito.bme.hu
Congress website: www.fib.bme.hu/ccc2017.html

GENERAL PROGRAMME

Wednesday 30 Aug. 2017	**Thursday 31 Aug. 2017**	**Friday 1 Sept. 2017**
Arrival Registration **Welcome Drink**	**9^{00} Opening** Technical Sessions Lunch Technical Sessions **Congress Dinner**	**9^{00} Technical Sessions** Technical Sessions Lunch **Technical Excursion**

EXHIBITION

A technical/commercial exhibition will be organized during the Congress
You are kindly asked to indicate your interest to participate as exhibitor.

TECHNICAL EXCURSION

New concrete structure for SAUSKA Winery in Tokaj

The three-storey part of the building under the ground level is an expansion unit, which is a rectangular-shaped, self-contained building block. Furthermore, the structure of the building part is a pillar-system, with reinforced concrete structures. The floor structures are reinforced concrete slabs, typically supported by points, flat on the top and bottom, and there are reinforced concrete basement walls on the edge. The roof slab is green roof designed which fits into the existing ground plane.

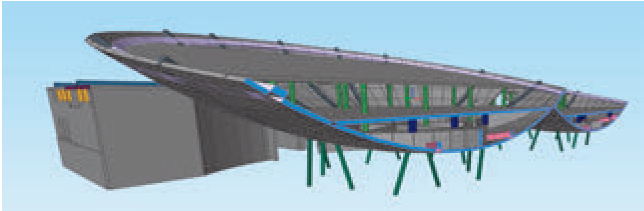

CONGRESS DINNER

A special Congress Diner will be organized. Details are available on the homepage of the Congress.

ACCOMPANYING PERSON'S PROGRAMME

Accompanying persons are warmly welcome to attend the Congress Special programme will be organized for them. Details are available on the homepage of the Congress.

CONGRESS VENUE

Tokaj – Cultural and Conference Complex
Tokaj, Serház street 55.
GPS: 48.12641525268555 | 21.41019630432129

CONGRESS TOPICS

Contributions focused on the following topics are invited.

Topic 1
TAILORED PROPERTIES OF CONCRETE
Environmentally compatible cements. New types of Aggregates. High performance admixtures. High strength and high performance concretes. Fibre reinforced concrete. Lightweight concrete. Green concrete. Applications.

Topic 2
ADVANCED REINFORCING AND PRESTRESSING MATERIALS AND TECHNOLOGIES
Metallic and non-metallic reinforcements. Internal and external reinforcements. Applications.

Topic 3
ADVANCED PRODUCTION AND CONSTRUCTION TECHNOLOGIES
Concrete structures meeting high requirements. Prefabrication. Design aspects. Applications.

Topic 4
ADVANCED CONCRETE STRUCTURES
Recent successful application of concrete for bridges, buildings and other structures.

Topic 5
MODELLING, DESIGN AND CODIFICATION

IMPORTANT DATES

15 April 2017 — Submission of Abstracts – Extended deadline

Ona page Abstracts are to be submitted to the Congress homepage including name(s), address(es), phone, fax and e-mail number(s) of author(s) together with the suggested Congress Topic where the abstract belong to.

15 May 2017 — Confirmation of acceptance of Abstracts

10 June 2017 — Submission of manuscripts

Accepted contributions will be either presented orally or in the Poster Session. Both oral and poster presentations will be published in the Congress Proceedings. The Poster Session will be continuously open during the Congress.

OFFICIAL LANGUAGE

The official language of the Congress is English. In addition, simultaneous translation into Hungarian and other languages can be organized.

www.fib.bme.hu/ccc2017.html